ENTRAINING HYDRAULIC JUMPS IN TWO-LAYER FLOWS

A report
submitted in partial fulfilment
of the requirements for the Degree
of
Master of Engineering
at the
University of Canterbury,
Christchurch, New Zealand

by
D. BEWICK

February 1974

ABSTRACT

This paper examines the region of rapidly varying flow in a two-layered density-stratified system. It is an extension of a previous analysis (Wilkinson & Wood, 1971) in which the theory for the case of stationary ambient fluid was developed. The analogous phenomenon in open channel hydraulics was the hydraulic jump.

In density stratified flows this phenomenon is referred to as an entraining hydraulic jump, or density jump, because ambient fluid is entrained into the faster flowing layer thereby changing its density. Unlike the open channel hydraulic jump, conditions either side of the entraining hydraulic (or density) jump are not uniquely related. A density jump with given flow conditions upstream has a range of possible states which may be attained downstream. The rate of entrainment of ambient fluid into the density jump, and the conditions downstream of the jump, are determined by the downstream control and the upstream conditions.

This project is an extension of this work to the case where the ambient fluid is in motion. The analytical and experimental work have demonstrated conclusively that there is a large increase in entrainment as the velocity of the ambient fluid is increased. This work should not only be of fundamental importance, but will also be of considerable interest in a number of geophysical situations and could be of great importance in the mixing of wastes in rivers and estuaries.

ACKNOWLEDGEMENTS

This project was conducted under the overall guidance of Professor H.J. Hopkins, Head of the Department of Civil Engineering, University of Canterbury.

I particularly wish to thank Professor I.R. Wood, not only for his original work in this field which provided the basis, and showed the need, for this project, but also for his guidance and enthusiasm during his supervision of this project.

The writer wishes to acknowledge his appreciation of the fine work done by the technical staff of the Department of Civil Engineering; and in particular mention Mr. H.S. Pearce for his work in building the laboratory equipment, carrying out modifications, and assisting with the experiments. Further thanks are due to Mr. H. Patterson for the excellent photographic work.

Thanks are also due to Dr. P.J. Bryant of the Department of Mathematics for his help with the Computer Program and expression for the wave velocity in a two-layered fluid.

Further thanks are offered to members of the University Computer Centre; the Ministry of Works, for financial assistance; and the typist, Mrs. Ball.

C O N T E N T S

	Page
Abstract	i
Acknowledgements	ii
Contents	iii
List of Figures	v
1. INTRODUCTION	
1.1 Density Currents	1
1.2 Hydraulic Jumps and Internal Hydraulic Jumps	3
1.3 Density Jumps	3
1.4 The Flow Regions of a Density Jump	6
1.5 The Entrainment Zone	6
1.5.1 The Wall Jet	6
1.5.2 Turbulent Entrainment in Stratified Flows	8
1.6 The Density Jump in a Stationary Ambient Fluid	10
2. THE DENSITY JUMP IN A MOVING AMBIENT FLUID	
2.1 Description	15
2.2 Analysis	18
2.3 The Solution for Infinite Depth	27
3. EXPERIMENTAL WORK	
3.1 Introduction	33
3.2 Apparatus	35
3.3 Velocity Determination	38
3.4 Photographic Technique	40
3.5 Density Determination	41
3.6 Procedure	41
4. LABORATORY EXPERIMENT RESULTS AND DISCUSSION	
4.1 Velocity Profiles	44
4.2 Density Distributions	44
4.3 The Effect of Non-Uniform Velocity Profiles and Density Distributions	45
4.4 Comparison of Experimental Results with Theory	47
4.5 The Effect of Boundary Friction	49

Page

5. THE COMPUTER PROGRAM

5.1 The Solution for Flows of Finite Depth 51

5.2 Computer Program Results 53

5.2.1 Theoretical Results for Laboratory Experiments 53

5.3 Comparison of Theories for Finite and Infinite Depths 54

5.4 The Downstream Froude Number when the Weir Height is Zero 55

5.5 The Wave Velocity in a 2-layer Fluid of Finite Depth 56

6. CONCLUSION AND RECOMMENDATIONS

6.1 Recommended Modifications 61

6.2 Further Studies 62

6.3 Conclusion 62

APPENDICES

Appendix A Typical Reduction of Test Data for a Single Experiment 65

Appendix B Error Analysis of a Typical Experiment 68

Appendix C Tables of Results 70

Appendix D Results Obtained by Wilkinson (1970) 76

Appendix E Calibration of Hot Water Flow Meter 77

Appendix F Computer Program 79

Appendix G Applications of Density Jump Theory in Thermal Power Stations 84

Appendix H The Huntly Thermal Power Station 86

Appendix I Recommended Modifications 91

Appendix J Notation 93

Appendix K References 96

LIST OF FIGURES

	Figure No.
Schematic Diagram of a Density Jump	1
Schematic Diagram of a Density Jump	2
Density Jump Controlled by a Broad-Crested Weir	3
A Non-Entraining Hydraulic Jump	4
A Flooded Hydraulic Jump	5
A Maximum Entraining Hydraulic Jump	6
Plot of Weir Height Against Downstream Froude Number	7
Schematic Diagram of a Flooded Jump	8
Point of Incipient Flooding	9
Photograph of a Jump with a Very Short Entraining Zone	10
Plot of Weir Height Against Downstream Froude Number for a Range of Velocities of Ambient Fluid	11
Laboratory Apparatus	12
Photograph of Laboratory Apparatus	13
Photograph of Selective Withdrawal	14
Hydrogen Bubble Apparatus	15
Hydrogen Bubble Traces, Photographs	16a,b,c,d
Typical Downstream Velocity Profiles	17
Typical Downstream Density Distributions	18
Experimental Results, v_*'s plotted	19
Froude Numbers, Experiment and Theory	20
Froude Numbers, $0 < v_* < 0.5$	21
Entrainments, Experimental and Theory	22
Entrainments, $0 < v_* < 0.5$	23
Graph of hf/y_1 against Theoretical q_{21}, labelled v_*'s	24a
Graph of hf/y_1 against Experimental q_{21}, labelled v_*'s	24b
Comparison of Theoretical Froude Numbers	25a
Comparison of Theoretical Entrainments	25b
Computer Plots of Weir Height Against F_2	26a,b,c,d

The Froude Number at h = 0 27

The Wave Velocity in a 2-Layer Fluid of Finite Depth 28a,b

Photographs of a Density Jump as v is increased 29a,b,c,d

Calibration Chart for Flow Meter 30

CHAPTER ONE

1. INTRODUCTION

1.1 DENSITY CURRENTS

The term "density current" is used to describe the motion of a fluid over, through, or under another fluid of slightly different density. Density currents may be divided into overflows, underflows, interflows, and plumes (which flow vertically upwards or downwards). The difference in specific weight of the two fluids provides the driving force for the motion. The density difference may be due to dissolved salts or a temperature variation. The term turbidity current is used when a suspension of solids causes the density difference. Density flows are generally miscible with the surrounding fluid. Density gradients in a fluid tend to suppress turbulence normal to that gradient, so that in certain cases density currents can flow for appreciable distances and only mix very slightly with the surrounding fluid. It is this feature of density flows that it is desirable to promote in power station cooling ponds.

Density underflow turbidity currents may occur when streams bearing suspended material enter a lake or reservoir. A zone of intense mixing is formed at the point where the river "plunges" beneath the lake surface to begin its underflow along the bed of the lake. Turbidity currents have been observed to travel hundreds of miles without loss of identity; and in the Grand Banks Turbidity Current of 1929, velocities of 55 knots were reported.

Density overflow currents occur when thermal power station cooling water or effluents from industrial processes and sewage treatment plants are discharged at temperatures higher than those of the receiving water. In an estuary, fresh river water which comes into contact with saline water and flows over the saline water forms a "salt wedge" adjacent to the bed of the estuary. Density current action is significant in the establishment of circulation patterns within estuaries and hence in the examination of estuarine siltation and pollution problems.

Selective Withdrawal is practised when water is drawn off from one stratum of a density stratified system without mixing with the water from adjoining strata. For example: cooling water should be drawn from the stratum of minimum temperature; water for domestic or industrial use should be drawn from a zone of low turbidity.

Density currents in the atmosphere are of considerable economic importance. For example: Katabatic winds (which form when air cooled by contact with cold ground flows downhill) are of importance to agriculture because of their influence on frost damage; also they may carry smoke or fog and so affect the visibility of airfields and ports. The accumulation of smog in valleys is a slightly different, but related, problem. In some regions such as the coasts of Greenland and Antarctica, kabatic winds may attain great strength (Ball 1956). Examples of turbidity currents in the atmosphere include dust storms such as the Sudan haboob, volcanic dust clouds, and powder snow avalanches. Data from experiments on density currents in hydraulic models has been used to study the motion of cold fronts.

1.2 HYDRAULIC JUMPS AND INTERNAL HYDRAULIC JUMPS

The hydraulic jump in an open channel has been extensively studied because of its practical importance as an energy dissipator in civil engineering work. (Henderson 1966). An almost exactly similar jump may occur with the flow of any fluid under a stationary lighter fluid. For example: the flow of water under kerosene, the flow of salt water under fresh water, or the flow of cold air under warm air. In the case of immiscible fluids with negligible viscosity and with the lighter fluid stationary, the equations are exactly similar to the hydraulic jump equations. The case where the upper fluid as well as the lower fluid is moving was studied by Yih and Guha (1955). Their analysis showed that with both layers flowing there are up to four mutually conjugate downstream states possible for a given upstream state.

1.3 DENSITY JUMPS

If two fluids of different densities are miscible, mixing or entrainment of one fluid into the other may occur in the turbulent region of an internal hydraulic jump. If entrainment is possible, the jump is accompanied by a change of density of the flowing fluid, and is called a "density jump" or "entraining hydraulic jump". The special case of the density jump in which the ambient fluid is stationary was studied by Wilkinson (1970) and Wilkinson and Wood (1971). The case when both fluids are flowing in the one direction gives rise to a similar jump but with increased entrainment, and it is this case that will be examined in detail in this report.

Density jumps are similar in many ways to open channel hydraulic jumps. However there are several points of difference between the two phenomena. Unlike the open channel hydraulic jump, flow conditions either side of the density jump are not uniquely related. The density jump with given flow conditions upstream has a range of possible states which may be attained downstream. The rate of entrainment of ambient fluid into the density jump and the flow characteristics downstream of the jump are determined by the downstream control and the upstream conditions.

Density jumps may occur when a fluid is discharged from an outlet under a horizontal boundary into a fluid of greater density, or over a horizontal boundary into a fluid of lesser density. A situation similar to the former case exists when heated cooling water is discharged from a power station onto the surface of a cooling pond.

Density jumps have also been observed in the atmosphere. Schweitzer (1953) observed the phenomena in Föhn Winds, and Ball (1959) and Lied (1964) noted their occurrence in Antarctica. Lied gives a particularly vivid account of meteorological measurements taken through a jump in katabatic flow. The depth of flow on the supercritical side of the jump was typically 60 to 100 feet and on the subcritical side 100 to 300 feet, varying with different jumps. Pressure drops of up to 20 m.b. were measured across the jump; in one instance, over a distance of only 60 yards. Lied's account of his walking through a jump is worth recounting.

"The experience of actually walking through a standing katabatic jump is somewhat unusual. Invariably the following sequence of events took place:

(i) The observer walked upslope in calm conditions, or with light and variable winds.

(ii) Taking measurements of pressure, temperature, and wind-speed and direction downhill from the jump while still in the calm air, the observer had the odd sensation of approaching a strongly roaring wall of drift snow, which was neither retreating nor advancing, and towering up to 300 feet above him.

(iii) Series of measurements were taken immediately outside the edge of the jump, whereafter the observer stepped into a totally different world, like walking through a door opening out into a full blizzard. At the very edge of the jump violently rotating swirls of wind and snow, with strong updrafts and downdrafts alternately forced snow up into his nostrils and eyes and at the next moment blew it down his neck. A severe buffeting was experienced.

(iv) At this point further measurements were taken. These showed a sudden drop of pressure, an immediate rise in temperature, and just inside the very turbulent edge of the jump, a violent increase in wind speed blowing downslope with strong gusts, and accompanied by moderate to dense drift snow.

(v) To make sure of his measurements the observer passed in and out of the jump several times repeating his observations on either side of it. He then walked upslope into the wind to obtain measurements well behind the turbulent edge of the jump.

(vi) Upslope the wind was usually stronger than near the edge, with denser drift, and the differences in pressure and temperature from the values obtained in the calm air also increased upslope.

(vii) Walking downslope with the wind behind him the

observer could determine the standing edge of the jump by the suddent increase in turbulence. On leaving the jump, the transition from highly turbulent to calm, or light and variable conditions usually occurred over a distance of only about 5 yards."

1.4 THE FLOW REGIONS OF A DENSITY JUMP

At this stage it is appropriate to describe briefly the flow regions of a density jump. This description applies to both the case of a stationary and moving upper layer. The density jump, or entraining hydraulic jump, consists of two distinct regions: an entrainment zone and a roller region. Nearly all the entrainment takes place in an entrainment zone, the entrainment mechanism in this zone being similar to that in a wall jet. Turbulent entrainment in stratified flows have been studied by Ellison and Turner (1959) and others. The roller region is similar to the normal nonentraining hydraulic jump. The formation of a roller at the downstream end of the jump is caused by the presence of a control such as a channel contraction, or a weir as in Figure 1.

1.5 THE ENTRAINMENT ZONE

The entrainment mechanism in the entrainment zone of a density jump is similar to that in a wall jet.

1.5.1 The Wall Jet

When a neutral jet of air or water strikes a surface at right angles and spreads out radially over it, it forms what is termed a wall jet. Such a flow is produced, for

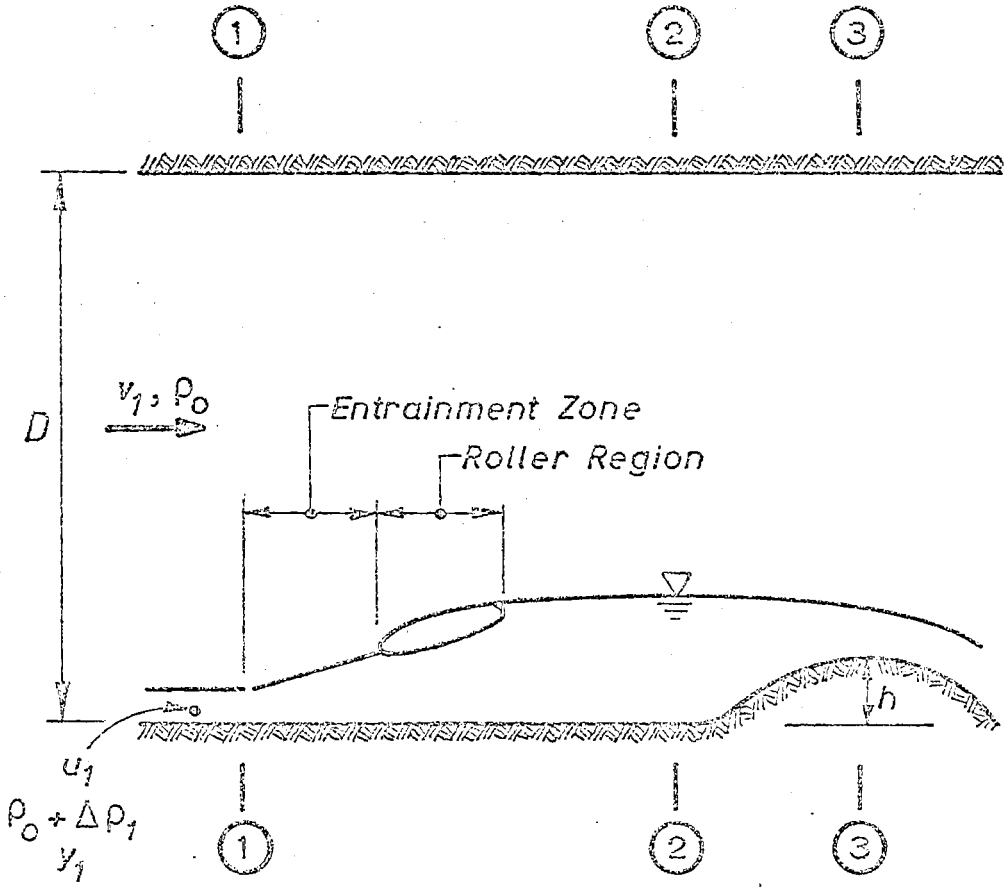

Fig. 1 : SCHEMATIC DIAGRAM OF A DENSITY JUMP

example, by a jet of water from a tap flowing into a partly full sink and spreading out over the bottom. Plane wall jets may also arise. If the water levels are different in two sections of a canal separated by a sluice, and if the sluice is slightly raised, the flow into the section with the lower water level will take the form of a wall jet.

In constructing an analytical similarity solution for the velocity profile, in the case of a radial jet, Glauert (1956) divided the jet into two parts. For the inner part, Glauert introduced the concept of an eddy viscosity distribution near the wall consistent with the Blasius power-law velocity profile, which may be expected to hold near the wall in any turbulent boundary layer flow outside a viscous sublayer. The outer part of the wall jet is governed by Prandtl's hypothesis that the eddy viscosity is constant across the layer and proportional to the product of the maximum mean velocity and the width of the layer.

Bakke (1957) verified experimentally the similarity solutions obtained by Glauert.

Kruka and Eskinazi (1964) investigated a plane, steady, turbulent wall-jet with negligible longitudinal pressure gradients in a moving stream. Following Glauert's reasoning they divided the flow up into two similarity regions. The inner or wall region extends from the wall to the point of maximum velocity, and the outer or free-mixing region extends from the maximum velocity point to the beginning of the free stream. Analytical similarity solutions were found for varying ratios (β') of free-stream to jet velocities.

The excess velocity, Δu_m (the maximum velocity in the jet, u_m , less the free stream velocity, v) was found to decay

as the longitudinal distance, x , raised to a power, a .

$$\Delta u_m = c\, x^a$$

An empirical relation describing the exponent a as a function of the velocity ratio β' showed that 'a' decreased when β' increased. Consequently the effect of raising the free stream velocity is to slow the rate of decay of Δu_m with the distance downstream.

1.5.2 Turbulent Entrainment in Stratified Flows

When a fluid is of a different density to its surroundings, it may flow as a relatively thin turbulent layer. The motion of this layer is governed by the rate at which it entrains the ambient fluid. The turbulent region of a density current grows with distance downstream as the ambient fluid becomes entrained in it. This implies a small mean velocity perpendicular to the main flow.

Ellison and Turner (1959) present a theory in which it is assumed that at high Reynolds numbers, viscosity effects can be ignored. Then it is taken that the entraining velocity normal to the direction of flow is proportional to the mean velocity of the density current. The constant of proportionality is termed the Entrainment constant, E . The entrainment parameter is a useful concept in that it expresses local entrainment at a section, in terms of local flow characteristics.

E is represented by $(\frac{u + v}{u})\ \frac{dy}{dx}$, or in stationary ambient flow simply by dy/dx , where u and y are the velocity and depth of the density current, v is the velocity of the ambient fluid, and x is in the direction of flow of

the density current. (x = distance downstream)

It can be shown that the spread of a self preserving neutral jet is linear with distance. Townsend (1956) measured $y = 0.15\,x$ giving an E of 0.075.

Bakke (1957) has published measurements of a wall jet in which the velocity profile resembles that of one half of an ordinary two-dimensional jet, modified by the presence of a thin boundary along the wall. He showed that the spread of the two dimensional wall jet was almost linear with downstream distance, with flow depth proportional to downstream distance raised to the power of 0.94. If the spread is assumed linear, the measurements lead to $y = 0.144\,x$ giving a value of E of 0.072.

The effect of stable stratification. A stable density gradient strongly inhibits turbulent mixing. Provided the Reynolds number is sufficiently large and density differences are small, E is a function of the Richardson number Ri, which is the inverse square of the densimetric Froude number, F. E was plotted against Ri for three experiments which gave reasonably consistent results. In most practical cases the layer will rapidly attain an equilibrium in which Ri does not vary with distance downstream, and the gravitational force on the layer is just balanced by the drag due to entrainment and boundary friction.

The fact that Ellison and Turner noted the analogy with hydraulic theory, making a distinction between shooting (supercritical) flow and tranquil (subcritical) flow in which entrainment is considered to be very small, suggested that Ellison and Turner were very close to discovering the fundamental theory of the entraining hydraulic jump.

Experiments in density overflows and underflows show that E falls off rapidly as Ri increases and is probably negligible when Ri is more than about 0.8. This implies that entrainment is zero in a subcritical density current. There is some difficulty in extending Ellison and Turner's reasoning to downstream controls other than the free overfall (F = 1.0).

The effect of motion of the ambient fluid. There is considerable interest in the question of how a steady velocity in the ambient fluid affects the flow of a wall plume travelling in the opposite direction to the ambient fluid. The meteorologist wishes to know how large an upper wind is necessary to destroy a katabatic flow at the surface; and the mining engineer is interested in how fast a downhill ventilating flow is needed to prevent a methane layer flowing uphill along the roof of a sloping mine roadway. It appears that there is a tendency for an opposing flow of ambient fluid to increase the apparent value of E . Ellison and Turner calculated that the velocity of upper wind necessary to reversea a katabatic wind flowing at 12 knots, is 24 knots.

1.6 THE DENSITY JUMP IN A STATIONARY AMBIENT FLUID

Wilkinson (1970) and Wilkinson and Wood (1971) studied the density jump in a two layered stratified system with one layer flowing and the other stationary. The particular case of a density jump controlled by a broad-crested weir downstream will be considered first.

1.6.1 Description

The density jump, in general, can be divided up into

two distinct zones; an entrainment zone and a roller region. Nearly all the entrainment which occurs takes place in the entrainment zone. These two zones are shown schematically in Fig. 2. The region of entrainment and mixing occurs at the upstream end of a density jump and the length of the entrainment zone is determined by the downstream control. Molecular diffusion between the layers is of a low order and is therefore neglected. The roller region is characterised by a flow near the interface in the reverse direction to the main flow. The interfacial slope of this roller is noticeably steep. This roller is similar in appearance to the roller associated with an open channel hydraulic jump and responds in a similar manner to a hydraulic jump if the height of a control weir downstream is adjusted. If the weir height (h) of Fig. 3 were increased, the roller region would extend further upstream and reduce the length of the entrainment zone. It is apparent, therefore, that increasing the weir height will cause a decrease in the entrained flow at the density jump and hence the flow in the layer downstream of the jump will be reduced.

If the weir height is increased further, a point can be reached where the roller extends the full length of the jump and entrainment effectively ceases. Such a jump will be referred to as a "non entraining jump" (see Fig. 4). Further increase of the weir height at this stage will cause the jump to flood so that the upstream end of the jump becomes submerged in dense fluid. There is no entrainment into a flooded jump (see Fig. 5).

If a controlling weir downstream of a density jump is lowered, the roller regions can be observed to migrate downstream. This causes the entrainment zone to lengthen,

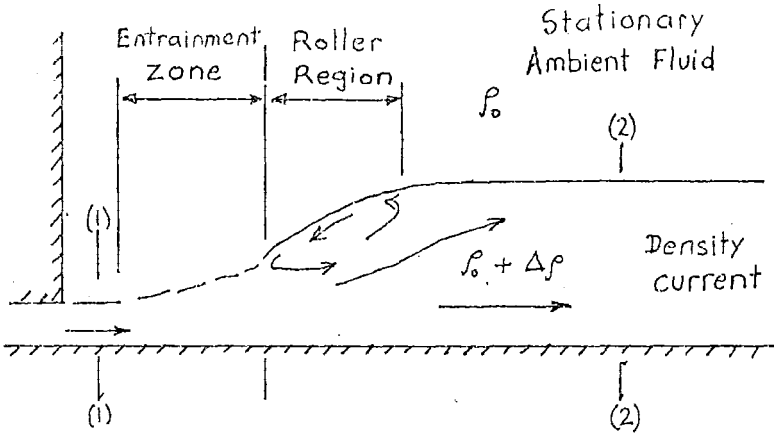

SCHEMATIC DIAGRAM OF A DENSITY JUMP.

FIGURE 2.

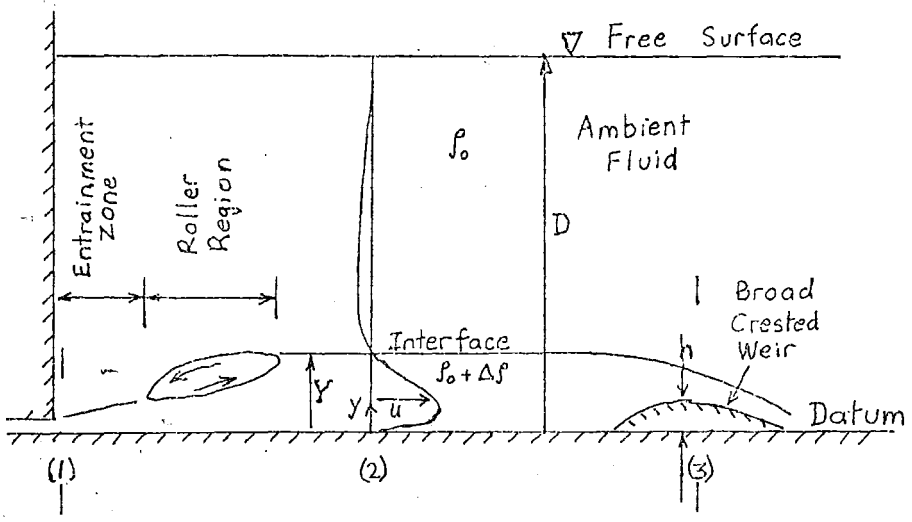

DENSITY JUMP CONTROLLED BY A BROAD-CRESTED WEIR

FIGURE 3

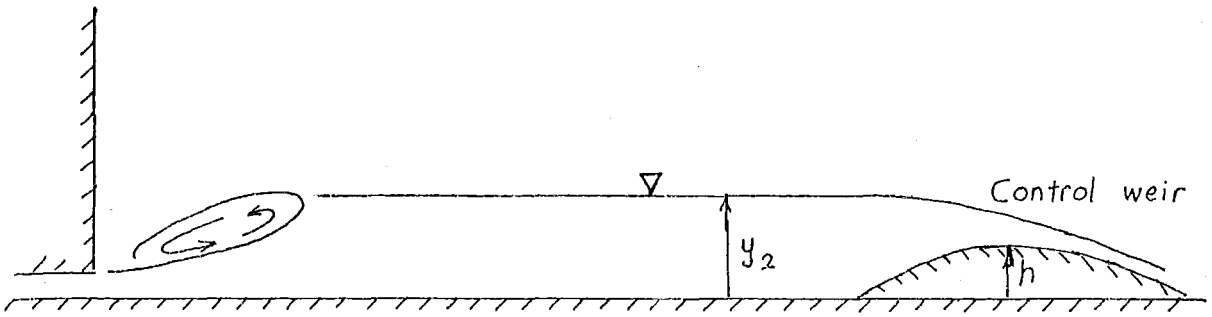

FIGURE 4.

A NON-ENTRAINING JUMP.

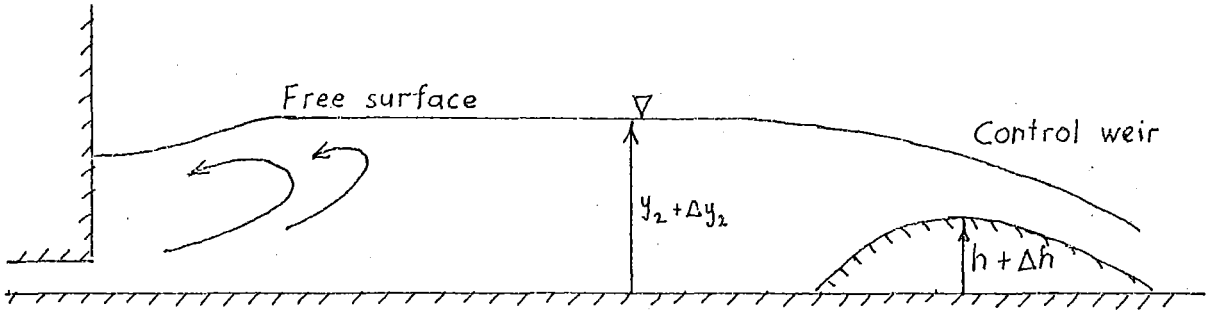

FIGURE 5.

A FLOODED HYDRAULIC JUMP.

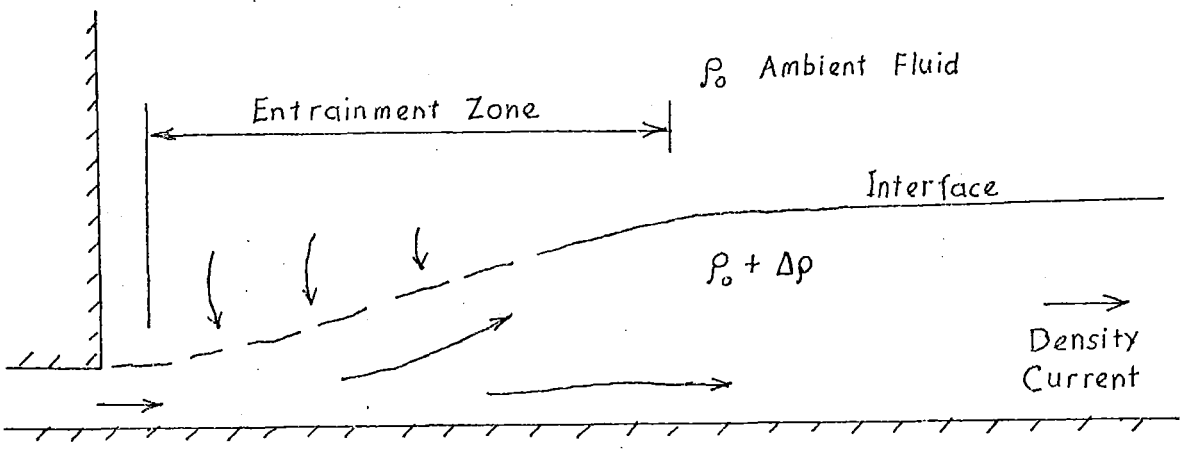

A MAXIMUM-ENTRAINING HYDRAULIC JUMP.

FIGURE 6.

JUMPS IN A STATIONARY AMBIENT FLUID.

and entrainment to increase, so that the flow in the layer downstream of the jump is also increased. A limit is reached when the entrainment zone occupies the entire length of the density jump, which is then of the maximum entraining type with no roller region. Such a density jump is shown in Fig. 6.

Other forms of control besides the broad-crested weir have been investigated, (Wilkinson 1970). These include the free overfall, sharp-crested weir, the undershot gate, the contraction, and friction on a sloping bottom.

1.6.2 Analysis of the Density Jump in Stationary Ambient Fluid

The analysis of the density jump in stationary ambient fluid is presented in Wilkinson and Wood (1971) and no attempt is made to reproduce it here. The analysis follows on much the same lines as the analysis for the moving ambient fluid except that allowance was made for non-uniform density and velocity distributions in the flowing layer.

It is assumed that there is no entrainment downstream of the jump. Use is made of the equation of continuity of density excess and the balance of hydrostatic pressure forces and fluid momentum between sections (1) and (2). The continuity and energy flux equations are used between sections (2) and (3). The flow is critical at the crest of the weir.

The equations are written in terms of the volume flow, q_v, the flow depth y, the flux of mass per unit span q_m, the flow force per unit span q_F, the energy flux per unit span q_E, the Froude Number F, measures of the non-uniformity of the velocity and density distributions in the momentum equation, s_m and s_H, and measures of the non-uniformity

of the velocity and density distribution in the energy flux equations, S_E and S_p.

It will be noted that the case of zero ambient flow is independent of the total depth D, and D can conveniently be considered to be infinitely large.

For a density jump controlled by a broad-crested weir of known height, conditions downstream of the jump can be predicted provided upstream conditions are known. This result is plotted in the form of a graph of hf/y_1 (f is a function of known upstream conditions and h the weir height) against F_2, (the downstream Froude number), for the case when S_m, S_H, S_E and S_p are all unity (see Fig. 7). It will be noted that this graph is exactly the same as that for the line $v_* = 0$ in the graph of hf/y against F_2 in the analysis of the density jump in moving ambient flow (Fig. 11).

Several interesting points arise from examination of the figure.

(a) When the weir height is of zero height, and in the absence of friction or any other downstream control, the Froude Number downstream of the jump will be unity and the jump is of the maximum entraining type.

(b) There is a maximum value of (hf/y_1) for which a solution is possible. It follows that if the weir height is raised above a maximum value, the jump will flood. There is no entrainment at a flooded density jump and rewriting the equations enable solution of the case of the flooded jump for different values of upstream Froude Numbers. The equation for one particular value of F_1 is plotted on Fig. 7.

(c) It can be seen that for an unflooded density

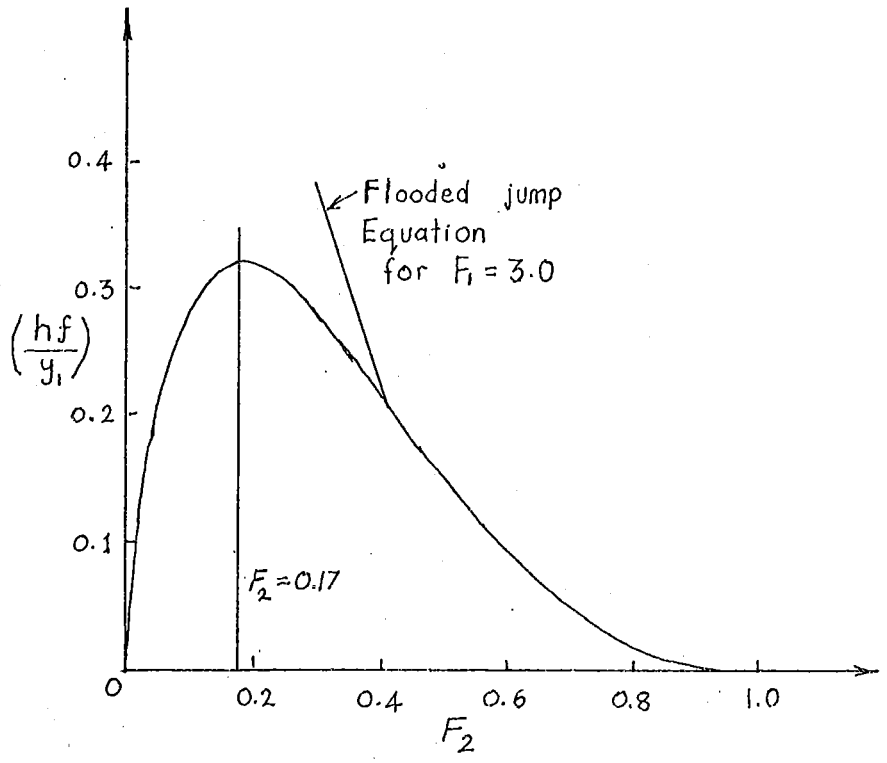

PLOT OF WEIR HEIGHT AGAINST FROUDE Nº DOWNSTREAM OF A DENSITY JUMP IN A STATIONARY AMBIENT FLUID

FIGURE 7

jump there are two possible values of F_2 . Physical arguments were used to show that only for the upper value of Froude Number is the flow state stable. Although the lower value of the Froude Number can be achieved by first flooding the jump and then lowering the control weir until the jump becomes non-entraining, a slight decrease in the weir height at the point will result in a dramatic change in form of the jump and the flow rate downstream. The jump will suddenly change to a density jump (in which the density changes) and there will be a rapid increase in F_2 .

The minimum stable F_2 for a density jump controlled by a broad-crested weir is 0.17, the Froude Number at which the critical weir height is reached. The maximum conjugate Froude Number, F_1 , upstream is that for a non-entraining jump and is equal to 13.2. Wilkinson (1970) showed that at upstream Froude Numbers greater than 13.2 the jump floods before the stage of zero entrainment is reached.

1.6.3 Experimental Results

Thermal density currents were used in the experiments, the warm layer flowing over the cooler ambient layer. Mean values of the characteristic density difference and the integral flow force and energy terms S_m , S_H , S_p and S_E were determined. Data from experiments were plotted on a graph similar to Fig. 7 and the agreement between theory and experiment was satisfactory. It should be noted, however, that the theoretical curve was plotted for the ideal case when it was assumed that the velocity and density distributions are uniform in the flowing layer. The closeness of the curve and the data indicated that the various integral factors compensate.

CHAPTER TWO

THE ENTRAINING HYDRAULIC JUMP IN A MOVING AMBIENT FLUID

2.1 DESCRIPTION

The density jump in a moving ambient fluid, like the density jump in stationary ambient fluid, consists of two distinct regions: an entrainment zone and a roller region. In experiments the entrainment process was made visible by injecting dye patches into the ambient flow in the vicinity of the density jump. It was observed that nearly all the entrainment occurs in the entrainment zone and there is virtually no entrainment in the roller region of the density jump.

The Entrainment Zone

The entraining zone of a density pump has been compared to the spread of a neutral jet. Neutral jets are jets in which the effect of a density gradient on entrainment is minimal. Some examples of neutral jets are plumes, forced plumes, vertical jets, and horizontal flows of a jet into ambient fluid of the same density (such as in a wall jet). In a neutral jet the densimetric Froude Number is infinite, and the Richardson number zero. And , if the depth of flow of a density current is very small, the Froude Number will also approach infinity. It follows, therefore, that the characteristics of the upstream end of a density jump for large values of the upstream Froude Number will approach those of a neutral jet.

When a neutral jet issues from a slot a severe velocity gradient between the moving fluid and the ambient fluid gives rise to high local shear. Eddies are generated in this zone of maximum instability and the ambient fluid is entrained into the jet. The amount of entrainment depends on the upstream conditions, the downstream control and the velocity of the ambient fluid.

Entrainment in the entrainment zone of a density jump falls off rapidly as the Richardson Number Ri increases and is probably negligible when Ri is more than about 0.8.

The Roller Region

The length and slope of the roller region is controlled by the height of the weir and the velocity of the ambient fluid. The effect on the roller of increasing the velocity of the ambient fluid is to increase the length and decrease the slope of the roller region.

At low ambient velocities, the roller region is characterised by a flow near the interface in the reverse direction to the main flow. At higher ambient velocities the interfacial part of the roller region will be flowing slightly slower than the ambient fluid. The low velocity gradient at the interface of the roller region compared with that in the entrainment zone causes a marked reduction in interfacial shear, resulting in reduced entrainment.

As there is negligible entrainment in the roller regions of the density jump, the roller region can be modelled mathematically as a non-entraining hydraulic jump, and represents a discontinuity in depth and velocity, but not in discharge nor density. The local Froude Number at

the end of the entrainment zone or the commencement of the roller region is therefore related to the Froude Number downstream of the jump by the same equation used to relate conjugate Froude Numbers in hydraulic jumps. Fig. 10 shows an hydraulic jump with a very short entraining zone.

The Effect of the Downstream Control

If the weir height is raised by a small amount, a positive surge will move upstream causing the roller region to migrate further upstream and entrainment at the jump will be reduced. Now the reduction in entrainment causes a reduction in the downstream flow and a new equilibrium will result with new values of depth and discharge downstream of the jump. By these changes the forces on either side of the jump may balance without movement of the jump. This corresponds with the normal hydraulic jump where, in a similar situation, the raising of the weir forces the jump to move upstream until losses allow the forces to balance again.

The continuous raising of the weir will eventually cause the jump to flood and entrainment will cease. (Figure 8). This is the point of incipient flooding. At the transition point the roller will cover the complete entrainment zone and the normal nonentraining hydraulic jump equations will apply. Further raising of the weir will cause some of the inflowing fluid to flow upstream behind the inlet, as shown in Figure 9. The inlet is now flooded.

If the weir is lowered, the roller region can be observed to migrate downstream. This causes the entrainment zone to lengthen and entrainment to increase, so that the flow in the layer downstream of the jump is also increased. A limit

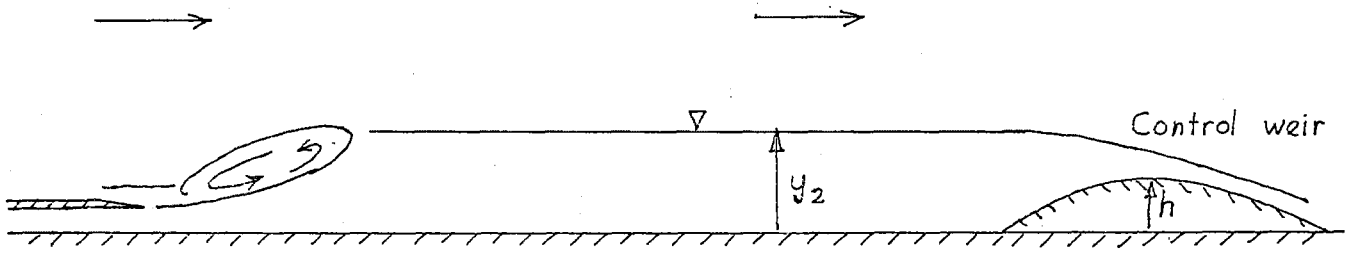

POINT OF INCIPIENT FLOODING IN A MOVING AMBIENT FLUID: A NON-ENTRAINING JUMP.

FIGURE 8.

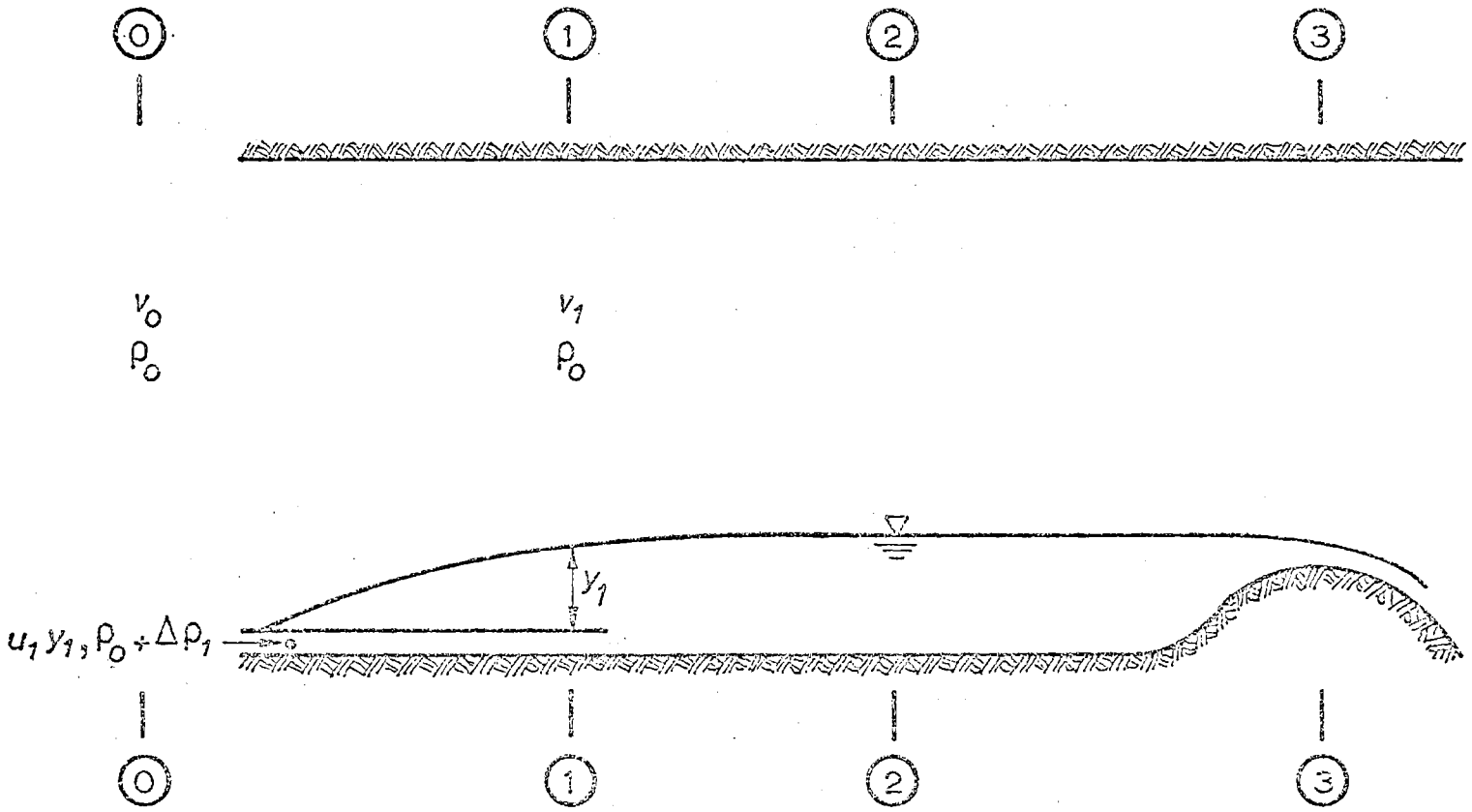

Fig. 9 : SCHEMATIC DIAGRAM OF A FLOODED JUMP

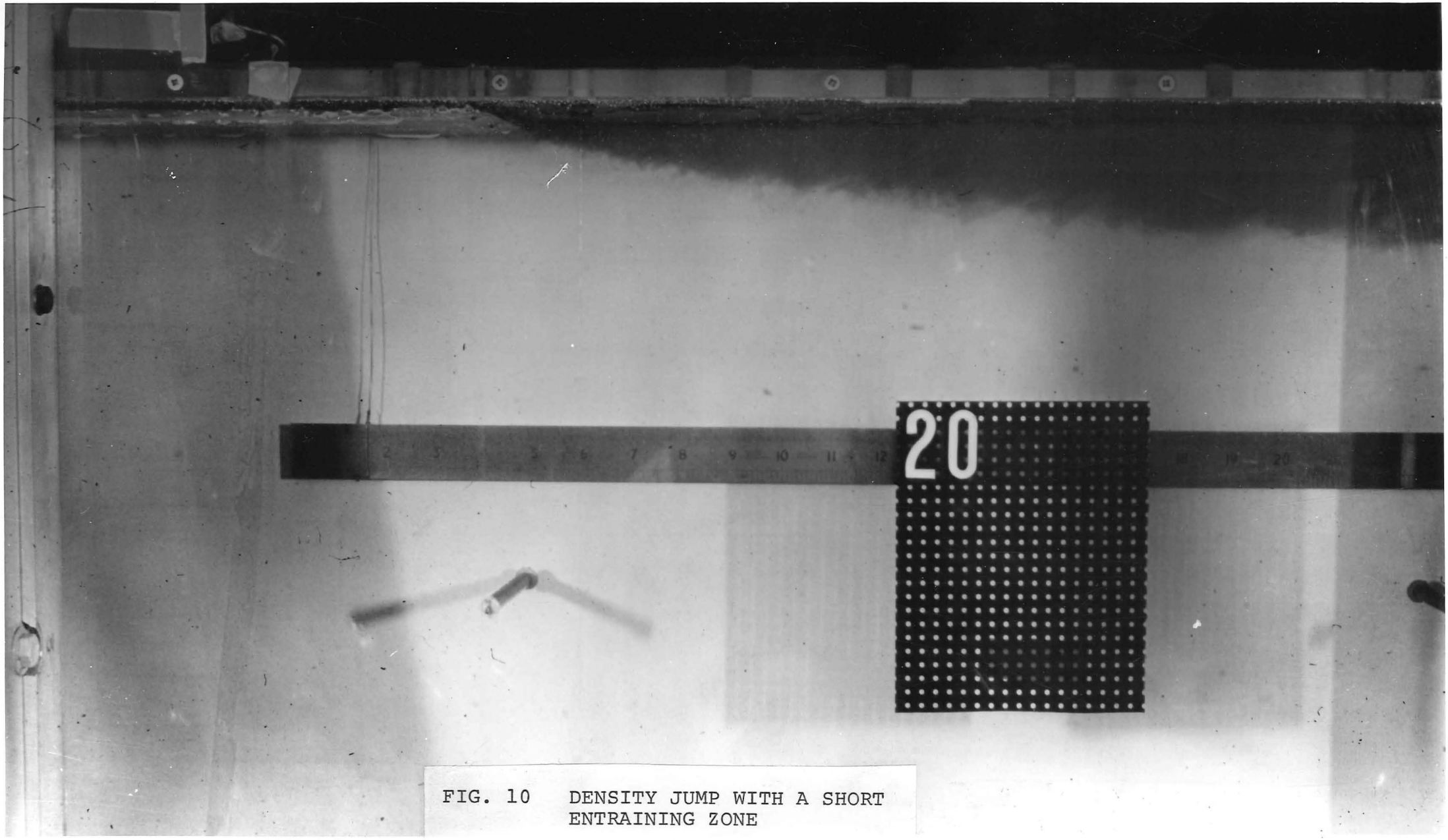

FIG. 10 DENSITY JUMP WITH A SHORT ENTRAINING ZONE

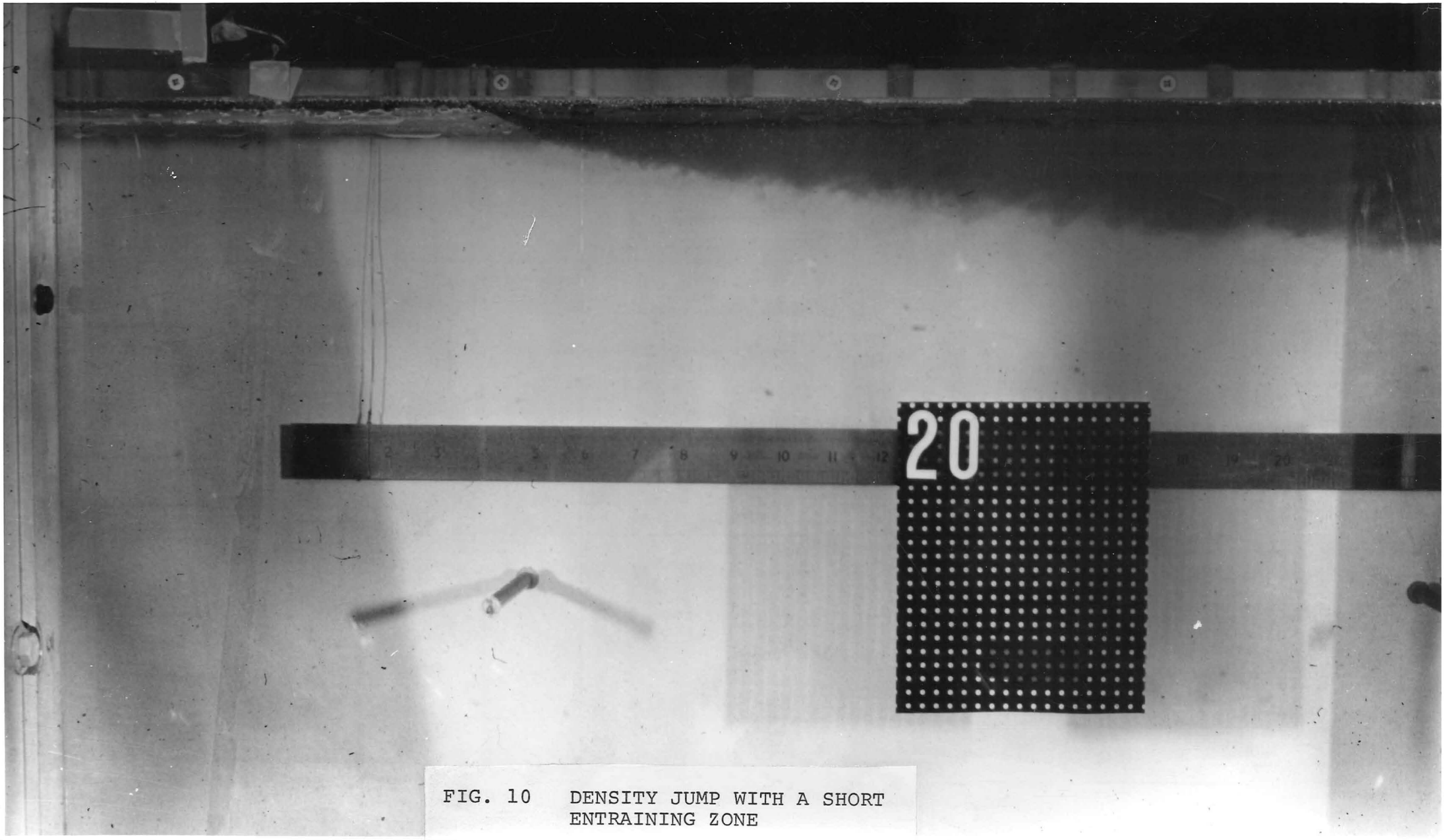

FIG. 10 DENSITY JUMP WITH A SHORT ENTRAINING ZONE

is reached when the entrainment zone occupies the entire length of the density jump, which is then of the maximum entraining type with no roller.

The Effect of a Moving Ambient Fluid

The case of zero velocity in the ambient fluid was studied by Wilkinson (1970). If the velocity of the ambient fluid is increased, the roller region is pushed downstream and the length of the entrainment region increases. The increase in entrainment increases the flow rate, depth and velocity; and decreases the density difference between the two fluids at sections (2) of Fig. 1. The driving force forcing the flow over the weir is reduced, and the depth y_2 increases slightly. The increase in velocity, and decrease in density difference offsets the increase in depth, so that the Froude Number increases.

As the ambient velocity is increased it becomes difficult to distinguish between the entrainment and roller regions, and turbulent entrainment extends for a considerable distance downstream before the flow becomes subcritical and conditions stable.

If the velocity of the ambient fluid is increased still further, a point is reached when the flow is supercritical the whole distance from the inlet to the weir. Supercritical flows are unstable and can entrain ambient fluid until the Froude Number reaches unity. Therefore it is expected that if the laboratory equipment were large enough, very large entrainments could be achieved.

2.2. ANALYSIS

The flows at sections (1), (2) and (3) (of Fig.1) are horizontal and therefore the pressure distributions are hydrostatic at these sections. Assumptions:

1. Bed friction is negligible.

2. The difference in densities of the two fluids is small.

3. There is no entrainment between sections (2) and (3).

4. Some of the ambient fluid (upper layer of Fig. 1) is entrained into the in flowing layer (lower fluid) between sections (1) and (2).

5. For ambient fluid particles that are not entrained, energy is conserved between sections (1), (2) and (3).

Equations considered in the analysis include:

1. Continuity of volume flux.

2. Continuity of density excess.

3. Conservation of energy in the ambient fluid (Bernoulli).

4. Bernoulli equation in the lower layer between sections (2) and (3).

5. Balance of hydrostatic pressure forces and fluid momentum between sections (1) and (2). (Benjamin (1962) labelled this term the "flow force").

6. Critical flow at the crest of the weir.

In the analysis of the entraining hydraulic jump in stationary ambient fluid (Wilkinson and Wood, 1971) allowance was made for non-uniform density and velocity distributions in the lower layer. However, it was decided for this investigation to assume that the velocity and density in each layer are constant at the sections considered.

Let the velocity, density and depth in the lower layer be u, $\rho + \Delta\rho$ and y, respectively. The total depth of the flowing layers is D. Let the velocity, density and depth of the ambient fluid be v, ρ_o and $(D - y)$

In steady flow, $\nabla(\rho u) = 0$, therefore, $q_\Delta = (\Delta\rho/\rho_o)ugy$ is constant in all sections. q_Δ is the flux of relative density excess times gravity per unit span.

In steady incompressible flow, $\nabla(u) = 0$

therefore, $q_v = [\, uy + v(d-y)]$ (2)

is constant at all sections.

q_v is the volume flux per unit span.

The mass flux (q_m) is also constant at all sections.

$$q_m = uy(\rho_o + \Delta\rho) + v\,\rho_o\,(d-y)$$

$$\frac{q_m\, g}{\rho_o} = g\,[\, u\,y + v\,(D-y)\,] + u\,y\,\frac{\Delta\rho}{\rho_o}\,g$$

$$\frac{q_m\, g}{\rho_o} = g\,q_v + q_\Delta \qquad (1)$$

The volume flux in the lower layer, (q), is

$$q = u\,y \qquad (3)$$

The densimetric Froude number, F, is defined as

$$F^2 = \frac{u^2}{\frac{\Delta\rho}{\rho_o}\,g\,y} = \frac{u^3}{q_\Delta} = \frac{q^2}{\frac{\Delta\rho}{\rho_o}\,g\,y^3} = \frac{q^3}{q_\Delta\, y^3}$$

Now if $q_{v*} = q_v/q_\Delta^{1/3} D$,

$q* = q/q_\Delta^{1/3} D$,

$V* = V/q_\Delta^{1/3}$

Then equation (2) may be written as

$$q_{v*} = q*\,[1 - V/u\,] + V*$$

$$= q*\,[1 - V*/F^{2/3}] + V* \qquad (4)$$

This equation will hold at all sections, but, in cases where there is no entrainment (between sections (2) and (3)), equation (4) may be divided into separate equations for the two layers. If q_u is the volume flux in the ambient fluid

$$q_u = v(D - y) \quad \text{and} \quad q_{u*} = \frac{q_u}{q_\Delta^{1/3} D} = q_{v*} - q*$$

$$\text{then} \quad q_{u*} = v* \left[1 - \frac{q*}{F^{2/3}} \right] \tag{5}$$

$q*$ is constant between sections (2) and (3).

It has been assumed that there is no energy loss in the ambient fluid, and, if the horizontal bottom is taken as datum, then the Bernoulli equation applied to any streamline in this layer yields

$$T_e = p + \frac{1}{2} \rho_o v^2 + \rho_o g D \tag{6}$$

where p is the pressure on the upper surface (Fig. 1) and T_e is the Bernoulli constant for streamlines in the upper layer (Ambient).

The fluid momentum equation may be written:

$$q_F = pD + \frac{1}{2} \rho_o g D^2 + \frac{1}{2} \Delta\rho g y^2 + \rho_o v (D - y) v + (\rho_o + \Delta\rho) u y u \tag{7}$$

where q_F is the flow force (Benjamin (1962)).

Next it is assumed that $\Delta\rho << \rho_o$. This is the normal Boussinesq approximation and implies that the density may be assumed constant and equal to ρ_o in all terms except the body force terms.

Equation (6) is used to eliminate the pressure term from (7) giving:

$$q_F + \frac{1}{2} \rho_o g D^2 - T_e D = \frac{1}{2} \rho_o v^2 D + \frac{1}{2} \Delta\rho g y^2 - \rho_o v^2 y + \rho_o u^2 y$$

$$\text{Now} \quad \frac{1}{2} \Delta\rho g y^2 = \frac{\frac{1}{2}\rho q_\Delta y}{u} = \frac{\frac{1}{2} \rho_o q_\Delta u y}{q_\Delta^{2/3} F^{4/3}} = \frac{\frac{1}{2} \rho_o q_\Delta^{1/3} u y}{F^{4/3}}$$

$$\text{Also} \quad \frac{1}{2} \rho_o v^2 D = \frac{1}{2} v*^2 \rho_o q_\Delta^{2/3} D$$

and $\rho_o v^2 y = \dfrac{\rho_o u y v^2}{q_\Delta^{1/3} F^{2/3}}$

and $\rho_o u^2 y = \rho_o q_\Delta^{1/3} F^{2/3} uy$

$$q_F + \frac{1}{2}\rho_o g D^2 - T_e D = \rho_o q_\Delta^{1/3} uy \left[F^{2/3} + \frac{1}{2F^{4/3}} - \frac{v^2}{q_\Delta^{2/3} F^{2/3}} \right] + \frac{v_*^2 \rho_o q_\Delta^{2/3} D}{2}$$

$$\frac{q_F - \frac{1}{2}\rho_o g D^2 - T_e D}{\rho_o q_\Delta^{2/3} D} = q_* \left[\frac{F^2 + \frac{1}{2}}{F^{4/3}} - \frac{v_*^2}{F^{2/3}} \right] + \frac{v_*^2}{2} \qquad (8)$$

Now in the lower layer, between sections (2) and (3), energy is conserved and, with the upstream horizontal bed taken as datum, we get

$$T_{el} = p + \rho_o g D + \frac{1}{2}(\rho_o + \Delta\rho) u^2 + \Delta\rho g (y + h)$$

where h is the bed level above the datum and T_{el} is the total energy level of the lower layer.

The Boussinesq approximation gives

$$T_{el} = p + \rho_o g D + \frac{1}{2}\rho_o u^2 + \Delta\rho g (y + h) \qquad (9)$$

Equation (6) is used to eliminate the pressure term from (9).

$$T_{el} - T_e = \Delta\rho g y (1 + \frac{h}{y}) + \frac{1}{2}\rho_o u^2 (1 - \frac{v^2}{u^2})$$

$$= \frac{\rho_o q_\Delta}{u} (1 + \frac{h}{y}) + \frac{1}{2}\rho_o q_\Delta^{2/3} F^{4/3} (1 - \frac{v^2}{u^2})$$

$$\therefore \frac{T_{el} - T_e}{\rho_o q_\Delta^{2/3}} = \frac{1}{F^{2/3}} \left[1 + \frac{h}{y} + \frac{F^2}{2} (1 - \frac{v_*^2}{F^{4/3}}) \right] \qquad (10)$$

The continuity equation (4) is applied between sections (1) and (2). Subscripts represent the values at the appropriate sections.

$$q_{*1}\left[1-\frac{v_{*1}}{F_1^{2/3}}\right]+v_{*1}=q_{*2}\left[1-\frac{v_{*2}}{F_2^{2/3}}\right]+v_{*2} \qquad (11)$$

The momentum equation (8) is applied between sections (1) and (2).

$$q_{*1}\left[\frac{(F_1^2+\frac{1}{2})}{F_1^{4/3}}-\frac{v_{*1}^2}{F_1^{2/3}}\right]+\frac{v_{*1}^2}{2}=q_{*2}\left[\frac{(F_2^2+\frac{1}{2})}{F_2^{4/3}}-\frac{v_{*2}^2}{F_2^{2/3}}\right]+\frac{v_{*2}^2}{2} \qquad (12)$$

Equations (11) and (12) yield the discharge ratio $q_{21}=q_{*2}/q_{*1}$

$$q_{*1}\left[\frac{(F_1^2+\frac{1}{2})}{F_1^{4/3}}-\frac{v_{*1}^2}{F_1^{2/3}}\right]-q_{*2}\left[\frac{(F_2^2+\frac{1}{2})}{F_2^{4/3}}-\frac{v_{*2}^2}{F_2^{2/3}}\right]$$

$$=\frac{1}{2}(v_{*2}-v_{*1})(v_{*2}+v_{*1})$$

$$=\frac{1}{2}(v_{*1}+v_{*2})\left[q_{*1}\left(1-\frac{v_{*1}}{F_1^{2/3}}\right)-q_{*2}\left(1-\frac{v_{*2}}{F_2^{2/3}}\right)\right]$$

$$\frac{q_{*2}}{q_{*1}}=\frac{\dfrac{F_1^2+\frac{1}{2}}{F_1^{4/3}}-\dfrac{v_{*1}^2}{F_1^{2/3}}-\frac{1}{2}(v_{*1}+v_{*2})\left[1-\dfrac{v_{*1}}{F_1^{2/3}}\right]}{\dfrac{F_2^2+\frac{1}{2}}{F_2^{4/3}}-\dfrac{v_{*2}^2}{F_2^{2/3}}-\frac{1}{2}(v_{*1}+v_{*2})\left[1-\dfrac{v_{*2}}{F_2^{2/3}}\right]}$$

$$q_{21}=\frac{\dfrac{F_1^2+\frac{1}{2}}{F_1^{4/3}}-\dfrac{v_{*1}+v_{*2}}{2}-\dfrac{v_{*1}}{2F_1^{2/3}}\left[v_{*1}-v_{*2}\right]}{\dfrac{F_2^2+\frac{1}{2}}{F_2^{4/3}}-\dfrac{v_{*1}+v_{*2}}{2}-\dfrac{v_{*2}}{2F_2^{2/3}}\left[v_{*2}-v_{*1}\right]} \qquad (13)$$

The continuity equation (5) for the ambient, between sections (2) and (3)

$$v_{*2}\left[1-\frac{q_{*2}}{F_2^{2/3}}\right]=v_{*3}\left[1-\frac{q_{*2}}{F_3^{2/3}}\right] \qquad (14)$$

The energy equation for the lower layer (10), between sections (2) and (3)

$$\frac{1}{F_2^{2/3}}\left[1+\frac{F_2^2}{2}\left[1-\frac{v_{*2}^2}{F_2^{4/3}}\right]\right]=\frac{1}{F_3^{2/3}}\left[1+\frac{h}{y_3}+\frac{F_3^2}{2}\left[1-\frac{v_{*3}^2}{F_3^{4/3}}\right]\right] \qquad (15)$$

$$=\frac{1}{F_3^{2/3}}\left[1+\frac{h\,F_3^{2/3}}{q_{*2}D}+\frac{F_3^2}{2}\left[1-\frac{v_{*3}^2}{F_3^{4/3}}\right]\right]$$

The definition of the Froude No. gives

$$y=\frac{q}{F^{2/3}q_\Delta^{1/3}}=\frac{q_* D}{F^{2/3}}$$

The assumption of no entrainment between sections (2) and (3) gives,

$$\frac{y_3}{y_1}=\frac{q_{*3}\,F_1^{2/3}}{q_{*1}\,F_3^{2/3}}=\frac{q_{*2}\,F_1^{2/3}}{q_{*1}\,F_3^{2/3}}$$

and equation (15) becomes,

$$\frac{1}{F_2^{2/3}}\left[1+\frac{F_2^2}{2}\left[1-\frac{v_{*2}^2}{F_2^{4/3}}\right]\right]=\frac{1}{F_3^{2/3}}\left[1+\frac{h\,q_{*1}\,F_3^{2/3}}{y_1\,q_{*2}\,F_1^{2/3}}+\frac{F_3^2}{2}\left[1-\frac{v_{*3}^2}{F_3^{4/3}}\right]\right] \qquad (16)$$

Now the conditions at section (1) and the value of h is known. Thus, the four equations 11, 12, 14, and 15 contain the unknowns q_{*2}, v_{*2}, F_2, F_3, and v_{*3}. The remaining equation required to close the system is obtained from the condition that at section (3) where dh/dx equals zero, dy/dx is finite.

The energy equations (6) and (9) are combined to eliminate the pressure term. Between sections (2) and (3), q is constant.

$$T_{el} - T_e = \frac{1}{2}\rho u^2 - \frac{1}{2}\rho v^2 + \Delta\rho g\ (y+h)$$

$$= \frac{1}{2}\ \rho\ (\frac{q}{y})^2 - \frac{1}{2}\rho\ (\frac{q_u}{D-y})^2 + \Delta\rho g\ (y+h)$$

The result is differentiated with respect to x, the distance downstream:

$$0 = -\frac{\rho_o q^2}{y^3}\ \frac{dy}{dx} - -\frac{\rho_o q_u^2}{(D-y)^3}(\frac{-dy}{dx}) + \Delta\rho g\ \frac{dy}{dx} + \Delta\rho g\ \frac{dh}{dx}$$

$$0 = \Delta\rho g\left[\frac{-dy}{dx}\cdot\frac{q^2}{(\frac{\Delta\rho}{\rho})\,g\,y^3} - \frac{q_u^2}{(\frac{\Delta\rho}{\rho})\,g\,(D-y)^3}\frac{dy}{dx} + \frac{dy}{dx} + \frac{dh}{dx}\right]$$

$$0 = \frac{dy}{dx}\left[1 - F^2 - \frac{q_u^2}{(\frac{\Delta\rho}{\rho})\,g\,(D-y)^3}\right] + \frac{dh}{dx} \qquad (17.1)$$

Now $$\frac{q_u^2}{(\frac{\Delta\rho}{\rho_o})\,g\,(D-y)^3} = \frac{v^2}{(\frac{\Delta\rho}{\rho_o})\,g\,(D-y)}$$

$$= \frac{v^2\ u\ y\ D}{u\ (\frac{\Delta\rho}{\rho_o})\,g\,y\,D\,(D-y)}$$

$$= \frac{v^2}{q_\Delta^{2/3}}\cdot\frac{u\,y}{q_\Delta^{1/3}D}\cdot\frac{D}{(D-y)}$$

$$= v_*^2\cdot q_*\cdot\frac{1}{(1-y/D)}$$

$$= v_*^2\, q_*\ \frac{1}{(1-q_*/F^{2/3})}\ ,\quad \text{since}\quad \frac{q_*}{F^{2/3}} = \frac{(\frac{u.y}{q_\Delta^{1/3}D})}{(\frac{u}{q_\Delta^{1/3}})} = \frac{y}{D}$$

$$= v_*^2\, q_*\ (\frac{F^{2/3}}{F^{2/3} - q_*})$$

and (17.1) becomes

$$0 = \frac{dy}{dx}\left[1 - F^2 - \frac{v_*^2\, q_*\, F^{2/3}}{F^{2/3} - q_*}\right] + \frac{dh}{dx} \qquad (17)$$

There is no entrainment between sections (2) and (3) and at section (3) $\frac{dh}{dx} = 0$ and $\frac{dy}{dx}$ is finite. Therefore,

$$F_3^2 + \frac{F_3^{2/3} v_{*3}^2 q_{*2}}{F_3^{2/3} - q_{*2}} - 1 = 0 \qquad (18)$$

There are now five non-linear simultaneous equations, (11, 12, 14, 15 and 18), in five unknowns, (v_{*2}, v_{*3}, q_{*2}, F_2, F_3), which may be solved for finite depths (D) on a computer (Chapter 5).

A simple case, however, is that when D is infinite. This solution may be calculated by hand giving the exact solution for infinite depth. It is worth noting at this stage that the case when D is infinite gives a reasonable approximation to the computer solution for D = 72.4 cms, for low values of v_* .

2.3 THE SOLUTION FOR INFINITE DEPTH

The solution obtained by Wilkinson and Wood (1971) was for the case where the total depth is very much larger than any other vertical dimension and the velocities in the ambient fluid tended to zero. The next most simple case is that D is very much larger than any other vertical dimension but the velocities in the upper layer are finite.

For this case $q_* = \frac{q}{q_\Delta^{1/3} D}$ tends to zero and, hence, the second term in equation (18) becomes small compared to unity giving

$$F_3^2 = 1 \tag{19}$$

The definition of the Froude Number and q_* give:

$$\frac{q_*}{F_2^{2/3}} = \frac{y_2}{D}$$

Equation 14 becomes:

$$v_{*2}\left[1 - \frac{y_2}{D}\right] = v_{*3}\left[1 - \frac{y_3}{D}\right]$$

Thus, when $y << D$,

$$v_{*2} = v_{*3} \tag{20}$$

The first terms on the right and left sides of (11) and (12) tend to zero, giving

$$v_{*1} = v_{*2} \tag{21}$$

Equation (13) can be simplified:

$$q_{21} = \frac{\frac{F_1^2 + \frac{1}{2}}{F_1^{4/3}} - v_*}{\frac{F_2^2 + \frac{1}{2}}{F_2^{4/3}} - v_*} \tag{22.1}$$

$$q_{21} = \frac{2F_1^2 + 1 - 2F_1^{4/3} v_*}{2F_2^2 + 1 - 2F_2^{4/3} v_*} \cdot \frac{F_2^{4/3}}{F_1^{4/3}} \qquad (22)$$

From (22.1), it is seen that the condition for no entrainment, ($q_{21} = 1$) and the jump is just flooded, Figure (2)), is independent of v_*

$$\frac{2F_1^2 + 1}{F_1^{4/3}} = \frac{2F_1^2 + 1}{F_2^{4/3}}$$

This equation is satisfied for $F_1 = F_2 = 1$, and, when this is not satisfied, it may be shown that the above reduces to the normal equation for an hydraulic jump:

$$\frac{2F_2^2 + 1}{2F_1^2 + 1} = \frac{F_2^{4/3}}{F_1^{4/3}} = \left(\frac{y_1}{y_2}\right)^2 \quad \text{since} \quad q_1 = q_2 = q_\Delta^{1/3} y F^{2/3}$$

$$\left(\frac{y_1}{y_2}\right)^2 \left(\frac{2F_1^2 + 1}{F_1^2}\right) = 2\left(\frac{y_1}{y_2}\right)^2 + \frac{1}{F_1^2}$$

$$\frac{1}{F_1^2}\left[\left(\frac{y_1}{y_2}\right)^2 - 1\right] = 2\left(\frac{y_1}{y_2}\right)^3 - 2\left(\frac{y_1}{y_2}\right)^2$$

$$\frac{1}{2F_1^2}\left(\frac{y_1}{y_2} + 1\right) = \left(\frac{y_1}{y_2}\right)^2$$

$$2F_1^2\left(\frac{y_1}{y_2}\right)^2 - \frac{y_1}{y_2} - 1 = 0$$

$$2F_1^2 - \left(\frac{y_2}{y_1}\right) - \left(\frac{y_2}{y_1}\right)^2 = 0$$

$$\frac{y_2}{y_1} = \frac{-1 \pm \sqrt{1 + 8F_1^2}}{2}$$

or

$$F_2 = \frac{F_1}{\left\{\frac{1}{2}\left[(8F_1^2 + 1)^{1/2} - 1\right]\right\}^{3/2}}$$

For given upstream values of F_1 and v_* it can be shown that maximum entrainment occurs when $F_2 = 1$ for all v_* :

$$q_{21} = \frac{k\, F_2^{4/3}}{2 F_2^2 + 1 - 2 v_{*1} F_2^{4/3}}$$

where $k = \left[2 F_1^2 + 1 - 2 v_{*1} F_1^{4/3}\right] / F_1^{4/3}$

$$\frac{d q_{21}}{d F_2} = 0 \; ; \; 0 = (2 F_2^2 + 1 - 2 F_2^{4/3} v_*) \cdot \frac{4}{3} F_2^{1/3} - F_2^{4/3} (4 F_2 - \frac{8}{3} F_2^{1/3} v_*)$$

$$(2 F_2^2 + 1 - 2 F_2^{4/3} v_*) \cdot \frac{4}{3} = F_2 (4 F_2 - \frac{8}{3} F_2^{1/3} v_*)$$

$$\frac{8}{3} F_2^2 + \frac{4}{3} - \frac{8}{3} F_2^{4/3} v_* = 4 F_2^2 - \frac{8}{3} F_2^{4/3} v_*$$

$$F_2^2 = \frac{1}{3} + \frac{2}{3} F_2^2$$

$$\therefore \quad F_2^2 = 1$$

Therefore q_{21} is maximum when $F_2 = 1$.

The theory for infinite depth shows that when $v_* = \dfrac{2 F_2^2 + 1}{2 F_2^{4/3}}$

then q_{21} will tend to an infinite value. However, in this case

$$y_2 = \frac{q_1}{q_\Delta^{1/3}} \frac{\left[2 F_1^2 + 1 - 2 v_* F_1^{4/3}\right]}{\left[2 F_2^2 + 1 - 2 v_* F_2^{4/3}\right]} \frac{F_2^{2/3}}{F_1^{4/3}}$$

also becomes infinite, and the requirement that D is very much greater than all other vertical dimensions is no longer satisfied and the solution breaks down.

The theory for the case of infinite depth implies that it should be possible to obtain large dilutions of the inflowing layer when

$$\left[\frac{2F_2^2 + 1}{2F_2^{4/3}} - v_* \right] \quad \text{is small} \qquad (23.1)$$

The minimum v_* required to make (23.1) equal to zero is $v_* = 1.5$. The theory for infinite depth however is not applicable for values of v_* as high as this. Therefore, the argument that large entrainments will occur when (23.1) is satisfied is not necessarily valid. Nevertheless, substantial increases in entrainment have been observed as v_* is increased.

Substituting (19) and (20) into (16) gives,

$$\frac{1}{F_2^{2/3}} \left[1 + \frac{F_2^2}{2} \left[1 - \frac{v_*^2}{F_2^{4/3}} \right] \right] = 1 + \frac{h}{y_1 F_1^{2/3} q_{21}} + \frac{1}{2} - \frac{v_*^2}{2}$$

and $$\frac{h}{y_1} = q_{21} F_1^{2/3} \left[\frac{1}{F_2^{2/3}} + \frac{F_2^{4/3}}{2} - \frac{3}{2} \right]$$

$$\frac{h}{y_1} = \frac{q_{21} F_1^{2/3}}{2 F_2^{2/3}} \left[2 + F_2^2 - 3 F_2^{2/3} \right] \qquad (24)$$

Substituting for q_{21} gives

$$\frac{h}{y_1} \quad \frac{2 F_1^{2/3}}{\left[2F_1^2 + 1 - 2F_1^{4/3} v_* \right]} = F_2^{2/3} \frac{\left[2 + F_2^2 - 3F_2^{2/3} \right]}{\left[2F_2^2 + 1 - 2F_2^{4/3} v_* \right]}$$

$$\text{ie} \quad \frac{hf}{y_1} = F_2^{2/3} \left[\frac{2 + F_2^2 - 3F_2^{2/3}}{2F_2^2 + 1 - 2F_2^{4/3} v_*} \right] \qquad (25)$$

$$\text{where} \quad f = \frac{2 F_1^{2/3}}{(2F_1^2 + 1 - 2F_1^{4/3} v_*)}$$

Equation 25 is plotted on Figure 11 and for given upstream and boundary conditions, $\left(F_1 , y_1 , h , v_* \right)$, the value

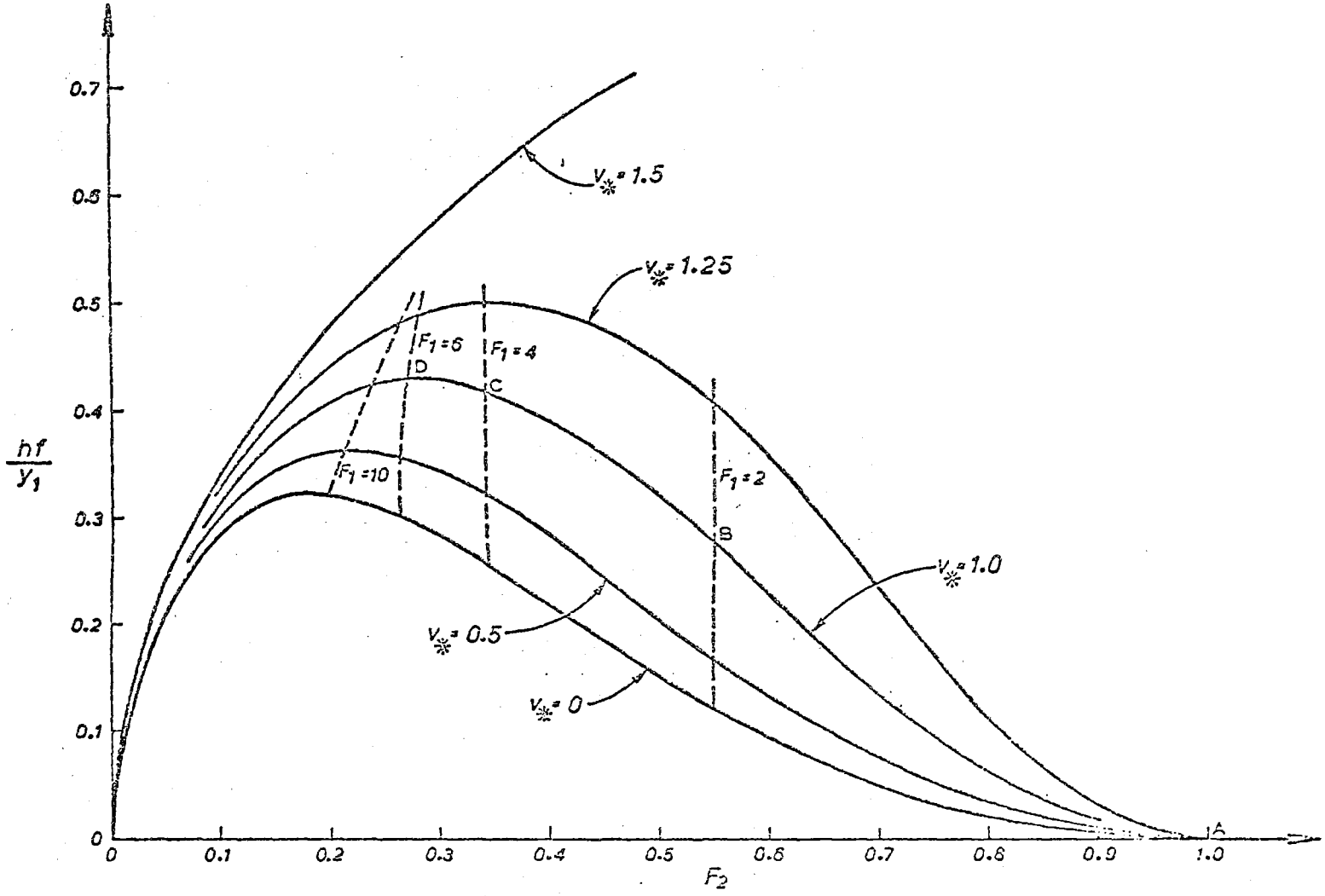

Fig. 11: PLOT OF WEIR HEIGHT AGAINST FROUDE NUMBER DOWNSTREAM OF A DENSITY JUMP FOR A RANGE OF VALUES OF DIMENSIONLESS VELOCITY IN THE AMBIENT FLUID.

– – – – Curves for incipient flooding. ——— Curve for constant V_*

$(\frac{hf}{y_1})$, and hence the value of F_2 can be obtained. Equations 22 and 23 then give the values of q_{21} and y_2, and the solution is complete.

It is now appropriate to discuss the behaviour of the jump using Figure 11. Firstly, when the weir height is zero in the absence of friction or any other control, the Froude number (F_2) is one or zero for all values of v_* less than 1.5. The case of a zero Froude number (F_2) implies no flow and is, therefore, not of interest. For the Froude number (F_2) of unity, the value of the discharge ratio is given by (22) with $F_2 = 1$,

$$q_{21} = \frac{\frac{2F_1^2 + 1}{F_1^{4/3}} - 2v_*}{3 - 2v_*}$$

and we note that with an increasing velocity (v_*) in the ambient fluid the amount of fluid entrained increases. However, when v_* approaches 1.5 the theory fails.

Consider a particular case with an upstream Froude Number of 7.55. When v_* is zero, $q_{21} = 2.14$, when v_* has the value of 1.0 then $q_{21} = 4.56$ (in both the computer result for a depth of 72.4 cms and the theory for the case of infinite depth). This dramatic increase in the amount of fluid entrained highlights the importance of velocities in the ambient fluid. It is again worth emphasising that when the weir height is zero and downstream Froude Number (F_2) equals 1.0 the entrainment is always maximum.

Consider now the case when $v_* = 1.0$ (curve ABCDO in Figure 11). As the weir is raised the value of $\frac{hf}{y_1}$ is increased, and the appropriate value of F_2 may be obtained.

The weir may be raised until the jump becomes flooded. At this stage there is no entrainment, $q_{21} = 1.0$ and equation (24) gives

$$\frac{hf}{y_1} = \frac{F_1^{2/3}\left[2 + F_2^2 - 3F_2^{2/3}\right] \cdot f}{2F_2^{2/3}} \qquad (26)$$

For a given F_1 and v_* the simultaneous solution of equations (25) and (26) give the point on the $\frac{hf}{y_1}$ graph at which the flooding of the jump commences. These solutions are the dashed lines on Figure 11. Thus, for an inflowing Froude Number of 2.0 and for v_* of 1.0, point B gives the value of $\frac{hf}{y_1}$ for incipient flooding. Point C is the solution for an inflowing Froude Number of 4.0. From this we note that the larger the inflowing Froude Number the further the weir may be raised without flooding. Also, from the curves of incipient flooding it can be seen that for a constant inflowing Froude Number and for all values of v_* less than 1.5 then the larger the value of v_* the higher the weir may be raised without flooding.

It is also important to note that for each value of v_* there is a maximum value of $\frac{hf}{y}$ which cannot be exceeded without flooding the jump. This corresponds to the maximum of the curves in Figure 11.

It can be shown that solutions of F_2 for values of $\frac{hf}{y_1}$ between the origin and the maximum are unstable to positive perturbations and need not be considered. An argument of this type may be found in Wilkinson and Wood (1971).

CHAPTER THREE

EXPERIMENTAL WORK

3.1 INTRODUCTION

In the analysis, the ambient fluid of density ρ_o and velocity v is the upper fluid in Figure 1. The incoming fluid of density $\rho_o + \Delta\rho$ and velocity u is the lower fluid.

This situation is reversed in the experimental work: the ambient fluid of density ρ_o and velocity v is the lower cold fluid, The incoming hot fluid of velocity u and density $\rho_o + \Delta\rho$ where $\Delta\rho$ is negative, becomes the upper fluid.

The theory applies equally to overflows (as in the experimental work) and underflows (as in the theory).

3.1.1 Definition of the Interfacial Depth y_2

Ellison and Turner (1959) defined the depth of their density currents as the mean of the depth of greatest velocity gradient and the depth of maximum density gradient. Wilkinson (1970) found these two depths to be equal and equal to the interfacial depth which he defined as the characteristic depth.

In the current series of experiments, large differences were observed between the visual interface, and maximum density and velocity gradients. It was decided to define the depth of interface as the mean of the three depths : the visual interface, and the depths of maximum density and velocity gradients.

3.1.2 Experimental Determination of the Downstream Froude No. F_2

The theoretical velocity profiles and density distribution at section (2) are assumed to be uniform. The experimental velocity profiles and density distributions are markedly non-uniform (see Figs. 17 and 18). It is necessary to take the non-uniformity in the density and velocity profiles into account when calculating the downstream Froude Number from experimental results by integrating from the boundary to the interface.

$$\text{Let} \quad \Delta_2 = \frac{\int_o^D u_2 (\Delta\rho/\rho)_2 \, g \, dy}{u_2 \, y_2} \tag{31}$$

$$\text{and} \quad \Delta_1 = (\Delta\rho/\rho)_1 \, g \, . \tag{32}$$

since the profile is uniform at section (1).

$$\text{Let} \quad k = \Delta_1/\Delta_2 \quad \text{and} \quad r = y_2/y_1 \tag{33}$$

$$\text{Then} \quad F_2 = \left(\frac{k}{r}\right)^{3/2} \cdot F_1 \tag{34}$$

The proof is as follows. The continuity equation is

$$q_\Delta = \int_o^D u \, (\Delta\rho/\rho) \, g \, dy = \text{const}$$

$$\text{and} \quad \Delta_2 = q_\Delta / u_2 \, y_2 \, ,$$

$$\Delta_1 = q_\Delta / u_1 \, y_1 = q_\Delta/q_1 \tag{35}$$

therefore,

$$k = q_2/q_1 = q_{21}$$

Now, from (35)

$$F_2^2 = \frac{u_2^3}{q_\Delta} = \frac{q_2^3}{q_\Delta \, y_2^3} = \frac{q_2^3}{q_1 \, \Delta_1 \, y_2^3}$$

and multiplying through by $\dfrac{y_1^3 \, q_1^2}{y_1^3 \, q_1^2}$ gives

$$F_2^2 = \frac{q_2^3 \, y_1^3 \, q_1^2}{q_1^3 \, y_2^3 \, \Delta_1 \, y_1^3}$$

$$\text{or} \qquad F_2^2 = \frac{k^3}{r^3} \cdot F_1^2 \qquad (34)$$

3.2 APPARATUS

Tank. The experiments were carried out at the University of Canterbury in the research tank located in the Department of Civil Engineering. The tank measured 4.57 m by 1.525 m, and was 1.1 m high. The glass sides of the tank were 1.27 cm thick. A constant head in the tank was maintained by using a 10 cm vertical pipe connected to waste at the bottom, and open at the top at the required head. To prevent the water level dropping below the required level, a 1.9 cm pipe was connected from the mains to the tank, and should empty into the tub. The tank was filled with mains supply water through a 7.6 cm pipe emptying into a tub in the bottom of the tank.

Covered Flume. A 3.66 m long covered flume was placed in the tank along one of the glass sides (Figures 12 and 13). The flume was 72.4 cm deep and 15.24 cm wide at the control sections. The cold water entry section was constructed with a 45 cm long inside wall in parabolic curvature, leading from a 15 cm diameter circular section to prevent separation at the entry and promote uniform flow in the flume. The base of the flume was 7.6 cm higher than the base of the tank, with a parabolic entry section. The outside wall and top of the flume were also shaped to prevent separation. The hot water inlet was located downstream of the cold water inlet, in the top of the flume. This section was 45 cm long, 6.35 mm deep and was constructed from 3.2 mm thick perspex with a gradual chamfer at section (1) where hot and cold waters meet. This perspex section was accurately located and held in place with narrow screws. An air trap (No.2) was located in this entry

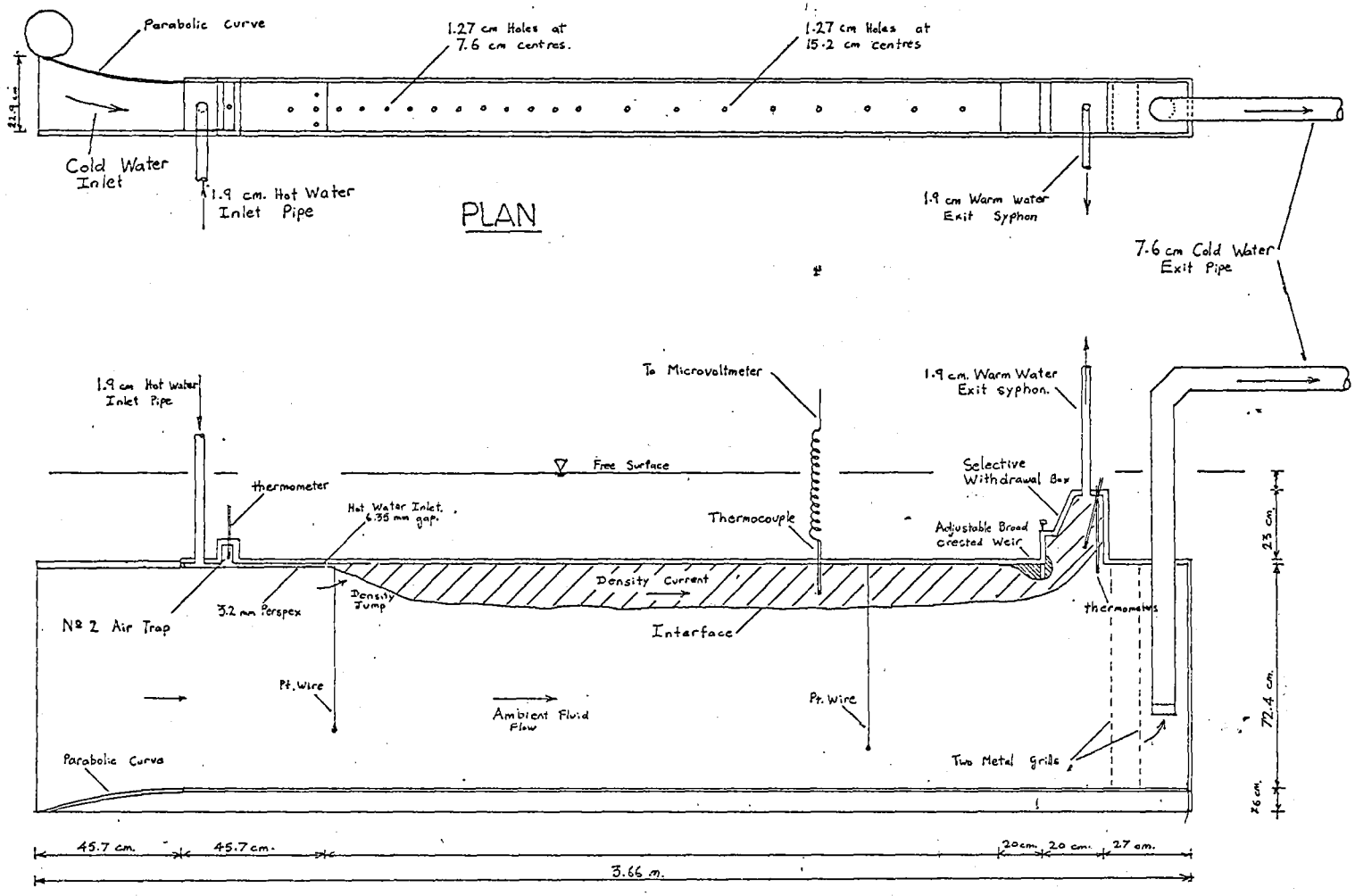

SIDE ELEVATION

END ELEVATION

FIGURE 12 : SCHEMATIC LAYOUT OF COVERED FLUME

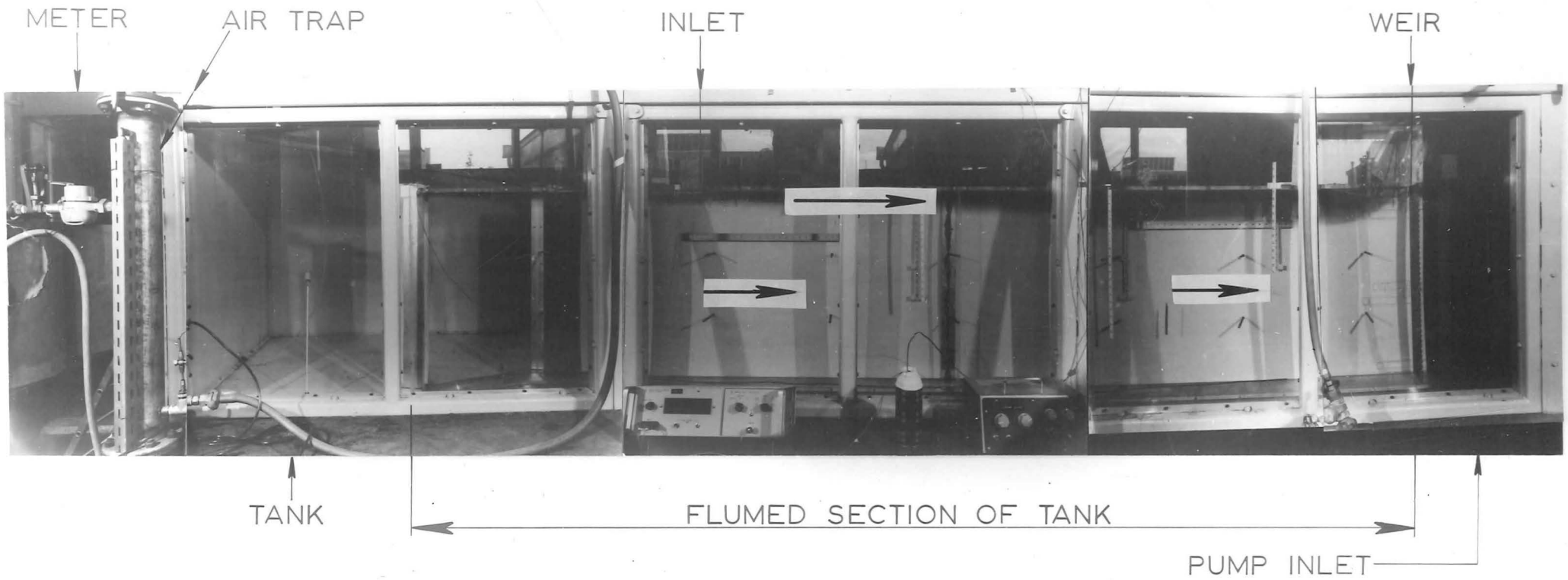

FIG. 13

-EXPERIMENTAL EQUIPMENT-

section (Fig. 12).

The sides of the flume were held together at regular intervals by 6.35 mm brass rods. Unfortunately these rods introduced Von Karmàn vortex streets which adversely affected the hydrogen bubble traces. (It is recommended that the top rod in the vicinity of section (2) be removed before further experiments are attempted.)

At intervals of at first 7.6 cms, then 15.2 cms, along the top of the covered flume, 1.27 cm holes were drilled and fitted with rubber bungs inserted until flush. The bungs could be removed to suck out air bubbles which formed in the top of the flume. The holes were also used for platinum wires, thermocouples, and hypodermic needles for injecting dye to observe entrainment.

Weir. An adjustable broad-crested weir was positioned near the far end of the top of the flume, with a vertical range of from 0 to 5 cms (Fig. 16).

Selective Withdrawal. Immediately behind the weir was a box in the roof of the flume leading to a pipe which acted as a syphon to facilitate the selective withdrawal of the warmer fluid only. The operator adjusted a valve on the syphon so that the interface between the warmer (dyed) layer and the cold layer came just inside the box (Fig. 14). Two thermometers were positioned in the box so that the position of the interface could be found if the dye was switched off.

The Cold Water System. Immediately behind the selective withdrawal box were two metal grills, the purpose of which was to enable cold water to be extracted from the flume without interrupting the uniform flow in the flume. Behind the grills, cold water was extracted through a 7.6 cm irrigation pipe

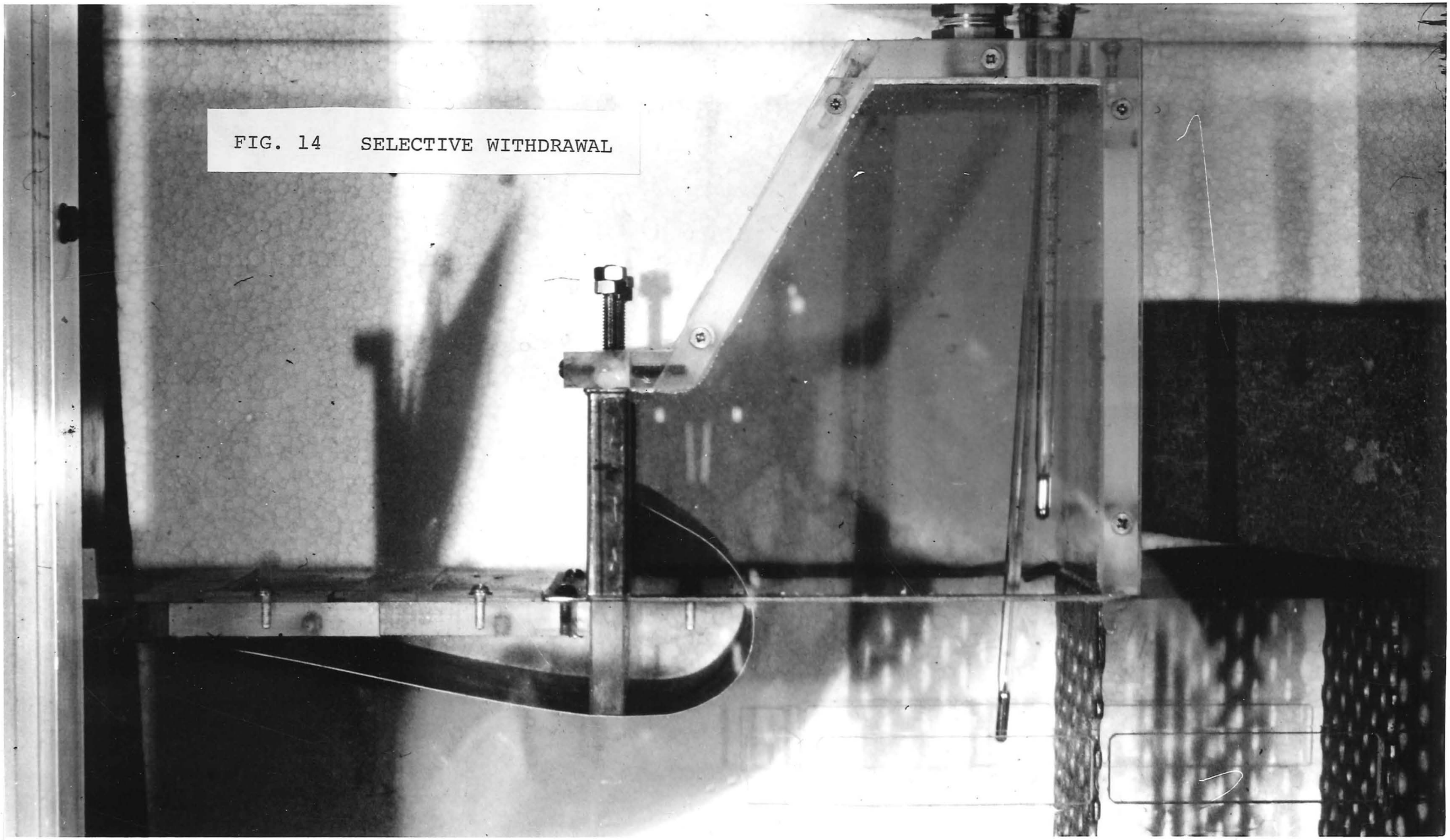

FIG. 14 SELECTIVE WITHDRAWAL

leading to the cold water pump with priming and bleeding valves. The pump was a Sigmund N-NA4(a) 3" pump of 35 ft head direct coupled with a Holroyd coupling to a Metropolitan Vickers 1420 rpm totally enclosed fan-cooled 3 Hp. electric induction motor. The pump proved to be too powerful for the experiments, making it difficult to control the 7.6 cm gate valve. It is recommended that a smaller $^{3}/_{4}$" self priming pump be installed. The 3" pump could still be used for very high flows (v = 4 cm/s) and to mix the water in the tank. A 1.9 cm pipe connected to the priming valve and the mains was used to prime the pump. A 7.6 cm irrigation pipe carried the cold water from the gate valve into a tub in the bottom of the tank. This tub (1m x 60 cm x 55 cm) was used to minimise turbulence in the tank.

The Hot Water System. Hot water passed through 1.9 cm plastic and rubber pipes, through a gate valve, flow meter, air trap (No.1), dye injection nozzle, another gate valve, another air trap (No.2), to the hot water inlet section of the covered flume. Hot water was supplied by two 182 litre cylinders with 2000 watt water heaters. These water heaters were only just adequate for the experiments run, and could only provide water at a constant temperature for about twenty five to thirty minutes (depending on the temperature of the hot water required). It is recommended that the heating capacity be increased so that experiments lasting several hours could be carried out. The flow of hot water was measured using a Kent "M2" type uniform meter with rotary positive piston, which was claimed by the makers to be extremely sensitive on all flows, and free from distortions caused by unequal expansion when measuring hot flows. An experiment

(Appendix E) indicated that the flow meter was accurate to within 1% for the range of flows considered.

Air Traps. The hot water supply contained an unusually large amount of dissolved air, and bubbles formed at the inlet section, under the top of the covered flume, and around thermocouple junctions. To overcome this problem two air traps were built. The first air trap was constructed from a 1 m length of 12 cm diameter vertical pipe, as in Fig. 13. Hot water entered near the top and flowed out near the bottom. At the very top was a bleeding hose with a surgical clip, to release air and facilitate draining. The second air trap was mounted in the hot water inlet section of the covered flume. It measured 15 cm by 5 cm by 5 cm high, with a rubber plug in the top, to release air. A thermometer was fitted to measure the temperature of the incoming hot water after an attempt to use a thermocouple in the inlet reach failed when it became coated with air bubbles.

Dye System. The incoming hot water was dyed so that

(a) the depth of the interface could be measured, and

(b) the interface could be observed so that the warmer layer only could be selectively withdrawn. The dye system was turned off for photographs of hydrogen bubble traces as the dye had the effect of reducing the amount of light. A 15 litre flask was mounted above the hot water cylinders to provide sufficient head for the solution of red food colouring to travel through 0.64 cm plastic pipe, surgical clip, and dye injection nozzle and valve into the hot water pipe.

3.3 VELOCITY DETERMINATION

The "hydrogen bubble technique" of flow visualisation

makes use of tiny hydrogen bubbles as flow tracers. The bubbles are generated by electrolysis at a fine non-reactive wire (usually platinum) stretched across the flow. A direct current is pulsed onto the wire cathode and a sheath of hydrogen forms around the wire. Surface tension causes immediate collapse of the sheath into tiny hydrogen bubbles which are swept away by the moving fluid. If the bubbles are suitably illuminated, and the period of pulsing is known, then the velocity profiles may be calculated from still photographs of the lines of bubbles after they have left the wire. Hydrogen bubble technique is very good for obtaining qualitative velocity distributions because these can be observed directly. Quantitative measurements, however, are another matter. The time required to obtain meaningul data from hydrogen bubble photographs is the major disadvantage of the technique. Also the method is not suitable for unsteady flows. The bubbles follow pathlines and unless the flow is steady significant errors can be introduced if the pathlines are interpreted as streamlines. An obvious source of error in velocity measurement using hydrogen bubble technique is caused by the rising of the bubbles. It is desirable therefore to have bubbles of the minimum possible size.

A hydrogen bubble generator was constructed in the Department to give short pulses of electricity of between 36 and 130 volts. It was found that a potential of 60 - 70 volts and a cycle length of 0.4 seconds gave reasonable results. The anode was a piece of thin copper tubing set in the bottom of the flume. The cathode was a 0.061 mm diameter platinum wire hung through the top of the flume and weighted by an electrically insulated lead sinker. (Fig. 15). A black screen was placed behind the inside wall of the flume as a background

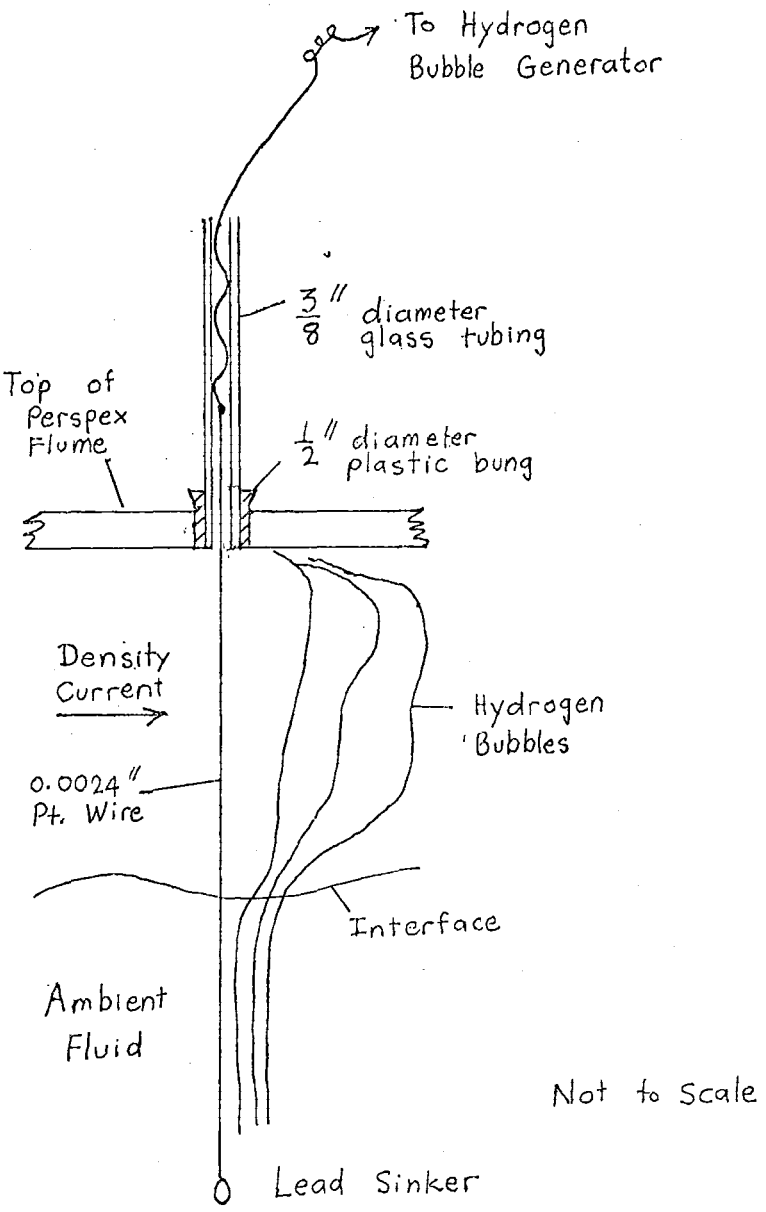

HYDROGEN BUBBLE APPARATUS

FIGURE 15

for the bubble traces. Illumination was provided by an electronic flash, synchronized with the camera shutter, directed down through the top of the flume so that the bubbles were illuminated from above. This avoided reflections which might have caused glare spots above on the photographs.

An electrolyte, 0.05 g/litre sodium carbonate solution was used, although sodium sulphate would perhaps have been better.

3.4 PHOTOGRAPHIC TECHNIQUE

The hydrogen bubble traces were photographed with an Asahi Pentax camera mounted 1.52 metres from the platinum wire, with a 135 mm telephoto lens, to reduce the divergence of light rays. [A reduction factor of 5% was still required when measuring the distance between traces because the ruler which appears in the photographs (for the scale) was 8.3 cm behind the platinum wire. This correction factor was verified by photographing two rulers, 8.3 cms either side of the platinum wire, and halving the difference in scales of the two rulers.]

The shutter speed was 1/60 second in order to fix the movement of the bubbles. With a lens aperture of F8, a reasonable depth of field was obtained which was necessary as the operation was carried out in a confined area.

35 mm high contrast line film (Agfa Ortho 25) was used. An electronic flashlight was held vertically above the hydrogen wire, with a screen placed to prevent light from the flash shining directly into the camera.

The black and white film was processed in high contrast line developer. 10" x 8" prints were produced on document copying

paper in order to preserve the high contrast which is necessary to produce a clear image of the hydrogen bubbles.

Considerable control ("burning in" and "holding back") was exercised in the printing process to bring out the ruler, hydrogen bubble traces, and the top of the tank (Datum for measurements).

Colour photographs were taken with a 35 mm wide angle lens, with an aperture of F16 and $^{1}/_{30}$ second shutter speed. Colour slides were made on Agfa chrome 50s film. Light was provided by four quartz iodine lamps producing a total output of 4000 watts.

3.5 DENSITY DETERMINATION

A 30 cm long adjustable calibrated thermocouple was mounted in the top of the covered flume at section (2) so that it could be raised and lowered as required. The cold junction was placed in a thermos flask packed with melting ice. The induced emf was displayed on a Hewlett Packard 3440 A Digital Microvoltmeter, which was claimed to have an accuracy of 0.1%. The variable sample rate was set at 5 samples per second. The temperatures corresponding to the voltmeter readings were read off a calibration curve, and the density of water at that temperature obtained from a table in the Handbook of Chemistry and Physics.

More accurate readings of the density differences may have been obtained if the cold junction of the thermocouple was placed next to the thermometer in the ambient fluid zone.

3.6 PROCEDURE

To ensure that all the necessary readings were taken

it was decided to adopt a standard procedure in the laboratory. Preliminary work is listed below. The hot water thermostats were set to the required temperature and heaters switched on. The tank was filled, electrolyte added, and the constant head apparatus checked. The microvoltmeter was zeroed and ice prepared for the cold junction. The cold water pump was primed and gate valve set for the required velocity of ambient fluid. The selective withdrawal syphon was checked. The hydrogen bubble generator and platinum wires were checked. It was found that if the generator is left on for 5 minutes prior to an experiment the platinum wire would release better bubble traces than when first switched on. The dye bottle was filled, air bubbles removed from the top of the flume, and the weir set at the required height. The first air trap was emptied of water. The photographic equipment was set in the required location and curtains, screens and lighting arranged.

Two alternate methods were used to determine the velocity of the ambient fluid. One was to photograph hydrogen bubbles released from a platinum wire at section (1) before the hot water is switched on. The second method was to mount the camera sideways at section (2) and photograph a deep enough field of view to be able to observe both the warm layer above and ambient fluid below the interface. Wherever possible, both methods were used and the results averaged.

The procedure adopted for a typical experiment is listed below. The cold water pump, syphon, and constant head system were all turned on. When the fluid became steady, the hydrogen bubbles at section (1) were photographed. The camera was then shifted to section (2), mounted sideways

and focused. The water was run to waste until the pipe warmed, then the first air trap was filled and the hot water pipe connected to the top of the covered flume in such a way that there were no sharp bends in the pipe. Dye was switched on. It was necessary to leave the system running for ten minutes to 1/4 hour before taking any readings. This ensures a steady state had been achieved. During this time the syphon was adjusted so that only the warm layer was withdrawn. The flow meter, ambient temperature and hot water thermometer were read. Air was released from the air traps whenever practicable. When conditions had become completely stable with the syphon only withdrawing the warm layer, the mean observed depth of the interface at section (2) was noted and the dye tap was turned off in preparation for the photographs of hydrogen bubble traces. Two themometers in the selective withdrawal box indicated the position of the interface and allowed one to check the withdrawal every couple of minutes when the dye was switched off.

A profile of temperature against depth at section (2) was taken. Five photographs of hydrogen bubble traces were taken at section (2). The dye was switched on again. A second profile of temperature against depth at section (2) was taken. The selective withdrawal system was again checked, and the mean observed position of the interface at section (2) again noted. The temperatures of the ambient and hot fluids were again noted and the flow meter checked.

An example of the calculations performed with each experiment may be found in Appendix A.

CHAPTER FOUR

LABORATORY RESULTS AND DISCUSSION

4.1 VELOCITY PROFILES

Figure 16(a) shows a typical hydrogen bubble trace taken at section (1) in a moving ambient fluid. Figures 16(b), (c) and (d) show typical bubble traces taken at section (2) with both layers moving. Note that the velocity in the ambient fluid is fairly uniform. Note also that in Fig. 16(d) the ambient velocity was greater than u_2. The theory for Experiment 25 predicted flooding.

Figure 17 shows four typical velocity profiles at section (2) in a moving ambient fluid. Note the marked non-uniformity of the profiles. The velocity profiles do not appear to become more nor less non-uniform as the ambient velocity is increased.

Once established, the velocity profiles remain fairly constant over the channel width. The density gradient within the moving layer inhibits turbulent diffusion in the y-direction. Therefore, velocity distributions, once established at the jump, tend to be self preserving or to change only very slowly. Density jumps represent discontinuity of flow energy. Energy is dissipated by turbulent shear forces at the jump and it is these turbulent eddies which determine the form of the downstream velocity distribution.

4.2 DENSITY DISTRIBUTIONS

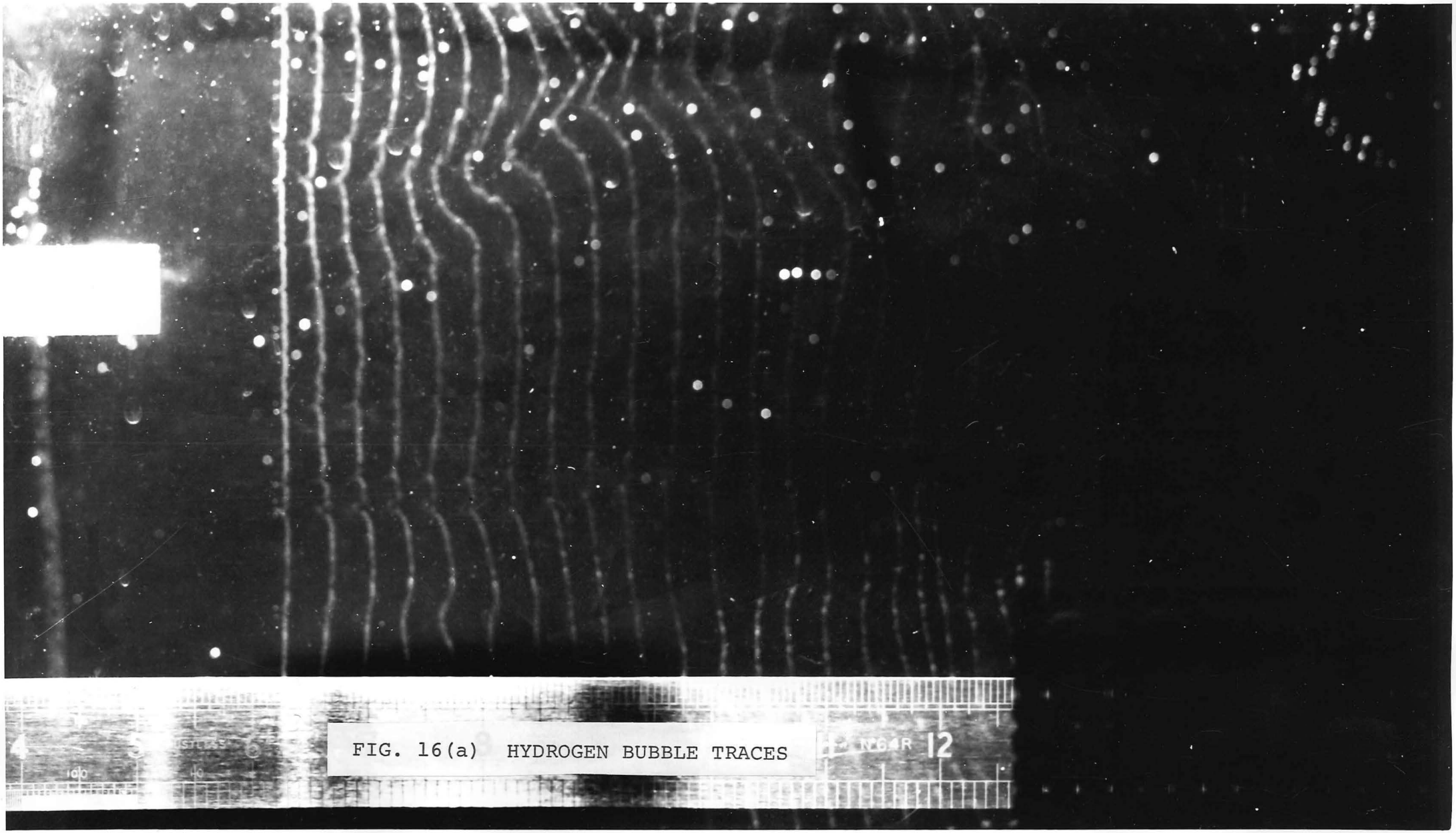

FIG. 16(a) HYDROGEN BUBBLE TRACES

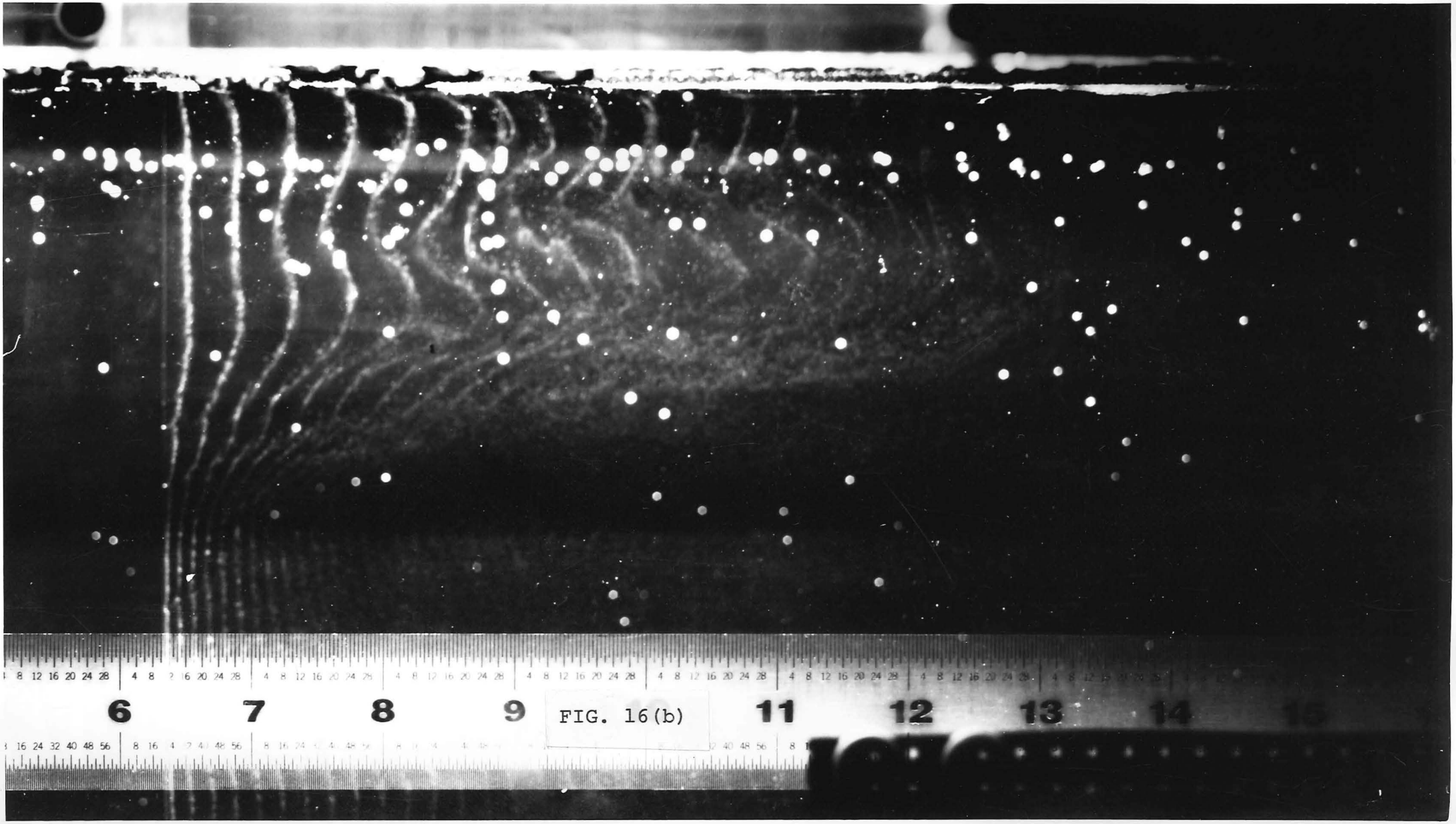

FIG. 16(b)

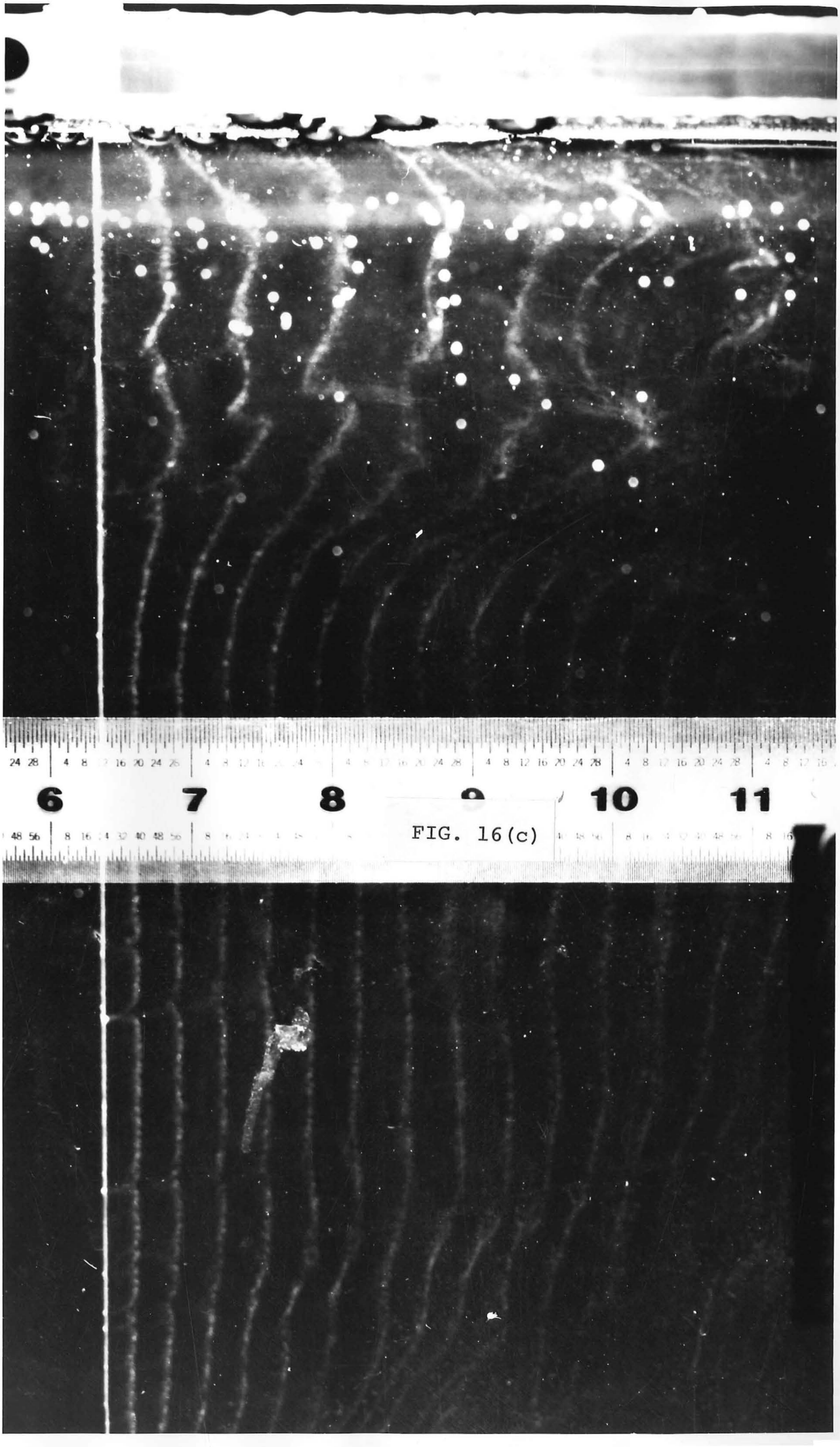

FIG. 16(c)

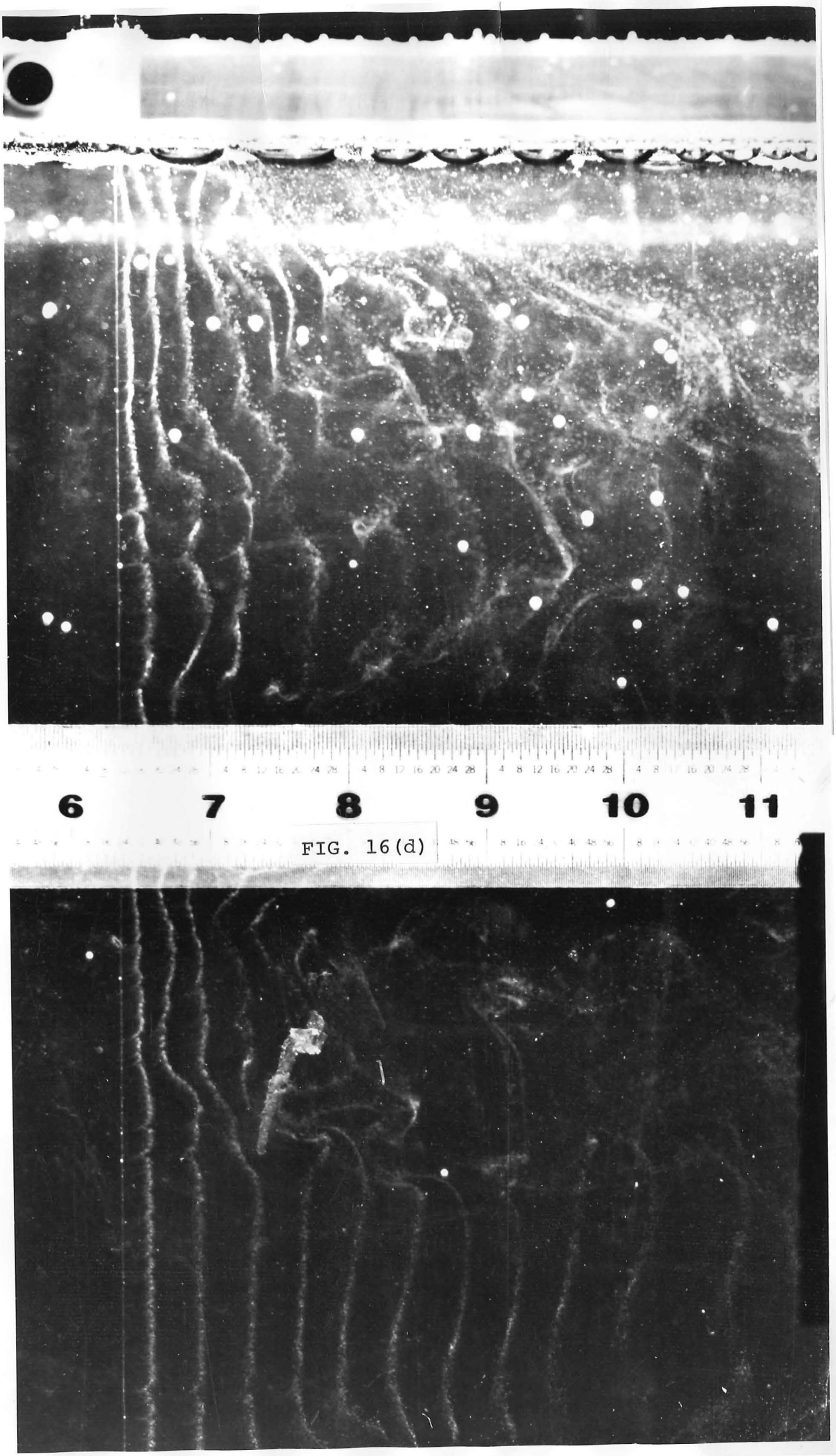

FIG. 16(d)

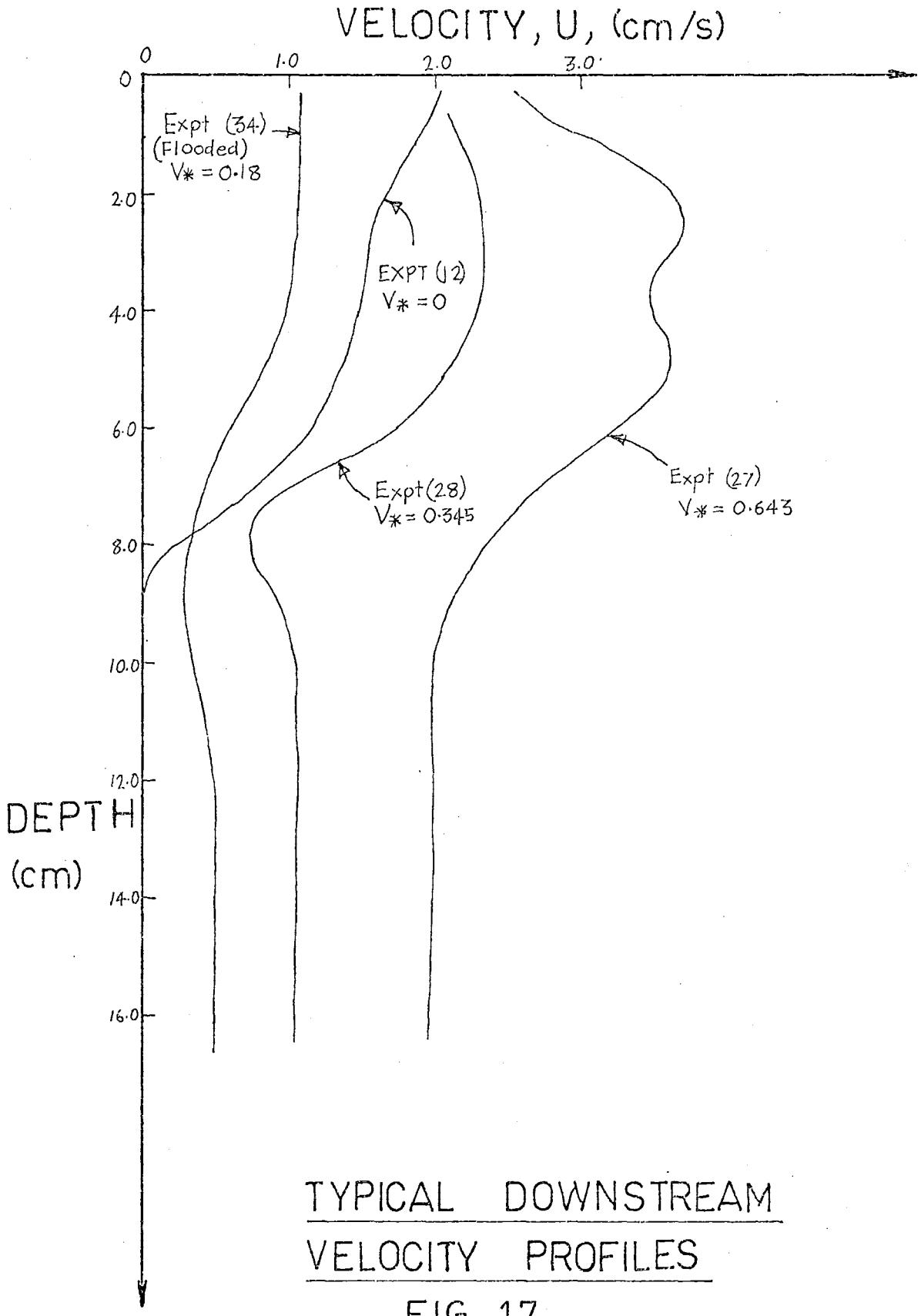

TYPICAL DOWNSTREAM VELOCITY PROFILES

FIG 17.

Figure 18 shows two typical density distributions downstream of a density jump. The density distribution in stationary ambient fluid has a rectangular, uniform profile. The density distribution in a fast moving ambient flow (v = 1.06 cm/s) had a marked triangular non-uniform profile.

The density distribution in a density current, downstream of a density jump, is seldom uniform. This non uniformity is a result of incomplete mixing of the density current and the ambient fluid. Uniformity is dependent on the extent of turbulent mixing in the jump after entrainment has occurred. If the roller region occupies most of the density jump, entrained ambient fluid is thoroughly mixed with the inflowing fluid in the roller region of the jump and the resulting density distribution approaches uniformity. Wilkinson (1970) reported that for zero ambient velocities, density jumps, with low downstream Froude numbers had uniform downstream density distributions; but that in the maximum entraining jump the resulting density distributions were markedly non-uniform.

4.3 THE EFFECT OF NON-UNIFORM VELOCITY PROFILES AND DENSITY DISTRIBUTIONS

It should be noted that the theory is based on the assumption that the velocity profiles and density distributions are uniform in the flowing layer. Wilkinson (1970) found that for the case of stationary ambient flow, the experimental data fitted closely to the curve of hf/y_1 against F_2 (Fig. 8), indicating that the various integral

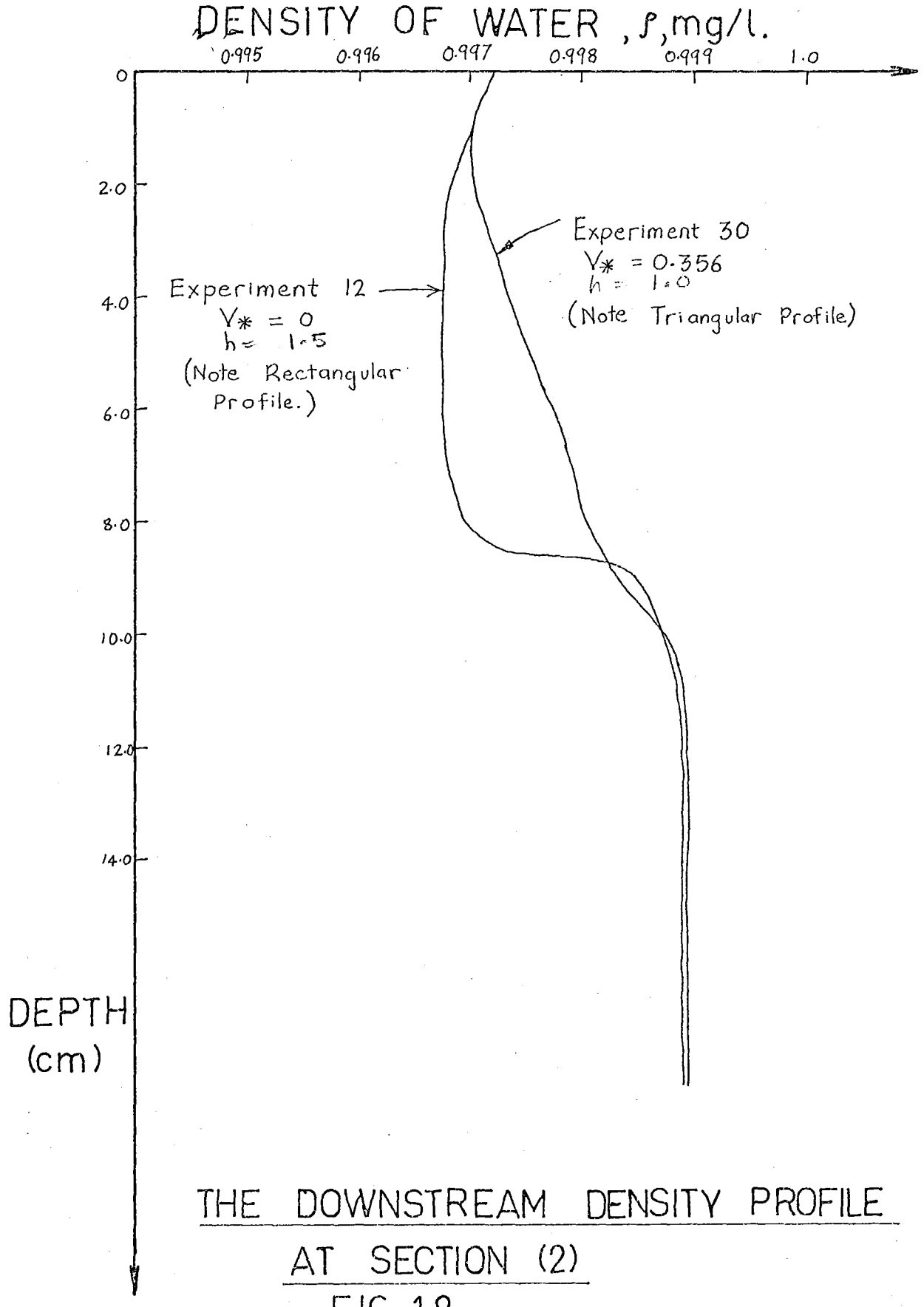

THE DOWNSTREAM DENSITY PROFILE AT SECTION (2)

FIG 18

factors compensate. It could be that for the case of moving ambient fluid, the density and velocity profiles are non-uniform to such an extent that the various integral factors may not compensate.

Wilkinson reported that both the velocity profiles and density distributions downstream of a density jump which had a constant upstream state became more non-uniform as the downstream Froude number increased in value; that is, as the height of the control weir decreased and entrainment increased. It would have been expected that an increase in the velocity of the ambient fluid, and corresponding increase in entrainment, leads to increased non-uniformity of the velocity profiles and density distributions. In fact, only the density distributions appeared to become more non-uniform as v_* increased; the velocity profiles remaining markedly non uniform irrespective of changes in v_* .

One effect of non-uniform velocity profiles and density distributions is that it is difficult to judge the depth of the interface. Large differences of two or three centimetres were found between the different y_2's: the depth of maximum change of density with depth; the depth of maximum change of velocity with depth; and the visual depth of the interface. No significant relationship was found between the three expressions for the depth except that the depth of maximum velocity gradient was less than the visual depth of interface in most cases.

The difficulty in determination of the depth of interface could be one explanation for the large differences in experimental and theoretical Froude Numbers and q_{21}'s,

particularly in experiments with high ambient velocities.

4.4 COMPARISON OF EXPERIMENT RESULTS AND THEORY

A typical reduction of test data for a single experiment may be found in Appendix A. Appendix B is an error analysis of a typical experiment. Note how small initial errors (1 and 2%) rapidly accumulate giving a 7% error in the theoretical value of F_2, but a 50% error in the experimental value of F_2; a 28% error in the theoretical q_{21}, and a 17% error in the experimental q_{21}. This indicates the necessity of obtaining experimental results of great accuracy. Recommended modifications in experimental technique are listed in Chapter 6, and recommended modifications to the laboratory equipment are listed in the appendix. Despite the large experimental error, all but one of the F_2 experimental results (excluding flooded jumps) were within 25% of the theoretical results for F_2. If experiments in which flooding occurred, $v_* > 0.5$, or $H < 0.5$ cms are excluded, all experimental F_2 results are within 15% of the theoretical F_2 results.

Also, all but two of the q_{21} experimental results (excluding flooded jumps) were within 50% of the theoretical q_{21} results. If those experiments in which jumps were flooded, $v_* > 0.5$ or $H < 0.5$ cms are excluded, all but two of the experimental q_{21} results are within 25% of the theoretical q_{21}'s.

Appendix C shows the results of all the experiments. For known upstream conditions and weir heights (Table 3), the predicted downstream conditions (Table 4 assuming infinite depth; Table 5 the computer results for D = 72.4)

may be compared with the downstream results obtained in the laboratory. (Table 6).

The values of v_* , the dimensionless ambient velocities,are plotted on a graph of weir height and a function of upstream conditions (hf/y_1) against the downstream Froude Number F_2 (Figure 19). It can be seen from this graph and the tables of results that agreement between experiments and theory ranged from satisfactory to poor. The experimental values of F_2 in experiments with very low weir heights was considerably lower than the theoretical values. This may be due to friction at the solid boundary acting as a downstream control. (See Section 4.5).

The experimental values of F_2 were plotted against the theoretical values of F_2 in Figure 20. There is a large scatter. The experimental value of entrainments, q_{21}, were plotted against the theoretical values in Figure 22. There is also a large scatter indicating a large experimental error.

The agreement between theory and experiment appeared to be slightly more satisfactory for low values of ambient velocity so the graphs were drawn again. Figure 21 shows experimental F_2's plotted against theoretical F_2's for only those experiments in which v_* was less than 0.5. Agreement between Theory and Experiment is now slightly more satisfactory. The results obtained by Wilkinson (1970) may be found in Table 7, Appendix D, and these were plotted on Figure 21 also. Figure 23 shows experimental q_{21}'s plotted against theoretical q_{21}'s for only those experiments in which $v_* < 0.5$. Agreement is a little more satisfactory. Wilkinson's results were also plotted, but

his experimental q_{21}'s were a lot lower than his theoretical q_{21}'s .

The effect of a moving ambient fluid, it has been shown theoretically, is to increase the entrainment. This is illustrated dramatically on Figure 24. Figure 24(a) shows the hf/y_1 plotted against the theoretical q_{21}'s; the numbers on the graph being the values of v_* . Figure 24(b) shows hf/y_1 plotted against the experimental q_{21}'s. Note the increase in q_{21} as v_* increases.

4.5 THE EFFECT OF BOUNDARY FRICTION

For weir heights of 0.5 cm and less the F_2's were a lot lower than predicted by theory and this is thought to be the result of friction at the solid boundary, the presence of which is thought to act as a control in the same way as the weir. That is, for small weir heights, the bed friction can be considered to act as an effective weir. As the weir height increases, the control switches from bed friction to the weir. Boundary friction was not included in the analysis, (a) because its neglect is a good approximation to density jumps at a free surface, and (b) the analysis would be difficult if friction was included.

Reynolds numbers in the density current at section (2) were of the order of 2000. Measured velocity distributions showed that this flow was turbulent, with a laminar boundary layer at the solid boundary. The ratio of interfacial shear to channel bed shear obtained by Wilkinson was of the order of 8% and is therefore neglected in the following derivation of an expression for the friction factor, f* .

If the boundary layer at the channel bottom and

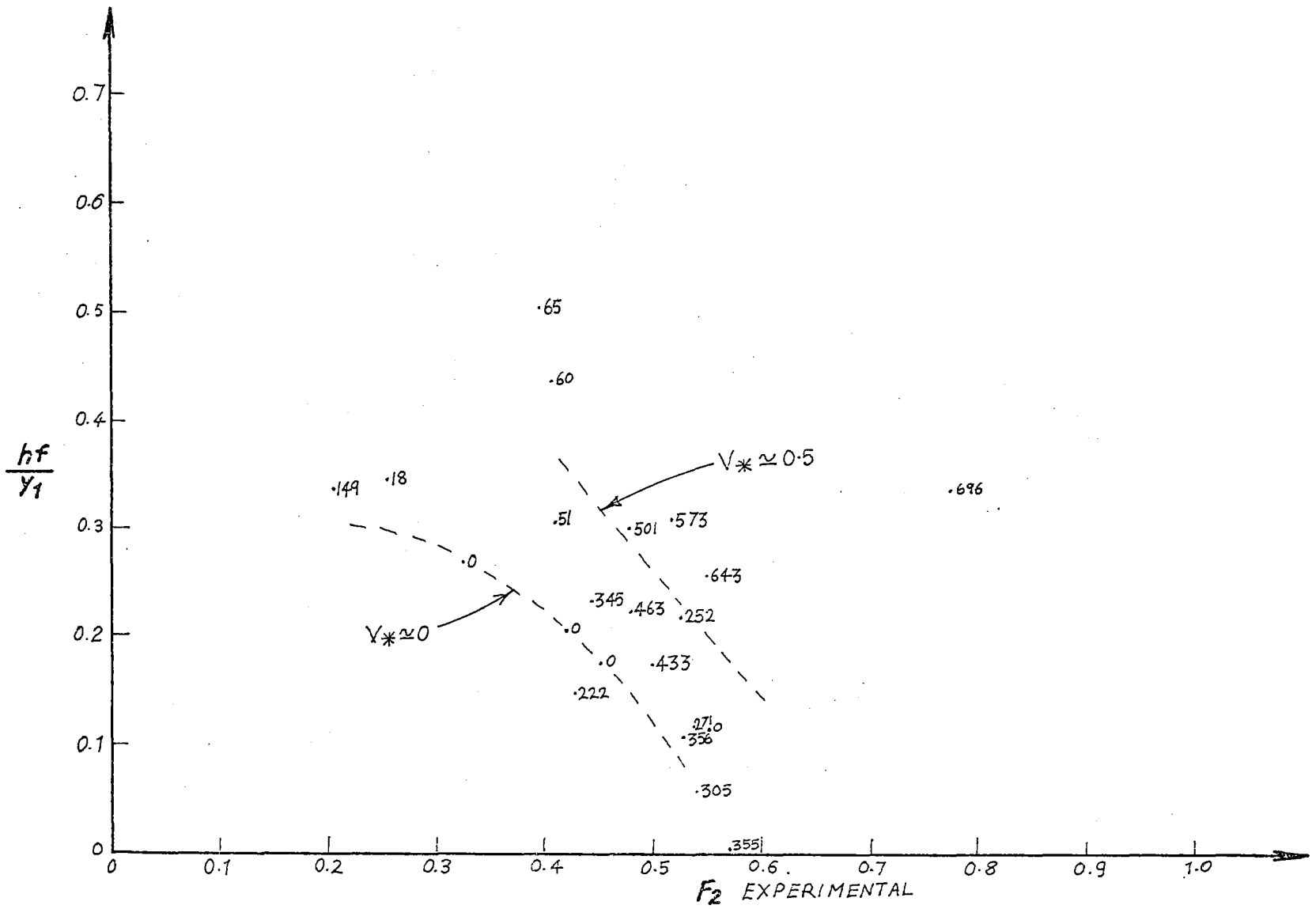

EXPERIMENT RESULTS; VALUES OF V_* PLOTTED

FIG 19

FIG 20

FROUDE NUMBERS ⊕:

EXPERIMENT AND THEORY

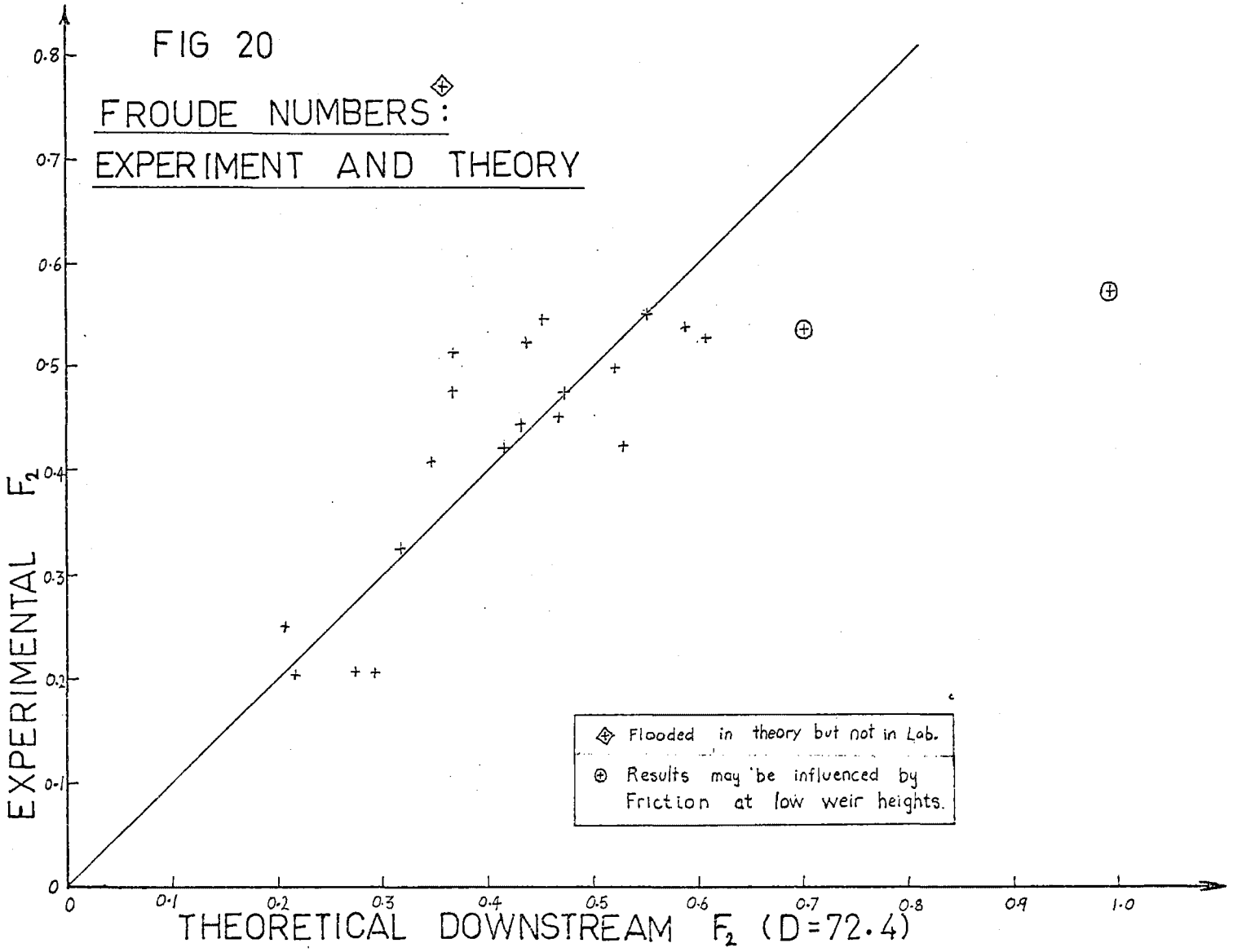

FIG 21

FROUDE NUMBERS,
EXPERIMENT & THEORY

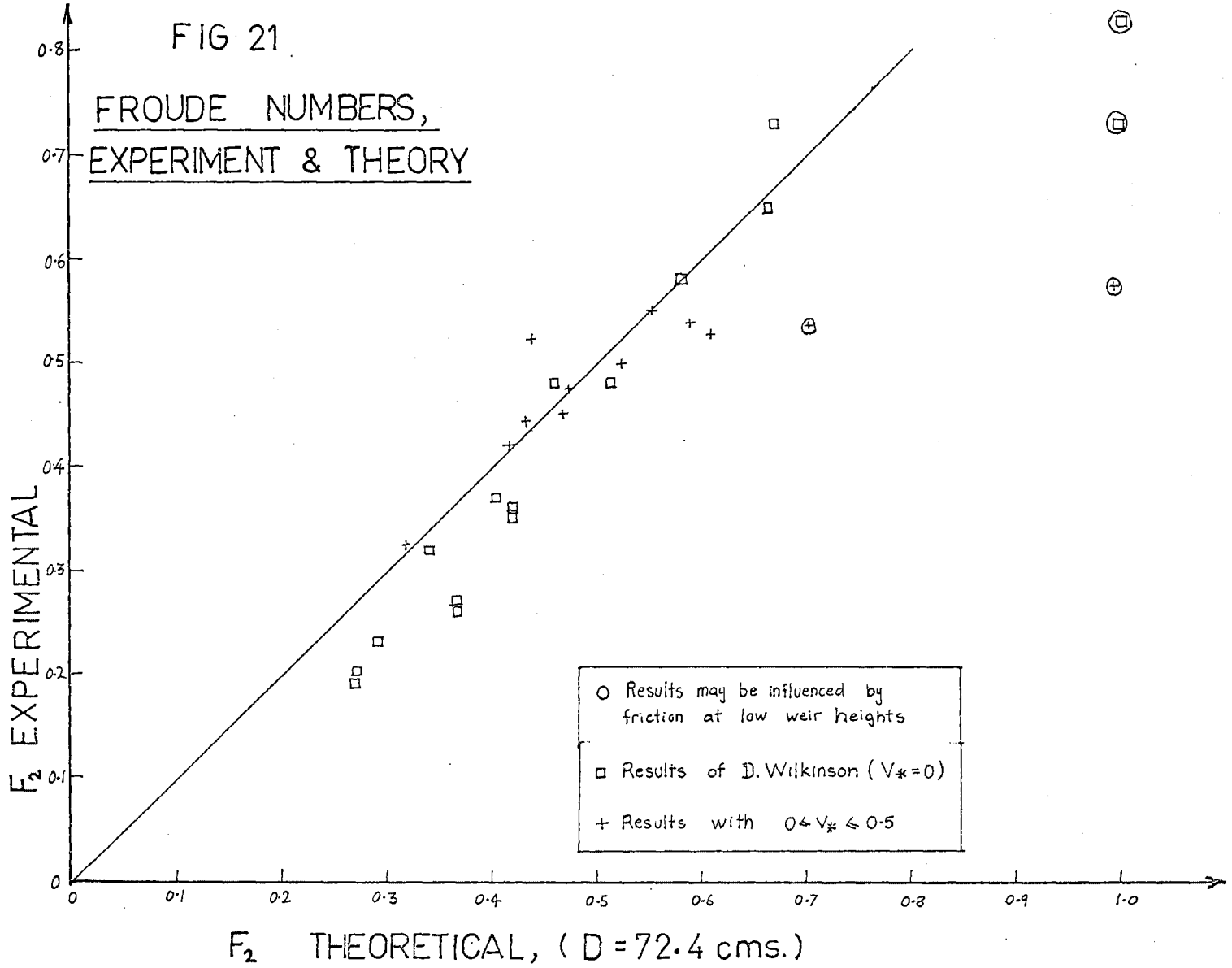

ENTRAINMENT, EXPERIMENT AND THEORY.

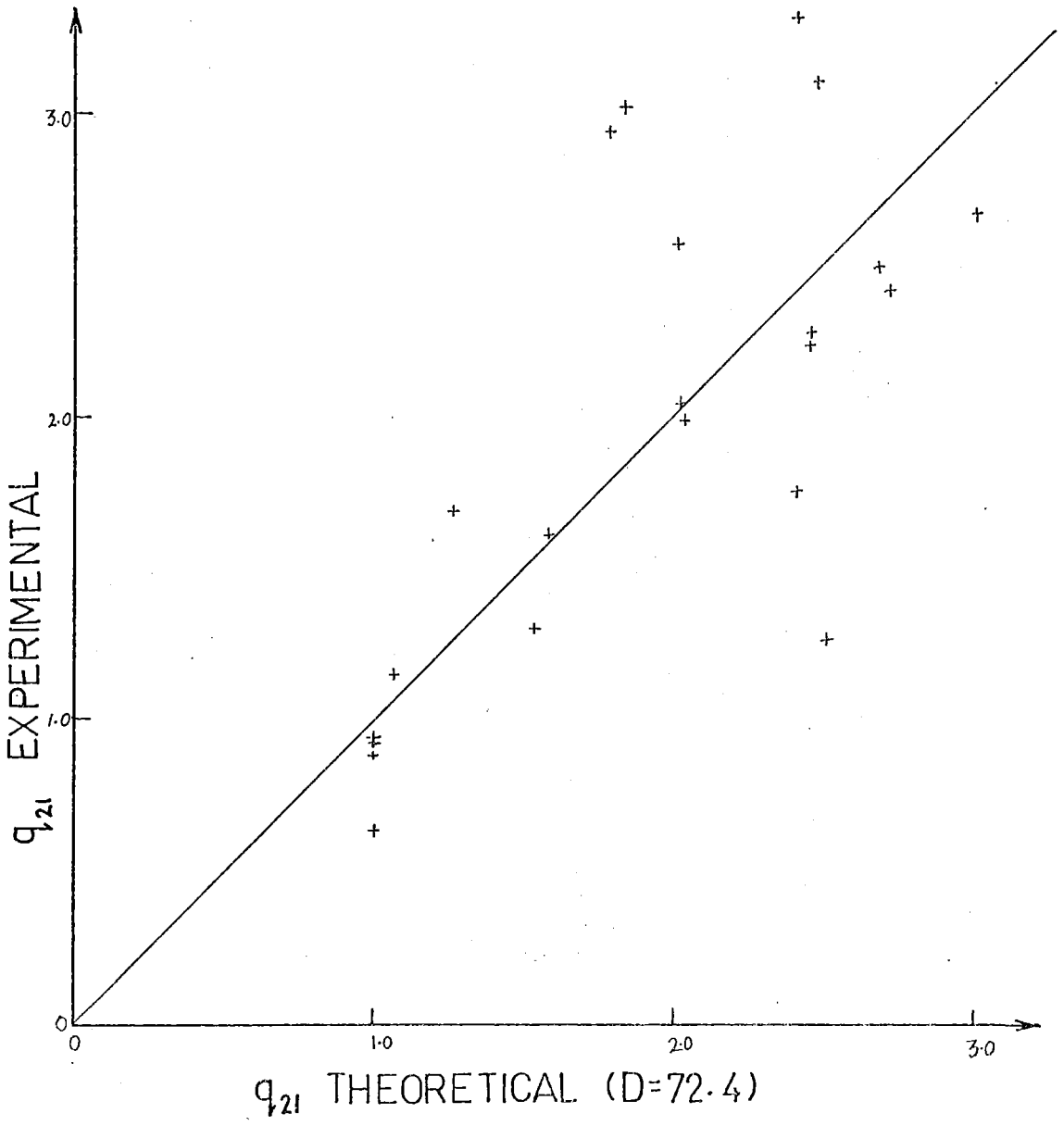

FIG 22

ENTRAINMENT, EXPERIMENT AND THEORY

$0 \leq V_* \leq 0.5$

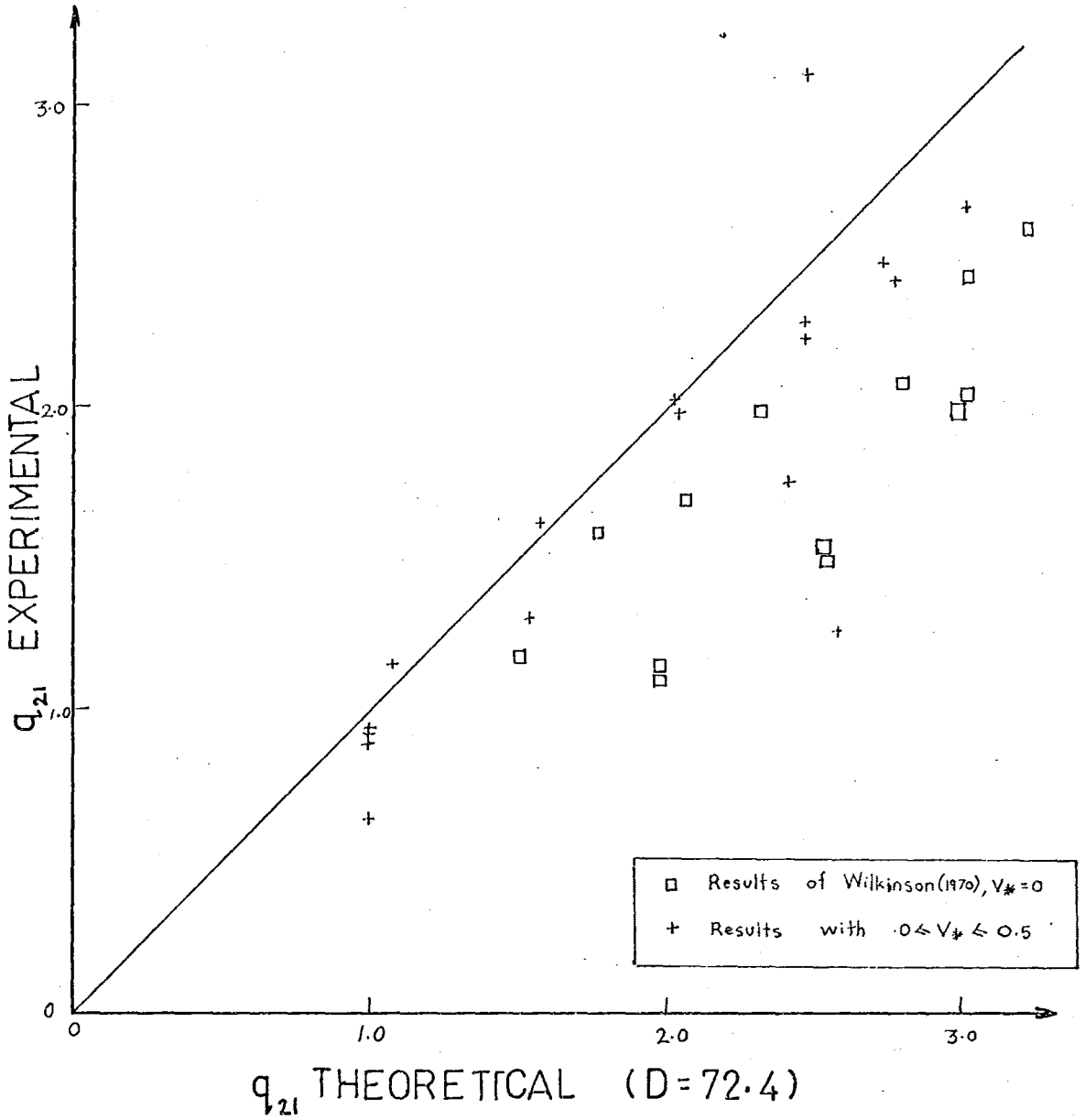

FIG 23

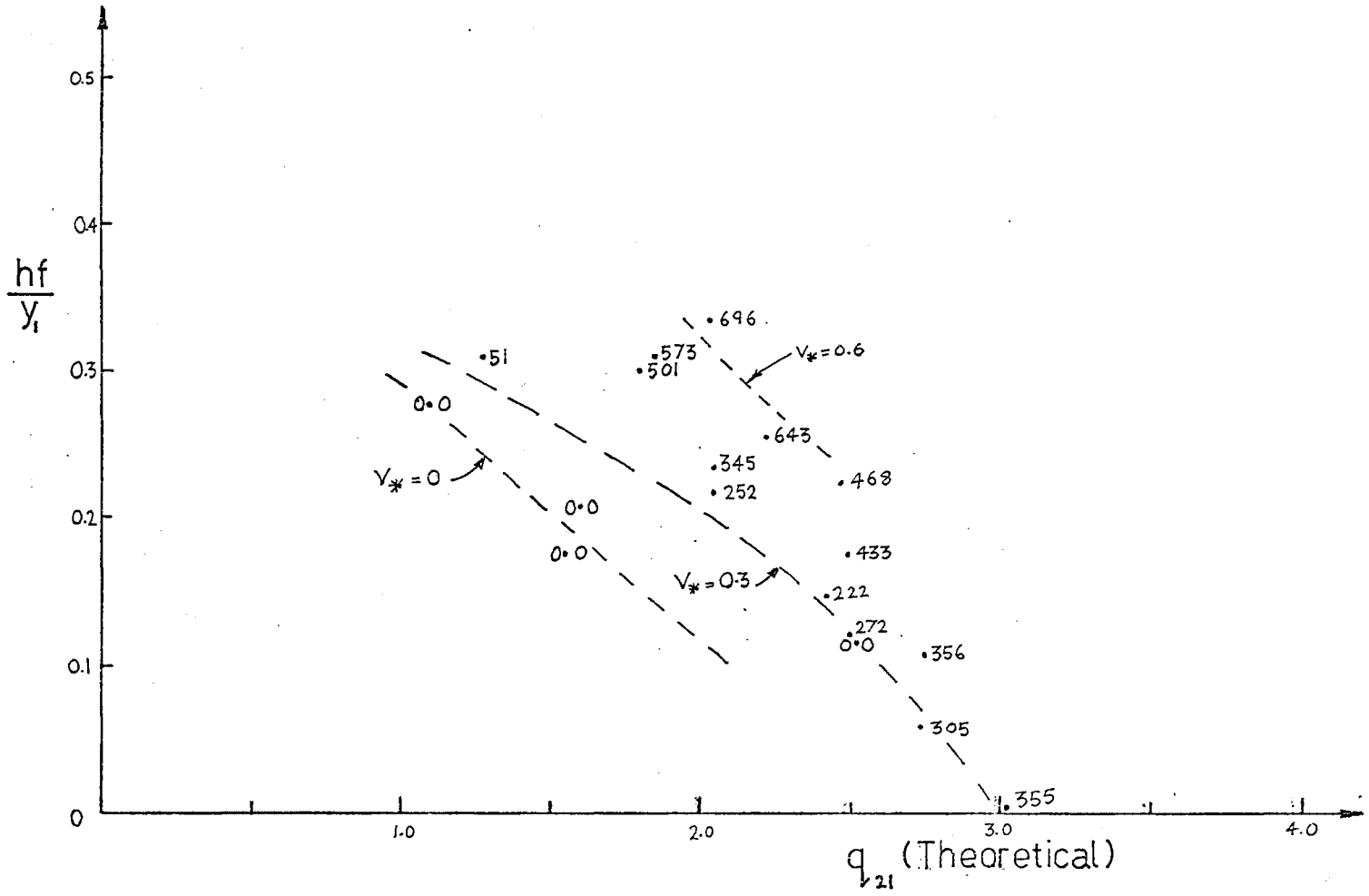

FIG. 24(a) : Graph of hf/y_1 against q_{21} (Theoretical) ; v_* plotted.

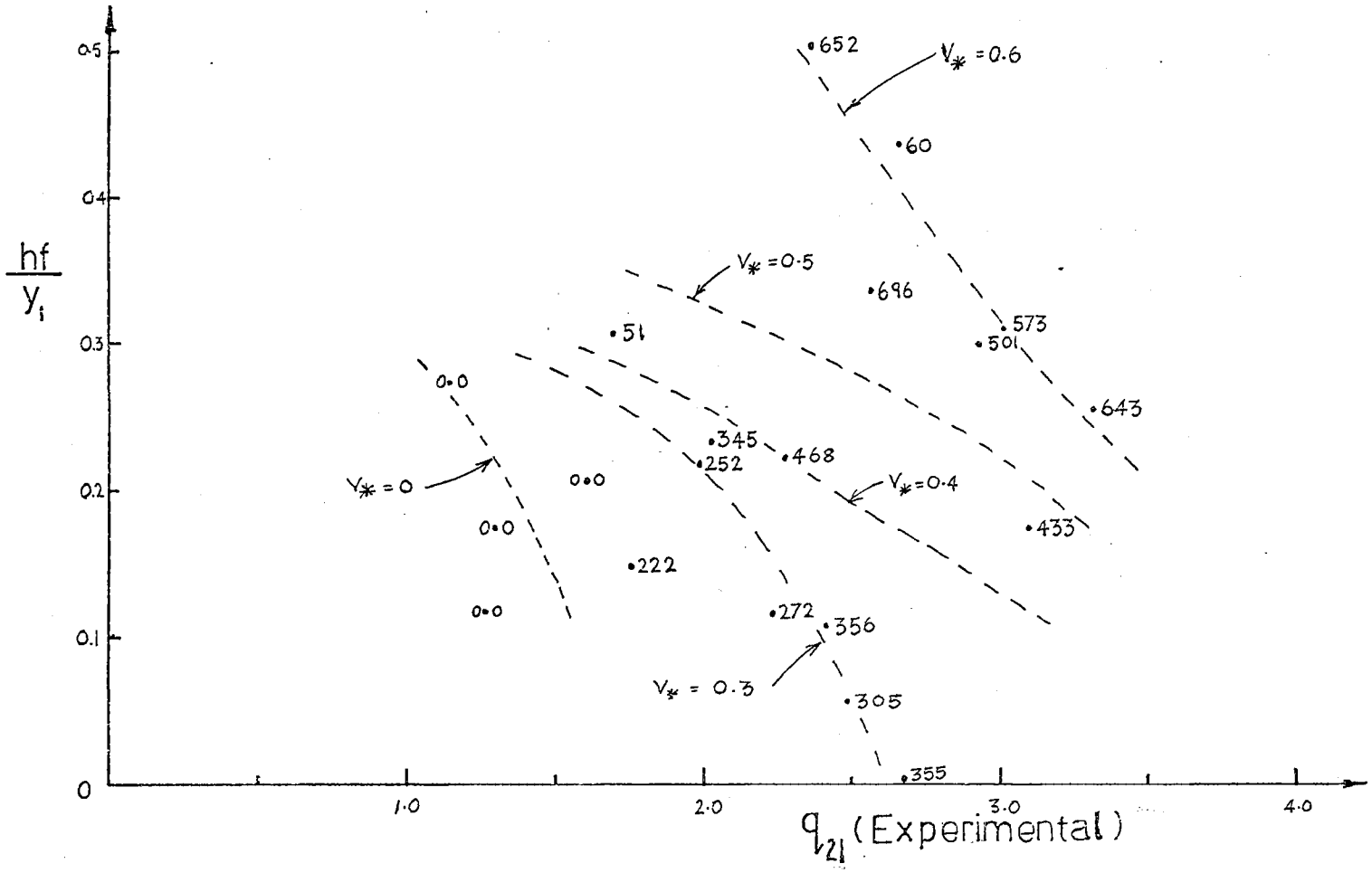

FIG. 24(b) : Graph of hf/y_1 against q_{21} (Experimental) ; v_* plotted.

sides remains laminar the Boundary Shear Stress, τ_w , may be written,

$$\tau_w = 2\mu \frac{\beta_2}{\beta_1} \frac{\bar{u}}{y} \quad , \quad \text{where}$$

β_1 = ratio of laminar boundary layer thickness to depth of the density current, y

β_2 = ratio of the velocity at the edge of a laminar boundary layer of the density current, to the mean flow velocity

$\bar{u}$,y = mean velocity and depth of density current

μ = dynamic viscosity

Wilkinson (1970 found that

$$\beta = \frac{2\beta_2}{\beta_1} = \text{constant} = 14.3$$

Therefore

$$\tau_w = \beta\mu \frac{\bar{u}}{y}$$

Streeter (1971) gives in equation (5.10.2), which holds for laminar or turbulent flow,

$$\tau_w = \frac{\rho f^* \bar{u}^2}{8}$$

where f^* = friction factor, and ρ = density.

Eliminating τ_w gives

$$f^* = \frac{8\beta\mu}{\beta \bar{u} y}$$

with $\mu = 2.6 \times 10^{-4}$ NS/m^2, $\rho = 1000$ kg/m^3 , $\bar{u} = 2$ cm/s , and $y = 8$ cm ,

then

$$f^* = 0.185 \ .$$

CHAPTER FIVE

THE COMPUTER PROGRAM

5.1 THE SOLUTION FOR FLOWS OF FINITE DEPTH

A computer program which could be used to solve the five equations (11, 12, 14, 15 and 18), for any value of depth D may be found in the appendix. The program is based on the Newton-Raphson iteration technique and was used on the Burroughs B6700 ALGOL Compiler.

The iteration technique is more easily described in terms of one equation and one unknown, Newton's approximation to a root: Let f_i be a function of x and f_i' its derivative with respect to x_i where x_i is the value of x at the ith iteration.

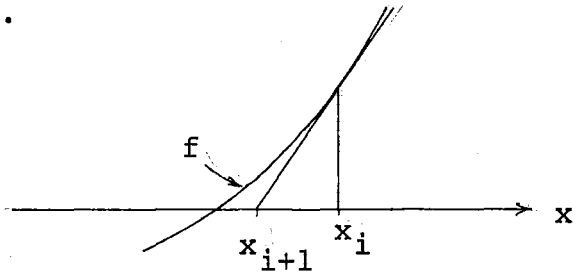

then

$$x_{i+1} = x_i - \frac{f_i}{f_i'}$$

where x_{i+1} is the value of x in the iteration following the ith iteration.

When there are five equations and five unknowns,

$f_i\ (x_1\ ,\ x_2\ ,\ x_3\ ,\ x_4\ ,\ x_5) = 0 \qquad (i = 1 \text{ to } 5)$

An initial approximation is $(x_1^o,\ x_2^o,\ x_3^o,\ x_4^o\ ,x_5^o)$

The Taylor expansion gives,

$$f_i\ (x_1^o + \Delta x_1\ , x_2^o + \Delta x_2\ ,\ \ldots\ x_5^o + \Delta x_5)$$

$$= f_i\ (x_1^o\ ,\ x_2^o\ ,\ \ldots\ x_5^o) + \frac{\partial f_i}{\partial x_1}\bigg|_o \Delta x_1 + \frac{\partial f_i}{\partial x_2}\bigg|_o \Delta x_2 + \ldots \frac{\partial f_i}{\partial x_5}\bigg|_o \Delta x_5$$

Putting $f_i(x^o + \Delta x) = 0$ gives five linear equations in five unknowns $(\Delta x_1,\ \ldots\ \Delta x_5)$ which, when solved simultaneously,

give a new value of $x = x + \Delta x$. Iteration continues until Δx becomes smaller than a predescribed error, or divergence takes place.

Solution convergence depends on good initial approximations. In the experiments the total depth D was 72.4 cms. For many cases the exact solution for infinite depth was found to be a suitable initial approximation for the case of $D = 72.4$ for convergence to occur. When difficulty was experienced in obtaining the required solution by this means, two alternative methods were used. The first, trial and error. The second, plotting a curve of hf/y_1 against F_2 for v_* increasing from 0 to the required v_* . (The curve of hf/y_1 against F_2 for $v_* = 0$ was in the same position for D = infinity as for $D = 72.4$. This was not the case for other values of v_*.)

The five equations (11, 12, 14, 15 and 18) were labelled $z[1]$ to $z[5]$ and these were differentiated with respect to the five unknowns (v_{*2}, v_{*3}, q_{*2}, F_2, F_3), labelled $x[1]$ to $x[5]$, giving twenty five derivatives labelled $Dz[1,1]$ to $Dz[5,5]$. These were operated on by a subroutine called DETLINEQN.

Input data includes v_{*1}(V1), F_1(F1), h(H), D(72.4 cms), q_Δ(QD), q_1(QO1), and five initial estimates of the five unknowns.

Output data includes the number of iterations required to obtain the solutions, the error, q_{21} , y_2/D , v_{*2} , v_{*3} , q_{*2} , F_2 , F_3 and the Jacobian.

There were at least three possible sets of solutions (branches) to the equations, and it was necessary to ensure that the initial estimates were close to the required solution

to prevent obtaining an extraneous solution.

The program was used to find theoretical solutions for all the laboratory experiments and also to plot charts of hf/y_1 against F_2 for the case when $D = 72.4$ cms for different values of v_* (0, 0.5, 1.0 etc.) by incrementing h by suitable small amounts (typically 0.01 cm).

5.2 COMPUTER PROGRAM RESULTS

The computer program was used to obtain theoretical downstream conditions for the case when the total depth $D = 72.4$ cms. The first program of Appendix F was used for one calculation only, for example, for a laboratory experiment. The second program will, for a constant value of v_* and a gradually decreasing weir height, give a set of values of hf/y_1 against F_2. The third program is a listing of a subroutine used in the solution of the non-linear simultaneous equations.

5.2.1 Theoretical Results for the Laboratory Experiments

The computer results for the laboratory experiments differed only slightly with the majority of theoretical results for the case of infinite depth. Froude Numbers varied mostly by 0 - 3%, but in one case was as high as 10%. Entrainments varied by from 0 - 3% usually, with one as high as 5%.

The laboratory experiment results differed by much more than this, so it can be said that the theory for infinite depth gives a reasonable approximation to the computer results for the laboratory experiments.

5.3 COMPARISON OF THE THEORIES FOR FINITE AND INFINITE DEPTHS

In Figure 25(a) the downstream Froude Number F_2 is plotted against v_* for the case of infinite depth and the case of $D = 72.4$. The upstream Froude Number F_1 remained constant at $F_1 = 7.55$. It can be seen that the curves, although equal when $v_* = 0$, diverge rapidly as v_* increases. The curve for $D = 72.4$ increases at first with increase of v_* until a maximum F_2 is reached at $v_* = 0.8$ and after this F_2 decreases as v_* increases. No computer solutions could be found for v_*'s greater than 1.0. The curve for infinite depth, on the other hand, continues to increase as v_* increases.

In Figure 25(b) the entrainments are compared. There is good agreement and in both the case of infinite depth and $D = 72.4$, q_{21} increases almost exponentially as v_* increases. Again, no computer solutions could be found for v_*'s greater than 1.0.

Figure 26 shows graphs of hf/y_1 plotted against F_2 for different v_*'s. Each graph is for a different upstream Froude Number F_1. In Figure 26(a), $F_1 = 4.0$, in Fig. 26(b), $F_1 = 7.55$, in Fig. 26(c), $F_1 = 8.0$ and in Fig. 26(d), $F_1 = 12.0$.

For stationary ambient fluid ($v_* = 0$) the graphs of hf/y_1 against F_2 are identical with the graph for infinite depth. As v_* increases, there are some significant differences.

(1) The curves for one particular value of v_* are not independent of the upstream Froude Number: as F_1 increases the curves for different v_*'s become closer together.

COMPARISON OF THEORETICAL FROUDE Nos.

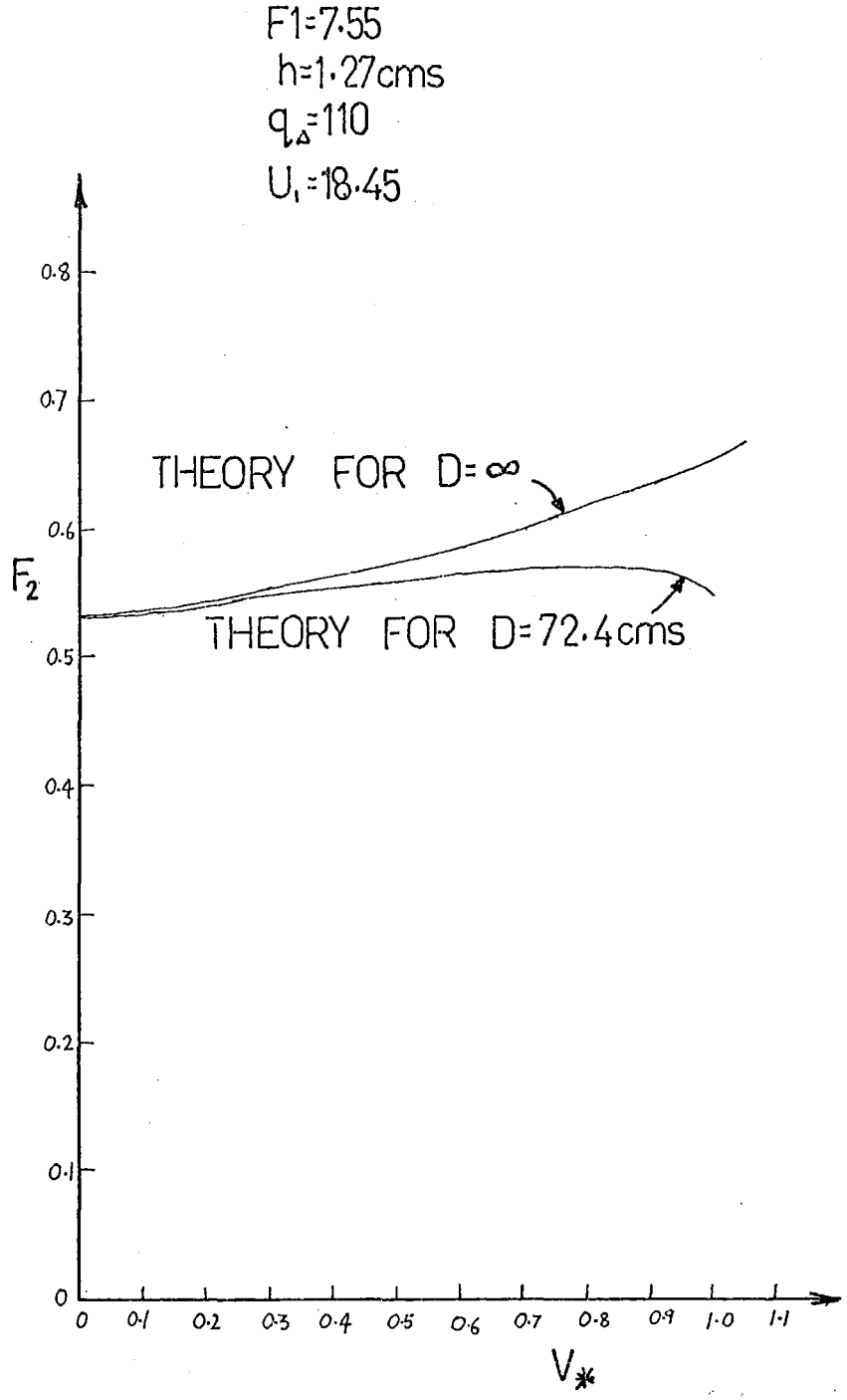

FIG 25(a)

COMPARISON OF THEORETICAL ENTRAINMENT

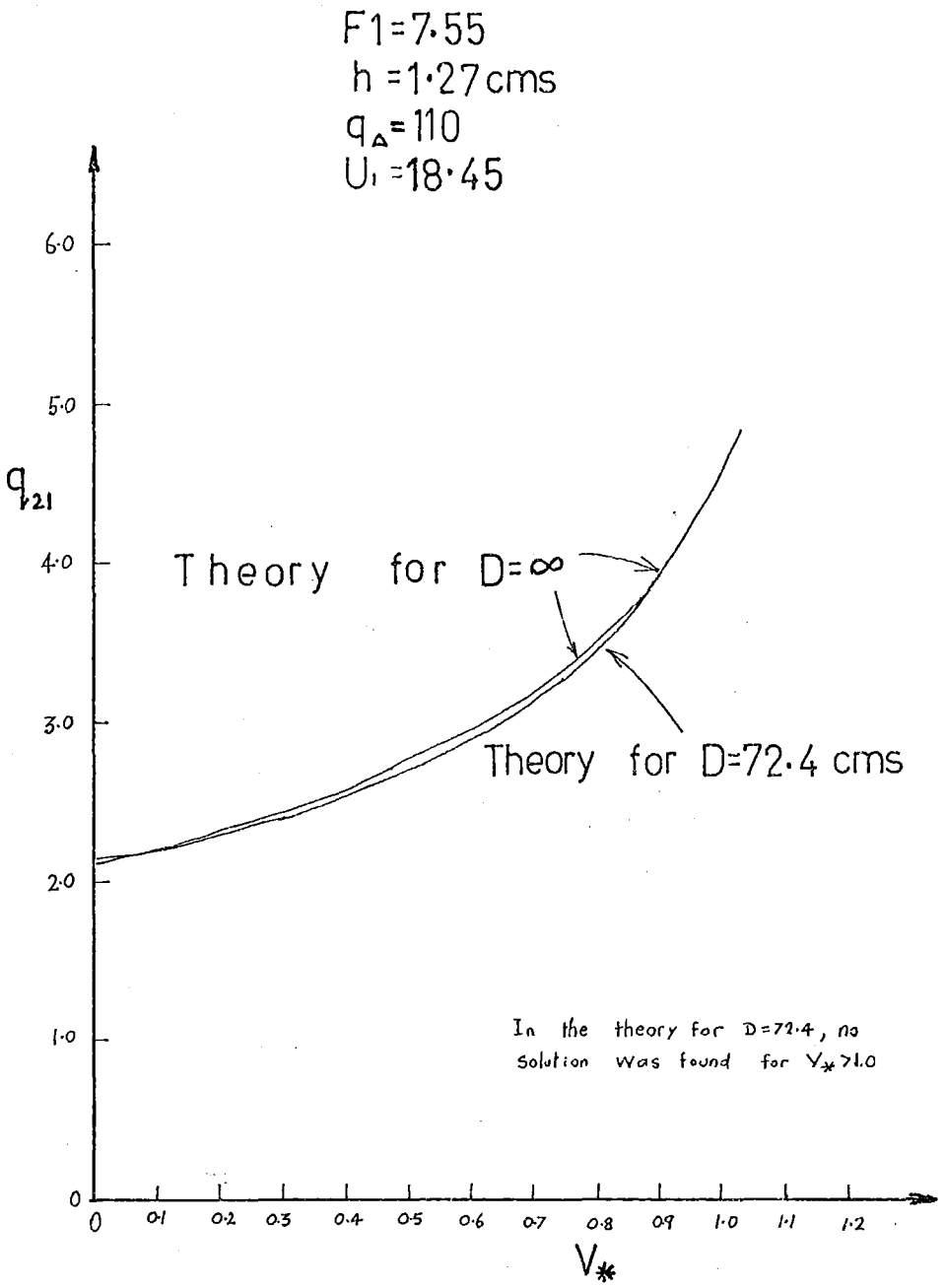

FIGURE 25(b)

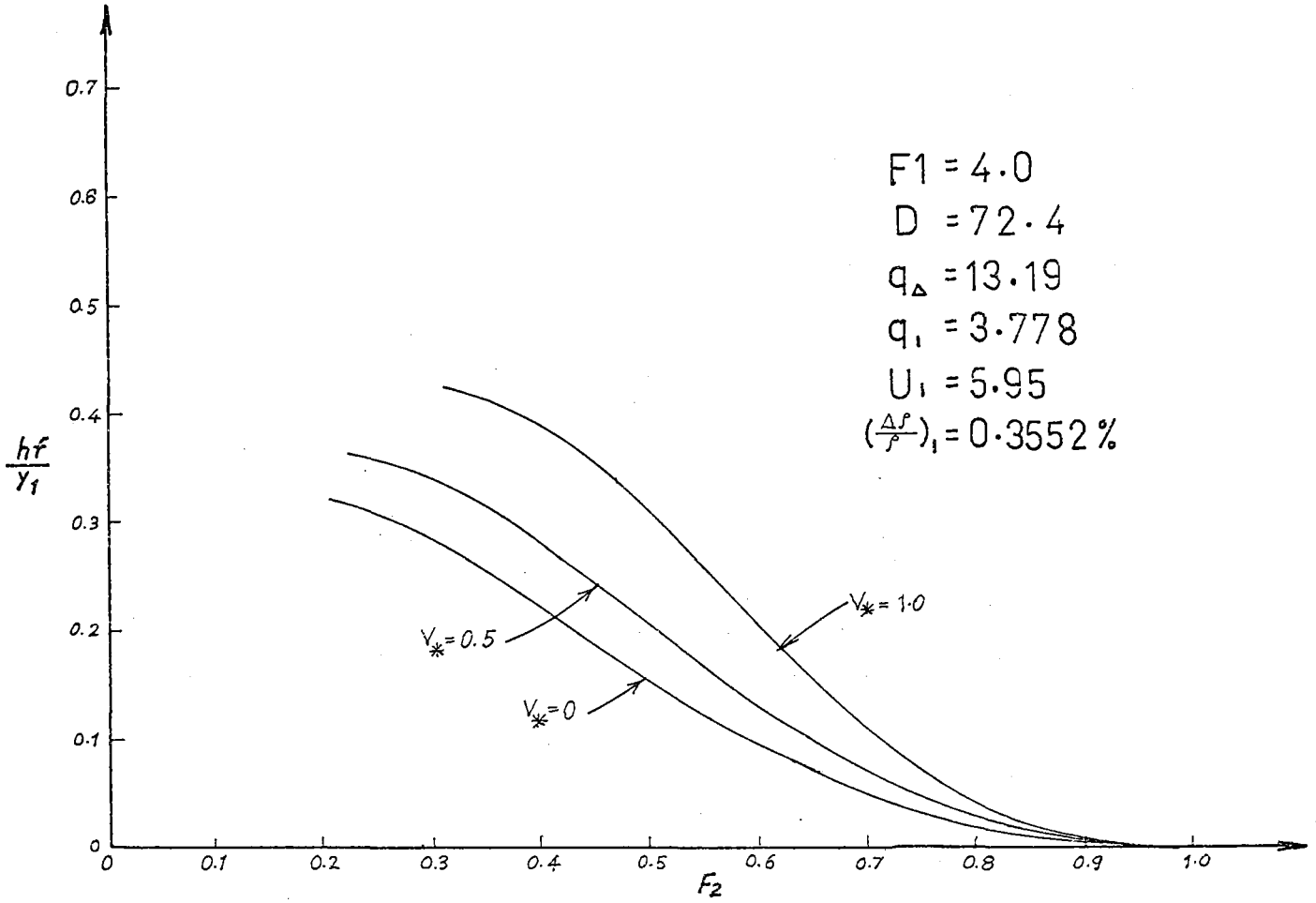

COMPUTER RESULTS FOR F1=4.0

FIGURE 26 (a)

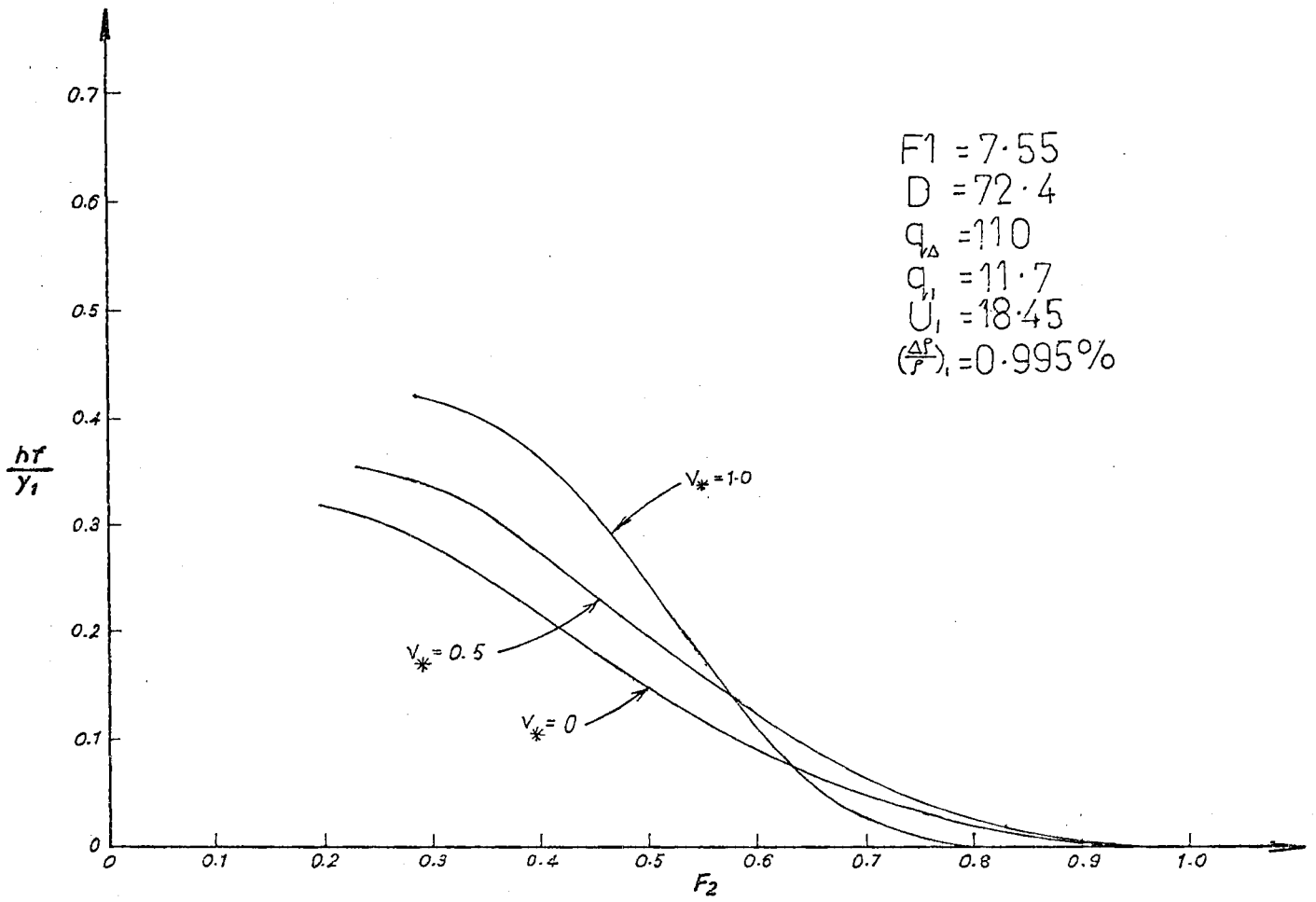

COMPUTER RESULTS FOR F1 = 7·55

FIGURE 26 (b)

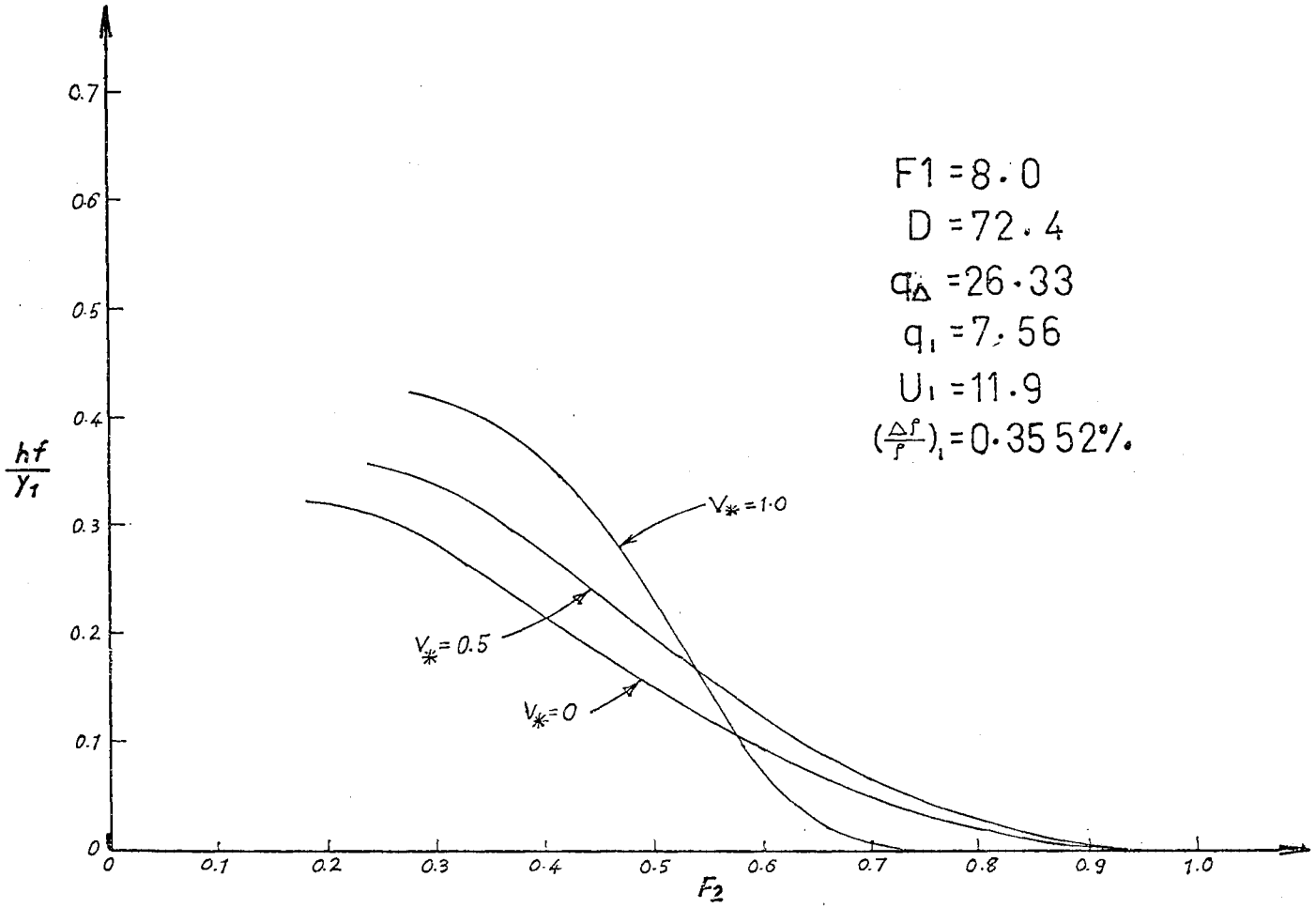

COMPUTER RESULTS FOR F1 = 8.0

FIGURE 26(c)

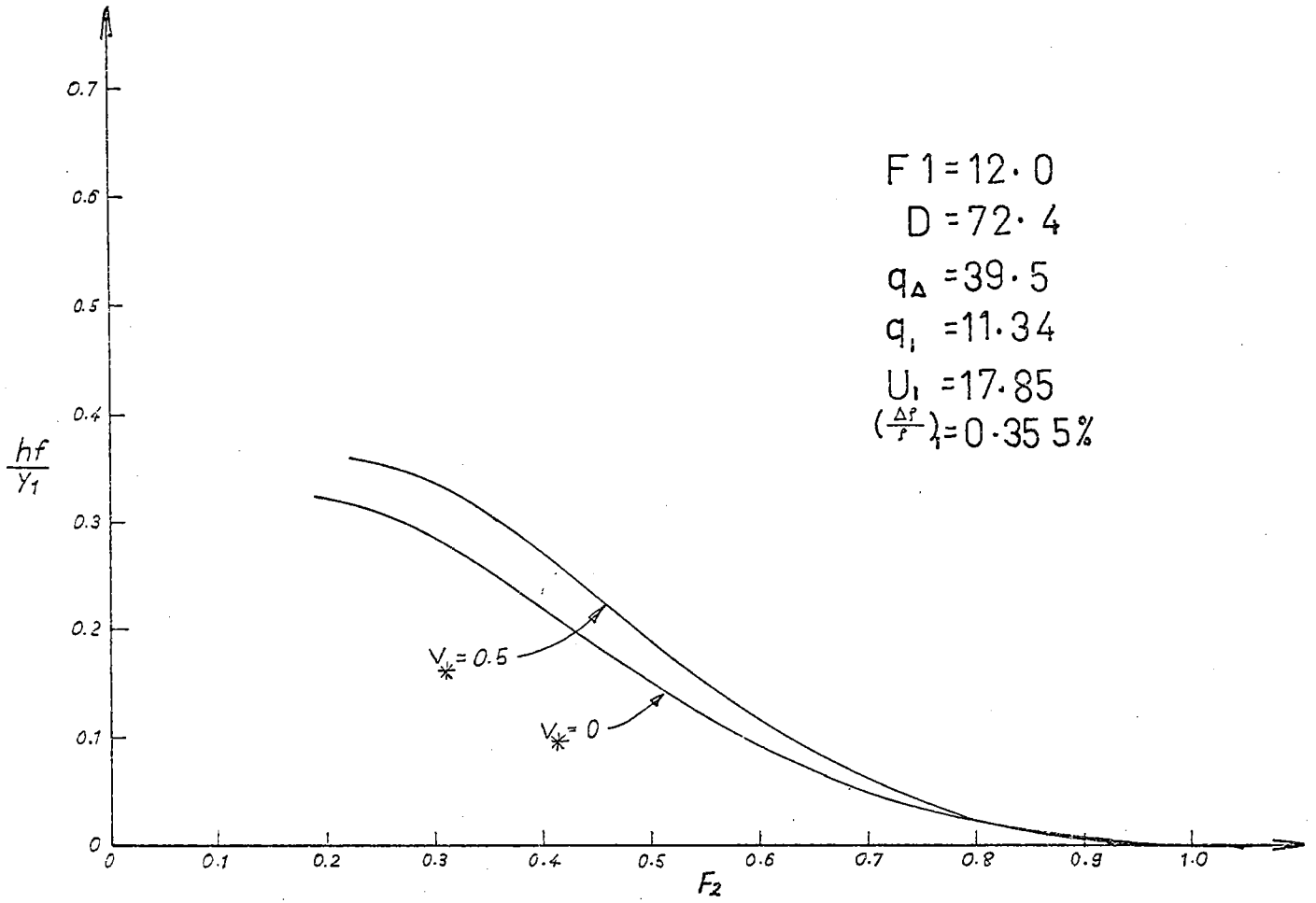

COMPUTER RESULTS FOR F1 = 12·0

FIGURE 26(d)

(2) The curves for very high v_*'s and high upstream Froude Numbers become steeper both as F_1 and v_* increase. At low weir heights and high F_1's the curves for high v_*'s cross over the curves for lower v_*'s .

(3) The downstream Froude Number for the case of a very low weir height depends on both v_* and upstream Froude Number. As both F_1 and v_* increase, F_2 decreases.

5.4 THE DOWNSTREAM FROUDE NUMBER WHEN THE WEIR HEIGHT IS ZERO

When the weir height is zero, the theory for infinite depth predicts that $F_2 = 1.0$ irrespective of values of v_* or F_1 . When the weir height is zero the theory for $D = 72.4$ predicts that F_2 will only be equal to zero when $v_* = 0$. F_2 becomes less than zero as both F_1 and v_* increase. For $F_1 = 7.55$, the decrease in F_2 with increase in v_* is plotted on Figure 27.

However, the downstream Froude Number should always be 1.0 when the weir height is zero, irrespective of the value of v_* . This is because at a free overfall, critical flow exists and a wave will neither travel up nor downstream ($w = 0$).

In a single layer fluid, the wave velocity, $w = v - c$ where $c^2 = gy$. Therefore,

$$w = v - \sqrt{gy}$$

and the Hydraulic Froude Number is

$$F = \frac{v}{\sqrt{gy}}$$

The wave velocity for a 2-layer fluid is given by

THE FROUDE NUMBER AT h=0

$F1 = 7.55$

$q_\Delta = 110$

$q_1 = 11.7$

$U_1 = 18.45$

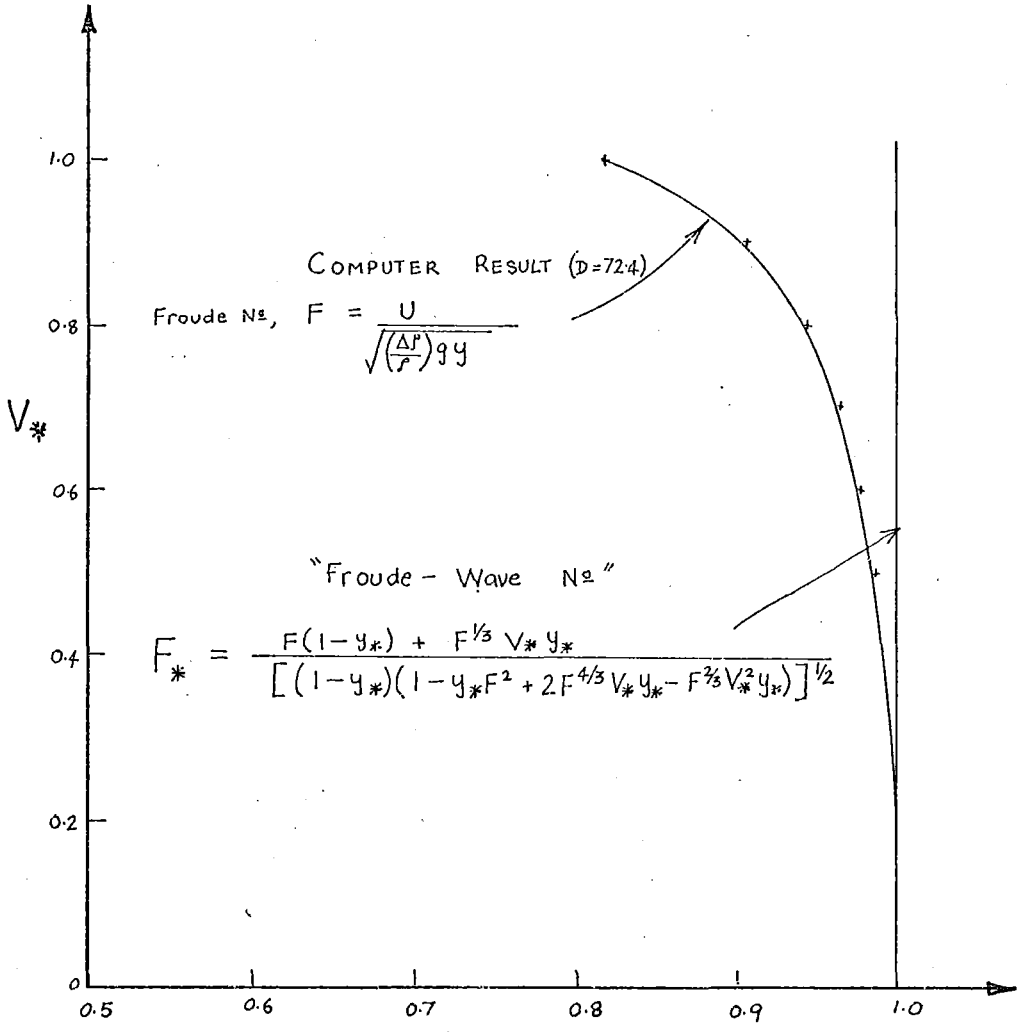

FIGURE 27

equation 28 and the corresponding Froude Number, which is called the "Froude Wave Number" (F_*), is defined by equations 29 and 31. (See section 5.4).

Critical flow exists when $F_* = 1.0$. This was verified by calculating F_* from equation 31 using the values of F_2 obtained to plot figure 27 and it was found that $F_* = 1.0$ for all values of v_*. (NB in equation 31 use the computer value of v_{*2} instead of v_*). The line $F_* = 1.0$ is plotted on Figure 27.

5.5 THE WAVE VELOCITY IN A 2-LAYER FLUID OF FINITE DEPTH

Let the speed of a wave at the interface be w (Fig. 28a). The ambient fluid has density ρ, velocity v and depth $(D-y)$. The lower layer has density $\rho + \Delta\rho$, velocity u and depth y. Impose $(-w)$ to make the situation steady (Fig. 28b). The wave height (z) is small. The two continuity equations are,

$$(u-w)y = (u-w+\Delta u)(y+z) = (u-w)y + y\Delta u + z(u-w) + z(\Delta u).$$

$$(v=w)(D-y) = (v-w+\Delta v)(D-y-z) = (v-w)(D-y) + (D-y)\Delta v - z(v-w) - z\Delta v .$$

Which give

$$\begin{aligned} y\,\Delta u + z(u-w) &= 0 \quad \text{or} \quad \Delta u = -(u-w)\,z/y \\ (D-y)\Delta v - z(v-w) &= 0 \quad \text{or} \quad \Delta v = (v-w)z/(D-y) \end{aligned} \qquad (27)$$

The energy equations are,

$$T_e = p + \rho gD + \tfrac{1}{2}\rho(v-w)^2 = p + p + \rho gD + \tfrac{1}{2}\rho(v-w+\Delta v)^2$$

$$T_{el} = p + \rho gD + \Delta\rho gy + \tfrac{1}{2}\rho(u-w)^2 = p + \Delta p + \rho gD + \Delta\rho g(y+z) + \tfrac{1}{2}\rho(u-w+\Delta U)^2$$

$$T_{el} - T_e = \Delta\rho gy + \tfrac{1}{2}\rho(u-w)^2 - \tfrac{1}{2}\rho(v-w)^2$$

$$= \Delta\rho g(y+z) + \tfrac{1}{2}\rho(u-w+\Delta u)^2 - \tfrac{1}{2}\rho(v-w+\Delta v)^2$$

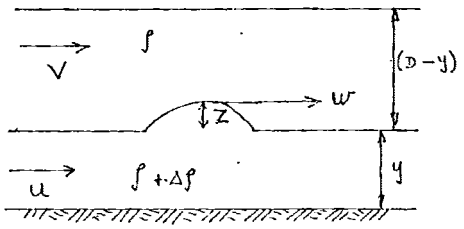

(a)

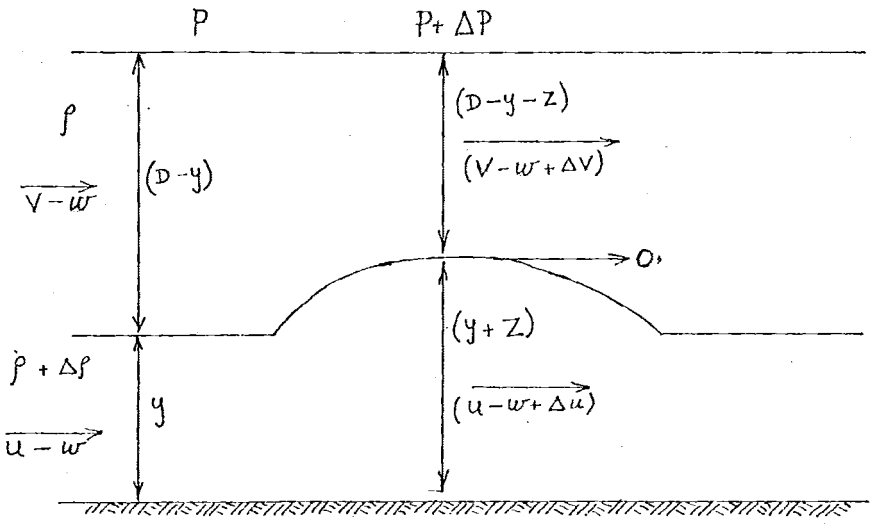

(b)

FIG.28: WAVE IN A 2-LAYER FLUID OF FINITE DEPTH

Linearise by neglecting products of Δu, Δv, z

$$\rho(v-w)\Delta v - \rho(u-w)\Delta u - \Delta\rho g z = 0$$

(27) gives

$$\rho\frac{(v-w)^2}{(D-y)} + \rho\frac{(u-w)^2}{y} - \Delta\rho g = 0$$

$$\frac{(v^2-2vw+w^2)}{(D-y)} + \frac{(u^2-2uw+w^2)}{y} - \frac{\Delta\rho g}{\rho} = 0$$

$$w^2\left[\frac{1}{D-y}+\frac{1}{y}\right] - 2w\left[\frac{v}{D-y}+\frac{u}{y}\right] + \frac{v^2}{D-y} + \frac{u^2}{y} - \frac{\Delta\rho g}{\rho} = 0$$

$$w = \frac{\frac{v}{D-y}+\frac{u}{y}}{\frac{1}{D-y}+\frac{1}{y}} - \left[\frac{\frac{2uv}{y(D-y)} - \frac{v^2}{y(D-y)} - \frac{u^2}{y(D-y)} + \frac{\Delta\rho g}{\rho}\left[\frac{1}{D-y}+\frac{1}{y}\right]}{\left[\frac{1}{D-y}+\frac{1}{y}\right]^2}\right]^{\frac{1}{2}}$$

$$w = \frac{vy+u(D-y)}{D} - \left[\frac{\frac{\Delta\rho g D}{\rho y(D-y)} - \frac{(u-v)^2}{y(D-y)}}{\frac{D^2}{y^2(D-y)^2}}\right]^{\frac{1}{2}}$$

$$w = \frac{vy+u(D-y)}{D} - \left[\frac{\Delta\rho g y(D-y)}{\rho D} - \frac{y(D-y)(u-v)^2}{D^2}\right]^{\frac{1}{2}} \qquad (28)$$

Note that the positive root is meaningless.

Equation (28) is the wave velocity in a 2-layer fluid of finite depth.

Now the wave velocity in a single-layer fluid of finite depth is $w = v - c$ where $c^2 = gy$.

then $w = v - \sqrt{gy}$

The Hydraulic Froude Number is $F = \frac{v}{\sqrt{gy}}$

The corresponding expression for the Froude number in a 2-layer fluid of finite depth may be written

$$F_* = \frac{\frac{vy - u(D-y)}{D}}{\left[\frac{\Delta\rho g y(D-y)}{\rho D} - \frac{y(D-y)(u-v)^2}{D^2}\right]^{\frac{1}{2}}} \qquad (29)$$

Equations (28) and (29) can be written in dimensionless form:

Let $v_* = v/q_\Delta^{1/3}$,

$u = F^{2/3} q_\Delta^{1/3}$,

$y_* = y/D$

$w_* = w/q_\Delta^{1/3}$

$$w_* = F^{2/3}(1-y_*) + v_* y_* - \left[\frac{(1-y_*)}{F^{2/3}} - (F^{4/3} - 2F^{2/3} v_* + v_*^2)(y_* - y_*^2) \right]^{\frac{1}{2}}$$

$$w_* F^{1/3} = F(1-y_*) + F^{1/3} v_* y_* - \left[(1-y_*)(1-y_* F^2 + 2F^{4/3} v_* y_* - F^{2/3} v_*^2 y_*) \right]^{\frac{1}{2}} \quad (30)$$

The Froude-wave number, F_*, becomes

$$F_* = \frac{F(1-y_*) + F^{1/3} v_* y_*}{\left[(1-y_*)(1-y_* F^2 + 2F^{4/3} v_* y_* - F^{2/3} v_*^2 y_* \right]^{\frac{1}{2}}} \quad (31)$$

Note that when $F_* = 1$, $w_* = 0$

Case (1) when D is infinite, y_* approaches zero

(30) gives $w_* F^{1/3} = F - 1$

and $w = 0$ gives $F = 1$ and $F_* = F$ (from (31))

Case (2), $w = 0$:

(30) becomes

$$F(1-y_*) + F^{1/3} v_* y_* = \left[(1-y_*)(1-y_* F^2 + 2F^{4/3} v_* y_* - F^{2/3} v_*^2 y_*) \right]^{\frac{1}{2}}$$

which reduces to

$$F^2 - F^2 y_* - 1 + y_* + F^{2/3} v_*^2 y_* = 0 \quad (32)$$

Now if $v_* = v_{*2} = v_{*3}$, and $F_2 = F_3 = F$, and $h = 0$ then equation (18) gives:

$$F^2(F^{2/3} - q_*) - F^{2/3} + q_* + F^{2/3} v_*^2 q_* = 0$$

Substituting $q_* = F^{2/3} y_*$, gives,

$$F^2 - F^2 y_* - 1 - y_* + F^{2/3} v_*^2 y_* = 0 \qquad (32)$$

Therefore, when $w = 0$, equation (30) reduces to equation (18).

Case (3). Kelvin-Helmholtz instability occurs when the term inside the square root sign of equation (30) is negative.

$$\left[(1 - y_*)(1 - y_* F^2 + 2F^{4/3} v_* y_* - F^{2/3} v_*^2 y_*)\right] < 0$$

$$\left[1 - F^2 y_* + 2F^{4/3} v_* y_* - F^{2/3} v_*^2 y_*\right] < 0$$

but $q_* = F^{2/3} y_*$

$$1 - q_* (F^{2/3} - v_*)^2 < 0$$

or

$$(F^{2/3} - v_*) > 1/q_*^{1/2} \qquad (33)$$

or

$$\left(\frac{u}{q_\Delta^{1/3}} - \frac{v}{q_\Delta^{1/3}}\right) > \frac{1}{9_*^{1/2}}$$

$$(u - v) > \frac{q_\Delta^{1/3}}{q_*^{1/2}} = \left[\frac{q_\Delta - D}{u\, y}\right]^{1/2} = \left[\frac{\Delta\rho}{\rho} g D\right]^{1/2} \qquad (34)$$

This condition would be satisfied in highly supercritical flow such as in the entry of a neutral jet.

When $v = 0$, (34) reduces to

$$F > \left(\frac{D}{y}\right)^{1/2}$$

When $v = 0.1\, u$, (34) becomes

$$F > \frac{1}{0.9} \left(\frac{D}{y}\right)^{1/2}$$

and when $v = 0.5\,u$, (34) becomes

$$F > 2\left(\frac{D}{y}\right)^{\frac{1}{2}}$$

When $v = 0$, F_1 would have to be greater than 10.7 for instability to occur in the present experiments, or 10.2 in the Wilkinson (1970) experiments.

Wilkinson noted that for Density Jumps controlled by a broad-crested weir, the minimum stable F_2 was 0.17, the conjugate F_1 being 13.2 ; and when $F_1 > 13.2$, the jump floods before the stage of zero entrainment is reached. This could be a result of Kelvin-Helmboltz instability.

In density currents of oil slicks over water, Wilkinson (1972) showed that dynamic instability occurred when the densimetric Froude Number upstream of a slick exceeded a critical value (approximately 0.529, depending on the magnitude of the density difference).*

Case (4). The graph of hf/y_1 against F_2 for D = infinity is NOT the same as the graph of hf/y_1 against F_* for D = 72.4, and v_* greater than zero. The reason for this is because v_* is not equal to v_{*2} in the computer results.

---

* The writer contemplates carrying out further research into this aspect.

CHAPTER SIX

CONCLUSION AND RECOMMENDATIONS

6.1 RECOMMENDED MODIFICATIONS

Modifications to the laboratory apparatus which should be carried out before any further experiments are attempted, are listed in Appendix H.

Recommended modifications in experimental technique include:

(1) Each experiment should be left for at least ¼ hour after adjusting v , the ambient velocity, although the syphon may be adjusted during this time.

(2) A camera should be mounted on its side opposite the downstream section to photograph hydrogen bubble traces in both the ambient fluid and density current. A second camera could be used to take colour photographs of two bays, including the inlet.

(3) A maximum of three and minimum of two operators would be required.

(4) Two thermometers should be placed in the tank, one at the top and one at the bottom. They should be compared occasionally to ensure that the tank has not become density stratified. A $1^{o}C$ difference would mean an appreciable error in the density profile at the downstream section. If stratification does occur, the 3 Hp. pump can be used to mix up the water in the tank.

(5) If the lighting is increased for photographs of hydrogen bubble traces it may be possible to run a very small flow of dye continually, and so avoid the problem of

cold dye liquor causing the temperature of the hot water to fluctuate when the dye is turned off and on.

6.2 FURTHER STUDIES

The results of most of the laboratory experiments suffered from a large experimental error and after modifications have been made, some further experiments should be studied. Temperature differences between hot and cold water should be kept within the range $8^{o}C$ to $10^{o}C$. One complete set of experiments could be made with $u_1 = 10$ cm/s, then another set, with $u_1 = 5$ cm/s. Values of h could be from 0 to 2.5 cms in steps of 0.5 cms. Values of the velocity of the ambient fluid, v, could range from 0 to 3.75 cm/s, in steps of 0.75 cm/s. If possible, experiments for one particular weir height could begin with $v = 0$ (or at auch a v that the inlet no longer floods) and v could be increased in steps of 0.75 cm/s until the roller region extends 1.5 m downstream. These experiments for each unchanged weir height should all be carried out without changing the upstream conditions.

6.3 CONCLUSION

It has been shown theoretically that, keeping the upstream conditions constant, a steady increase in ambient fluid velocity will cause entrainment, or q_{21}, to increase in an almost exponential manner, until $v_* = 1.0$, after which the theory breaks down. Analysis of the laboratory experiment results shows that a marked increase in entrainment will result if the ambient velocity is increased or

the weir height is lowered. Figures 29 are four photographs of an entraining hydraulic jump as the ambient velocity is increased. The upstream conditions and weir height were not adjusted for the duration of the experiment. In Figure 29(a) the jump is flooded and v_* is very low. In Figure 29(b), the jump is not quite at the point of incipient flooding, and the entrainment zone is very short. In Figure 29(c), v_* is increased further and the roller has moved downstream. Note the dye becoming entrained. In Figure 29(d), v_* is increased further still and the jump has moved a long way downstream. Note that very little of the dye released is entrained in the long roller region. Note also that there appears to be only a negligible increase in depth y_2 in Figure 29(a), (b) and (c).

When the weir height is very low, laboratory experiments give much lower Froude Numbers than those expected from theory. This is thought to be caused by boundary friction acting as a control in a similar manner to a weir, at very low weir heights. As the weir is raised, the control switches back to the weir.

When the weir height is zero, the theoretical Froude Numbers for a depth of 72,4 cms were lower than expected and decreased when v_* increased. This was caused by the definition of the Froude Number. The (densimetric) Froude Number is not the correct Froude Number to describe critical flow in a finite depth 2-layer fluid. The true Froude Number is a function of the speed of a wave travelling at the interface of the two fluids, and for this reason, a "Froude Wave Number" was introduced. As expected, the F_*

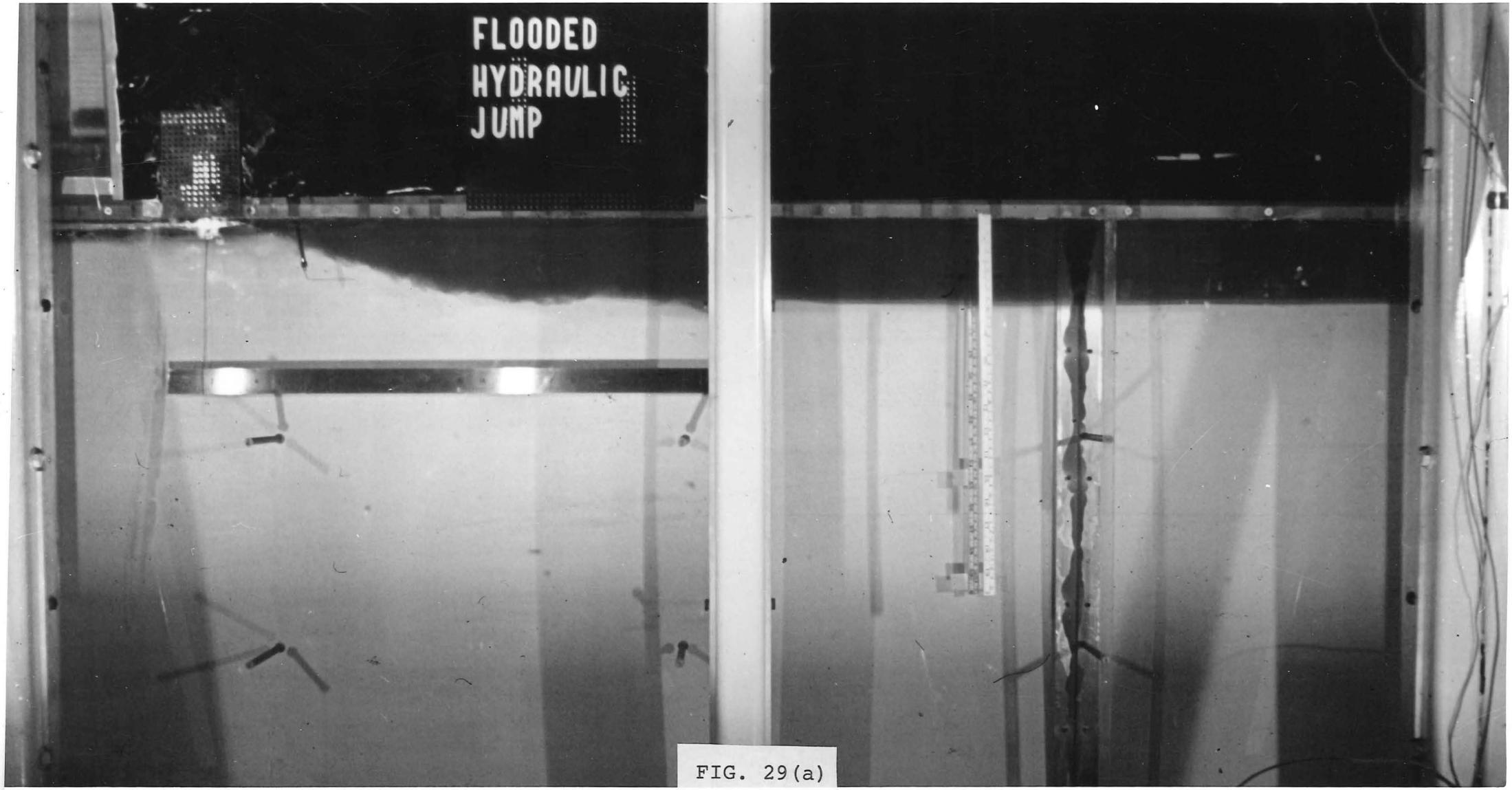

FIG. 29(a)

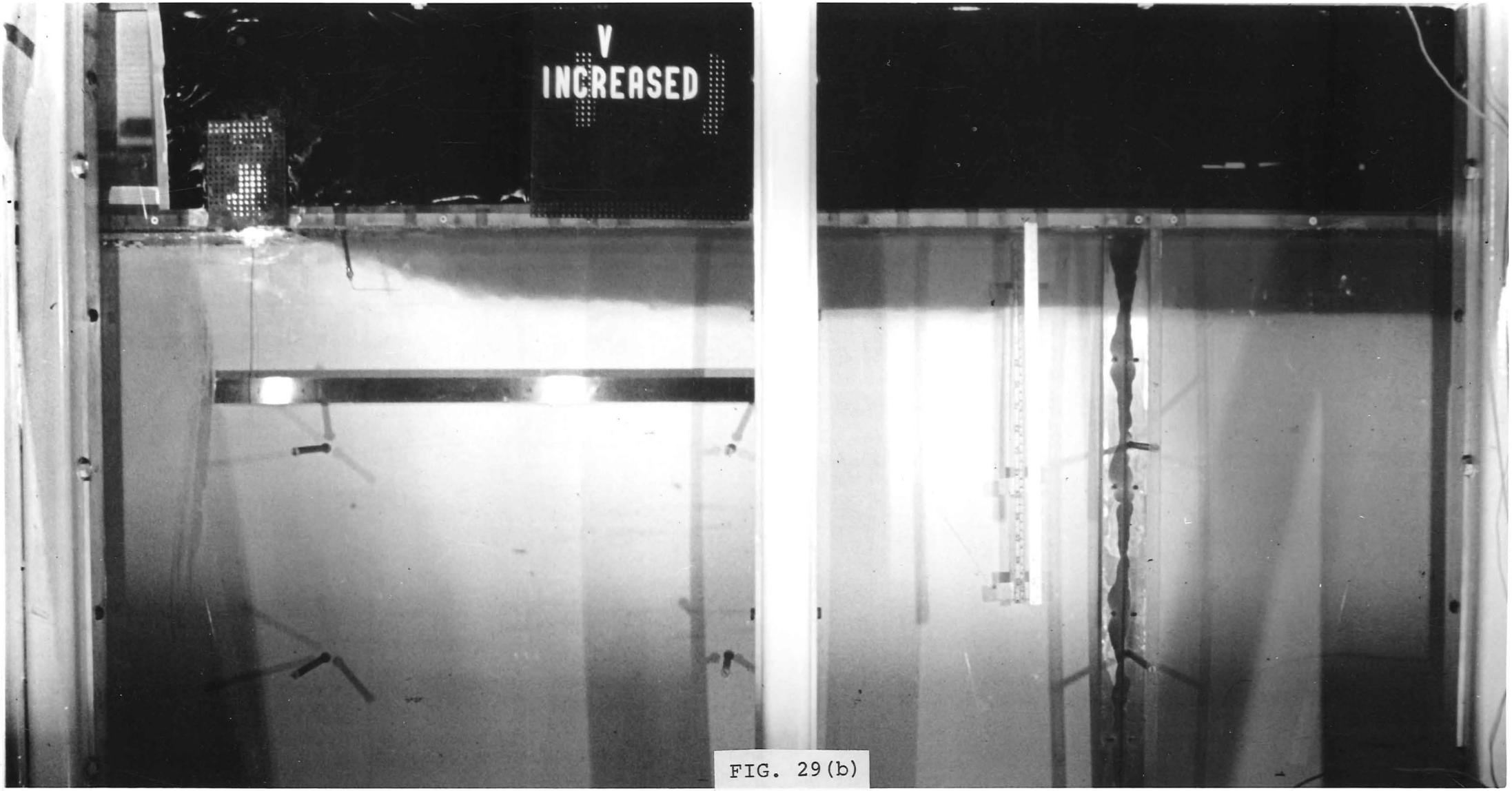

FIG. 29(b)

FIG. 29(c)

FIG. 29(d)

calculated from the computer results was exactly 1.0 when the weir height was zero, and remained at 1.0 as v_* increased.

When the weir height is zero, the theory for infinite depth predicts that $F_2 = 1.0$, irrespective of the value of F_1 . This is because when the depth is infinity, F_* reduces to F .

For low value of v_* (less than 0.5), the theory for infinite depth gives a very good approximation to the computer result for the case when $D = 72.4$ cms.

A relatively large experimental error lead to a large scatter in the laboratory experiment results. If experiments in which flooding occurred, $v_* > 0.5$ or $h < 0.5$ are neglected, the results are a little more satisfactory.

Some modifications required to be made to the laboratory equipment have been listed, and some suggestions have been made with which the experimental technique could be improved. Some further experiments which could very profitably be carried out, have been listed.

APPENDIX A

TYPICAL REDUCTION OF TEST DATA FOR A SINGLE EXPERIMENT

Experiment 28

Upstream Conditions:

T_a = 16.6 °C		Ambient Temperature
T_h = 32.35 °C		Temperature of hot water
ΔT = 15.75 °C		Temperature Excess
ρ_a = 0.99887		Density of Ambient Fluid
ρ_h = 0.99494		Density of hot water
$\frac{\Delta\rho}{\rho}$ = 0.393%		The density difference (equal to the mean density difference since the density distribution is uniform)
Q_1 = 1.522 gals/min		Flow $Q = u_1 \cdot b \cdot y_1$ (b = 15.24 cms)
u_1 = 11.85 cm/sec		Velocity, at inlet, of hot water
y_1 = 0.635 cms		Inlet depth
q_1 = 7.52 cm^2/sec		Flow per unit width
F_1 = 7.57		The upstream Froude Number, $F_1^2 = \frac{u_1^2}{(\Delta\rho/\rho)_1 \cdot g \cdot y_1}$
q_Δ = 29.01		$q_\Delta = (\Delta\rho/\rho)_1 \cdot u_1 \cdot g \cdot y_1$
v_1 = 1.06 cm/s		Velocity of Ambient Fluid
v_{*1} = 0.345		$v_{*1} = v_1/q_\Delta^{1/3}$ dimensionless ambient velocity
f = 0.0732		$f = \frac{2F_1^{2/3}}{2F_1^2 + 1 - 2F_1^{4/3} v_{*1}}$
h = 2.0 cms		Height of weir, 2.3 metres downstream from inlet

$hf/y_1 = 0.231$

Approximate Theoretical Results, (Assuming $D = \infty$, and $v_* = v_{*1} = v_{*2} = v_{*3}$)

$F_2 = 0.442$ (Downstream Froude No., from graph of $hf/y - v - F_2$).

$q_{21} = 2.06$ $\quad q_{21} = \left[\frac{2F_1^2 + 1 - 2F_1^{4/3} v_*}{2F_2^2 + 1 - 2F_2^{4/3} v_*}\right] \cdot \left[\frac{F_2^{4/3}}{F_1^{4/3}}\right]$

$q_2 = 15.5\ cm^2/s$ $\quad q_2$ = downstream flow per unit width $= q_{21} * q_1$

$u_2 = 1.78$ cm/s $\quad u_2$ = downstream velocity = $F_2^{2/3} \cdot q_\Delta^{1/3}$

$y_2 = 8.69$ cms $\quad$ Downstream depth $(y_2 = q_2/u_2)$

Theoretical Results, Computer Output, Assuming D = 72.4 cms

$F_2 = 0.4335$	Downstream Froude No.
$y_2 = 8.659$ cms	Downstream depth of density current
$u_2 = 1.76$ cm/s	Downstream velocity of density current
$q_2 = 15.24\ cm^2/s$	Downstream flow per unit width
$q_{21} = 2.0265$	$q_{21} = q_2/q_1$
$v_{*2} = 0.349$	Dimensionless ambient downstream velocity
$v_{*3} = 0.3298$	Dimensionless ambient velocity at weir
$F_3 = 1.004$	Froude No. at the weir.

Experiment Results

$y_2 = 9.1$ cms	Maximum gradient of density distribution
$y_2 = 8.5$ cms	y_2 observed, using dye, to interface
$y_2 = 7.0$ cms	Maximum gradient of velocity profile
$\bar{y}_2 = 8.2$ cms	Interfacial depth (average y_2)

The mean density distribution was obtained from the temperature distribution, tabulated below: (Temperatures obtained from calibrated thermocouple)

TABLE 1

y_2, cms	T°C	ρ (G/Ml)
1	26.25	.99675
2	26.5	.99668
3	26.25	.99675
4	25.75	.99688
5	25.75	.99688
6	25.25	.99701
6.5	25.0	.99708
7	24.75	.99714
7.5	24.5	.99720
8	24.25	.99726
8.5	23.5	.99745
9	22.0	.99780
9.5	19.25	.99839
10	18.25	.99858
10.5	17.75	.99867
20	17.0	.99880

The mean velocity distribution was obtained from 5 separate sets of hydrogen bubble traces:

$$\bar{u}_2 = \int_o^D \frac{u_2 dy}{\bar{y}_2} = 1.87 \text{ cm/s.}$$

$$q_2 = \bar{u}_2 \bar{y}_2 = 15.3 \text{ cm}^2/\text{s}$$

$$q_{21} = 2.04$$

Calculation of the characteristic density difference (Δ_2):

$$\frac{\Delta_2}{g} = \frac{1}{\bar{u}_2 \bar{y}_2} \int_o^D u_2 \left(\frac{\Delta\rho}{\rho}\right)_2 . dy$$

obtained by numerical integration of measured velocity and density distributions.

TABLE 2

y_2 (cm)	$y_2/\bar{y}_2$	u_2 cm/s	ρ_2(g/ml)	$(\Delta\rho/\rho)_2$ %	$u_2(\Delta\rho/\rho)_2$ %
.8	.1	2.15	.99675	.2126%	.457%
2.5	.3	2.29	.99669	.2184	.500
4.1	.5	2.27	.99688	.1993	.453
5.7	.7	1.86	.99699	.1883	.350
7.4	.9	.77	.99719	.1683	.129
		9.34			1.89%

$$\frac{\Delta_2}{g} = \frac{1.89\%}{\bar{u}_2 \cdot 5} = 0.2024\%$$

$$\frac{\Delta_1}{g} = \left(\frac{\Delta\rho}{\rho}\right)_1 = 0.3931\%$$

$$k = \frac{\Delta_1}{\Delta_2} = 1.943 \qquad r = \frac{y_2}{y_1} = 12.91 \qquad F_2 = F_1 \left(\frac{k}{r}\right)^{3/2} = 0.4417$$

APPENDIX B

ERROR ANALYSIS OF A TYPICAL EXPERIMENT

Experiment 28

T_a =	16.6 ± 0.2 °C	Ambient Temperature
T_h =	32.35 ± 0.2 °C	Temperature of hot water
ΔT =	15.75 ± 0.4 °C	Temperature excess
ρ_a =	.99887 ± .000034	Density of Ambient Fluid
ρ_h =	.994944 ± .000065	Density of hot water
$(\Delta\rho/\rho)_1$ ≐	.00393 (±2.5%)	$\Delta_1/g = (\Delta\rho/\rho)_1$
q_1 =	7.52 (± 1%) cm^2/s	$q_1 = u_1 y_1$ Upstream flow per unit width
u_1 =	11.85 (± 1%) cm/s	Velocity of hot water, upstream
y_1 =	0.635 (± 1%) cm	Depth of inlet slot (Depth of upstream flow)
F_1 =	7.57 (± 2.76%)	Upstream Froude No. $F_1 = u_1/\sqrt{(\Delta\rho/\rho)_1 g y_1}$
v =	1.06 (± 4.0%)	Velocity of ambient fluid
v_* =	0.345 (± 5.5%)	$v_* = v/q_\Delta^{1/3}$
q_Δ =	29.0 (± 4.5%)	$q_\Delta = (\frac{\Delta\rho}{\rho})_1 u_1 g y_1$
f =	0.0732 (± 8.74%)	$f = 2F_1^{2/3}/(2F_1^2 + 1 - 2F_1^{4/3} v_*)$
h =	2 (± 1%) cms	Height of weir
hf/y =	0.231 (± 10.7%)	
F_2 =	0.442 (± 7.05%)	Downstream Froude No., Approximate Theory
q_{21} =	2.06 (± 27.7%)	$q_{21} = \dfrac{(2F_1^2 + 1 - 2F_1^{4/3} v_*).F_2^{4/3}}{(2F_2^2 + 1 - 2F_2^{4/3} v_*).F_1^{4/3}}$.
q_2 =	15.5 (± 28.7%)	Downstream Flow per unit width, Approximate Theory.
u_2 =	1.78 (± 6.2%)	Downstream velocity (Approximate Theory)
y_2 =	8.69 (± 34.9%)	Downstream depth (Approximate Theory)

Experiment Results

u_2 error = 6.1% (Average error of 5 sets of readings)

$\bar{u}_2$ = 1,868 (± 6.1%) cm/s Mean velocity downstream

$\bar{y}_2$ = 8.2 (± 9.7%) Depth downstream

q_2 = 15.3 (± 15.8%)

q_{21} = 2.04 (± 16.8%)

$(\Delta\rho/\rho)_2$ error = 8.5%

$u_2(\Delta\rho/\rho)_2$ error = 14.6%

Δ_2/g = .2024 (± 20.7%)

Δ_1/g = .393 (± 2.5%)

k + 1.94 (± 23.2%) $k = \frac{\Delta_1}{\Delta_2}$

r = 12.9 (± 9.2%)

F_1 = 7.57 (± 2.8%)

F_2 = 0.442 (± 51.4%) $F_2 = (k/r)^{3/2}.F_1$

N.B. 50% error in experimental value of F_2 to be expected.

APPENDIX C

LABORATORY EXPERIMENT RESULTS

The following four pages tabulate the results of twenty-four laboratory experiments.

All figures have been reduced to three significant figures. All readings are in metric units, distances in centimetres except for distances downstream (metres).

The following notes may be useful.

*y_2 (obs) is the observed depth of the interface.

*y_2 ($\Delta\rho/\Delta y$) is the depth of maximum density gradient.

*y_2 ($\Delta u/\Delta y$) is the depth of maximum velocity gradient.

*y_2 is the mean depth of interface.

*1 The downstream distance is the distance from the entry section to the position where conditions first become stable.

*2 In experiment 12, q_2 (lab. expt.) is very much less than expected.

*3 Odd results in expt. 18 are due to difficulties in reading photographs because of an incorrect setting on the hydrogen bubble generator.

*4 Before experiment 20, section (2) was observed at 1.0 m downstream; for all the remaining experiments section (2) was observed at 1.6 m downstream. This change was necessary because some of the experiments required a considerable distance before downstream conditions became stable.

*5 In Experiment 22 there was a large unexpected difference between the experimental and theoretical values of q_2.

*6 In laboratory experiments 24 and 25 there was no flooding observed, although both the theories predicted flooding.

*7 In laboratory experiment 32, the value of F_2 was much lower than that expected by theory.

*8 Experiments 33 and 34 were at the point of incipient flooding and the experimental values of q_{21} slightly less than 1.0 because of a flow behind the entry.

*9 The theory used for experiments 33 to 36 (instead of the computer results for D = 72.4) was open channel flow theory, since there was no entrainment and the ordinary hydraulic jump formulae apply.

*10 Experiments 35 and 36 were completely flooded with a significant flow behind the entry section explaining why the experimental values of q_{21} were so low.

TABLE 3 RESULTS: UPSTREAM PARAMETERS

Expt No.	u_1 cm/s	v_1 cm/s	h cm	ΔT ^oC	$\frac{\Delta\rho}{\rho}$ %	F_1	v_{*1}	q_1 cm^2/s	$\frac{hf}{y_1}$
7	14.1	0	1.5	38.8	1.29	4.98	0	8.95	.272
8	15.3	0	1.0	41.0	1.39	5.2	0	9.7	.172
9	11.8	0	1.5	21.6	.581	6.2	0	7.48	.206
10	9.5	1.65	1.5	21.8	.584	5.21	0.51	6.05	.308
12	14.3	0	1.5	15.1	.368	9.45	0	9.09	.118
16	11.9	1.32	1.5	15.6	.383	7.68	.433	7.53	.174
18	12.0	0.65	1.5	14.3	.337	8.24	.222	7.58	.149
20	12.0	.762	2.05	14.8	.371	7.90	.252	7.61	.217
21	11.9	1.36	2.0	13.8	.332	8.25	.468	7.52	.222
22	11.8	1.54	2.5	15.7	.390	7.6	.501	7.52	.300
23	12.0	2.03	3.0	13.5	.331	8.34	.696	7.60	.333
24	11.7	1.82	3.5	15.3	.385	7.54	.60	7.41	.437
25	11.8	1.98	4.0	15.4	.385	7.58	.652	7.35	.502
26	11.9	1.78	2.5	16.1	.401	7.55	.573	7.58	.309
27	11.8	1.98	2.0	15.9	.395	7.54	.643	7.51	.253
28	11.8	1.06	2.0	15.8	.393	7.57	.345	7.52	.231
29	12.0	.844	1.0	16.0	.403	7.48	.272	7.53	.115
30	11.8	1.06	1.0	14.9	.356	7.95	.356	7.52	.108
31	12.0	.957	0.5	16.8	.413	7.52	.305	7.65	.058
32	11.9	1.10	0	16.4	.405	7.51	.355	7.57	0
33	12.18	.436	3.6	15.9	.332	8.46	.149	7.73	.338
34	12.0	.495	4.0	12.3	.278	9.12	.180	7.62	.343
35	6.97	.336	4.0	10.6	.236	5.74	.155	4.42	.634
36	6.54	.894	3.5	11.7	.267	5.07	.404	4.15	.718

TABLE 4 RESULTS: THEORY FOR D = INFINITY

Expt. No.	F_2	y_2 cms	u_2 cm/s	q_2 cm^2/s	q_{21}
7	.328	4.3	2.3	9.9	1.1
8	.475	4.88	3.1	15.1	1.56
9	.424	6.1	1.96	12.0	1.60
10	.384	4.98	1.72	8.55	1.41
12	.562	10.7	2.18	23.2	2.56
16	.528	9.49	1.99	18.9	2.51
18	.542	9.61	1.95	18.7	2.47
20	.445	8.9	1.77	15.8	2.07
21	.473	9.88	1.76	17.4	2.32
22	.379	8.59	1.60	13.7	1.83
23	.376	10.4	1.52	15.7	2.07
24	flooding indicated by theory				
25	flooding indicated by theory				
26	.381	8.72	1.63	14.2	1.87
27	.483	9.32	1.89	18.8	2.51
28	.442	8.69	1.78	15.5	2.06
29	.60	8.55	2.21	18.9	2.51
30	.622	9.67	2.16	20.9	2.78
31	.718	8.5	2.52	21.4	2.8
32	1.0	7.47	3.11	23.2	3.07
33	*.218	7.29	1.06	7.73	1.0
34	*.217	8.04	.993	7.97	1.05
35	* flooded, off chart				
36	* flooded, off chart				
	* flooded in lab. experiment				

TABLE 5 RESULTS: THEORY FOR D = 72.4 cms.

Expt No.	F_2	y_2	u_2	q_2	q_{21}	v_{*2}	v_{*3}	F_3
7	.318	4.27	2.25	9.63	1.08	-.002	-.002	1.0
8	.468	4.87	3.07	15.0	1.54	-.015	-.015	1.0
9	.419	6.06	1.96	11.9	1.59	-.019	-.018	1.0
10	.346	4.76	1.60	7.63	1.26	.534	.516	.996
12	.553	10.6	2.16	22.8	2.51	-.069	-.066	1.0
16	.522	9.49	1.97	18.7	2.49	.436	.414	.992
18	.530	9.54	1.92	18.3	2.41	.195	.186	.998
20	.436	8.90	1.74	15.5	2.04	.244	.230	.998
21	.475	10.5	1.77	18.5	2.46	.481	.452	.990
22	.366	8.60	1.57	13.5	1.79	.533	.500	.992
23	.357	10.5	1.47	15.3	2.02	.765	.706	.980
24	imaginary results (flooding)							
25	imaginary results (flooding)							
26	.367	8.72	1.59	13.9	1.83	.614	.576	.989
27	.454	9.95	1.82	18.1	2.41	.684	.642	.982
28	.434	8.66	1.76	15.2	2.03	.349	.330	.996
29	.589	8.50	2.19	18.6	2.47	.249	.240	.997
30	.610	9.60	2.14	20.5	2.73	.337	.323	.995
31	.704	8.45	2.49	21.0	2.74	.276	.268	.996
32	.994	7.37	3.10	22.8	3.01	.316	.316	.994
33*	.218	7.29	1.06	7.73	1.0			
34*	.209	7.87	1.03	7.62	1.0			
35*	.272	4.85	.913	4.42	1.0			
36*	.293	4.25	.978	4.15	1.0			

* From Open Channel Flow Theory (flooded)

TABLE 6 RESULTS: LABORATORY EXPERIMENTS

Expt No.	F_2	y_2	u_2	q_2	q_{21}	y_{2*} (obs)	y_{2*} ($\Delta\rho/\Delta y$)	y_{2*} ($\Delta u/\Delta y$)	dist (m) *1
7	.324	4.5	2.3	10.4	1.15		4.5		
8	.45	4.75	2.66	12.6	1.3		4.75	5.16	
9	.418	6.5	1.85	12.1	1.61	6.5	6.5	7.5	
10	.41	6.0	1.70	10.2	1.70	6.25	6.0		
12*2	.55	8.67	1.33	11.4	1.26	8.75	8.5	8.5	
16	.498	9.17	2.54	23.3	3.1	10	9.5	8	
18*3	.426	8.5	1.56	13.3	1.75	10	8.5		0.6
20*4	.521	8.9	1.69	15.1	1.98	8.75	8.9	9.1	0.5
21*5	.478	10.0	1.71	17.1	2.28	11	10	9.17	1.0
22*6	.478	9.64	2.28	22.0	2.93	11.3	8.5	9.17	0.8
23*6	.773	7.5	2.6	19.5	2.56	7.0	7.5	8.0	0.8
24	.405	10.0	1.97	19.7	2.66	10	10	10	1.4
25	.393	10.5	1.66	17.5	2.37	11.2	11.0	9.5	1.2
26	.515	8.72	2.63	22.8	3.01	8.8	9.0	8.2	1.0
27	.547	7.53	3.30	24.8	3.31	8.0	8.0	6.6	1.4
28	.442	8.2	1.87	15.3	2.04	8.5	9.1	7.0	0.4
29	.538	8.56	1.97	16.8	2.23	8.75	10.0	6.93	1.0
30	.527	8.62	2.1	18.1	2.41	8.75	9.5	7.6	0.5
31	.536	8.27	2.3	19.1	2.49	9.0	8.5	7.3	0.8
32*7	.573	7.64	2.65	20.2	2.67	8.75	6.5	7.68	0.9
33*8	.205	8.08	.884	7.14	.924	8.15	8.3	7.79	
34*9	.252	9.1	.795	7.23	.948	9.5	9.0	8.85	
35*10	.207	7.3	.392	2.86	.646	7.3	7.3	7.3	
36*10	.206	6.5	.572	3.72	.896	6.8	6.5	6.2	

APPENDIX D

RESULTS OBTAINED BY WILKINSON (1970) FOR DENSITY JUMPS CONTROLLED BY A BROAD-CRESTED WEIR

$v_* = 0$ in each case

TABLE 7

Upstream Conditions			Theoretical Results		Experimental Results		
F_1	f	$\frac{hf}{y_1}$	F_2	q_{21}	F_2	$k = q_{21}$	$r = \frac{y_2}{y_1}$
10.5	.0433	0	1.0	3.21	.83	2.60	14.0
10.7	.0422	.063	.667	3.01	.73	2.44	14.4
10.5	.0433	.105	.583	2.79	.58	2.09	14.7
9.7	.0481	.175	.468	2.31	.48	2.00	14.8
9.7	.0481	.220	.402	2.05	.37	1.70	15.1
9.7	.0481	.265	.339	1.76	.32	1.59	15.1
9.7	.0481	.290	.290	1.50	.23	1.19	14.5
16.5	.0238	0	1.0	4.33	.73	3.05	24.5
16.5	.0238	.065	.664	4.00	.65	2.90	25.4
16.5	.0238	.145	.513	3.49	.48	2.50	26.2
16.3	.0242	.210	.420	2.99	.35	2.00	26.4
16.3	.0242	.260	.347	2.53	.26	1.50	26.0
16.3	.0242	.300	.271	1.97	.19	1.10	25.3
16.2	.0243	.300	.271	1.97	.20	1.15	25.5
16.4	.0240	.260	.347	2.54	.27	1.55	26.0
16.5	.0238	.210	.420	3.02	.36	2.05	26.2

F_2 (Experimental) was plotted against F_2 (Theoretical) on Figure 21, together with the results obtained by the present writer, for $0 \leqslant v_* \leqslant 0.5$.

q_{21} (Experimental) was plotted against q_{21} (Theoretical) on Figure 23, together with the results obtained by the present writer, for $0 \leqslant v_* \leqslant 0.5$.

APPENDIX E

CALIBRATION OF HOT WATER FLOW METER

At a constant rate, water flowed through the flow meter into a weighed 20 gallon container mounted on scales. The flow meter reading was noted. Times were taken at the start and finish. When starting, the pipe, flowing, was moved towards the container, and the stopwatch started. When a required number of gallons as registered on the flow meter had flowed into the container, the pipe, still running, was moved away from the container and the stopwatch stopped. The container was weighed to determine the amount of water in the container.

Table 8 lists the results. A graph of inverse flow rate, as measured on the flow meter against the weighed inverse flow rate is shown in Figure 30. The flow meter readings are in imperial gallons.

Rather higher errors were recorded for very fast flows. It is likely that the errors for high flows were influenced by the experimental technique. It was difficult to synchronise timing with the period of flow into the container, during high flow rates.

At flow rates similar to those used in laboratory experiments (about 1 gallon per 40 seconds) the error observed was about 1%. It was concluded that the reading on the flow meter was accurate enough for the laboratory investigation.

It is relevant here to note that in flows of hot water, condensation formed on the glass of the flow meter,

making readings difficult.

TABLE 8

Weight Water (kg)	Weight x 0.22 (gal)	Time secs	Flow Meter (gal)	Secs/ gallon (meas.)	Secs/ gallon (meter)	Error %
47.2	10.4	55	10.05	5.29	5.47	3.5
46.6	10.28	74	10	7.2	7.4	2.8
46.6	10.28	107	10	10.4	10.7	2.8
46.0	10.1	205	10	20.3	20.5	1.0
45.95	10.1	155.7	10	15.4	15.57	1.0
23.3	5.12	162.8	5	31.8	32.56	2.4
22.85	5.03	293	5	58.1	58.6	0.6
23.0	5.05	239	5	47.4	47.8	1.0
22.9	5.04	629.6	5	125	126	0.8

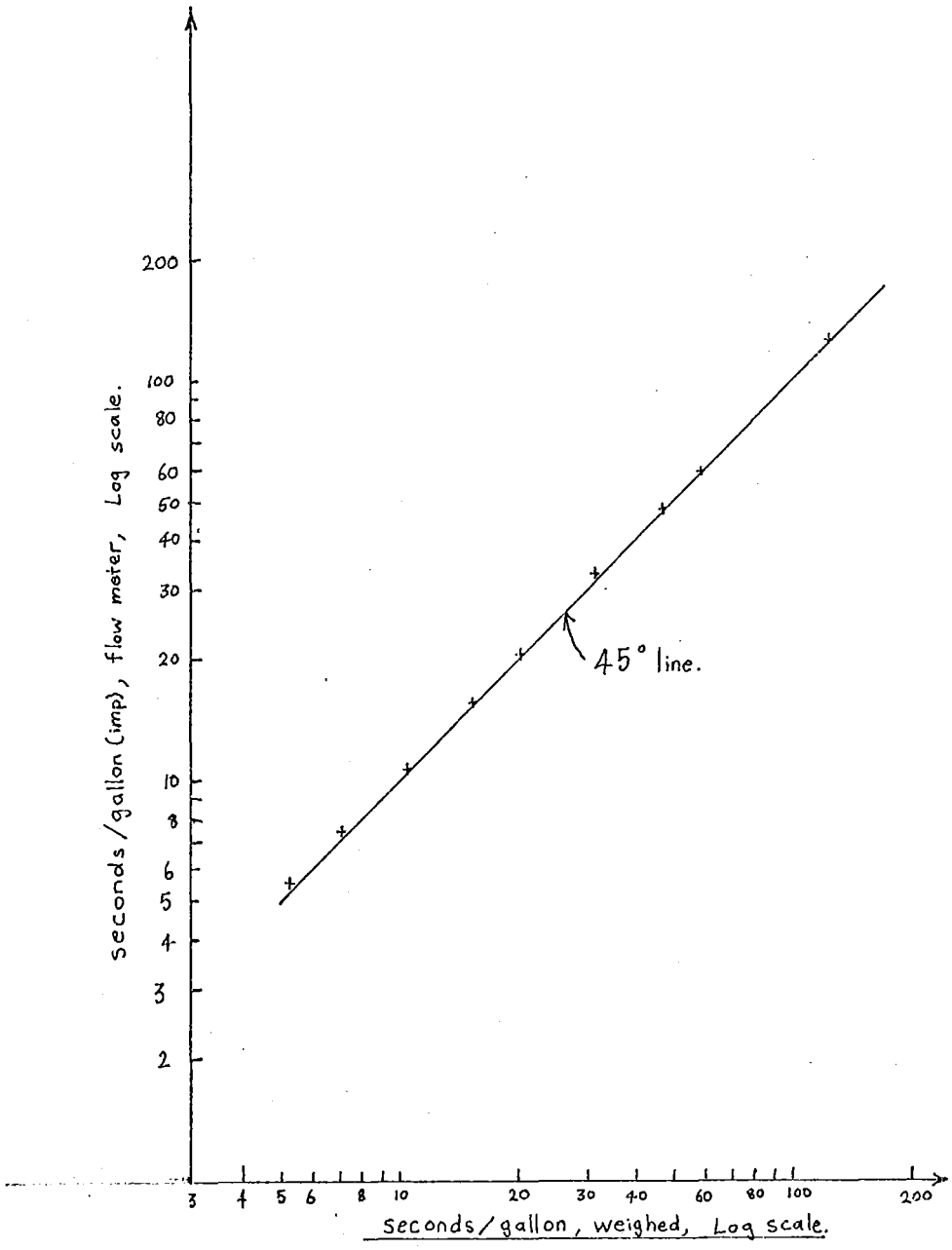

HOT WATER FLOW METER CALIBRATION CHART

FIGURE 30

APPENDIX F
COMPUTER PROGRAMME

```
BURROUGHS B6700 ALGOL COMPILER- VERSION 2.5.000,    MONDAY, 12/17/73,

                                    N E W T O N
                                    = = = = = =

BEGIN ARRAY DZ[0:5,0:5],X,XO,X1,X2,DX,Z[0:5];

LABEL L;                                                                1
INTEGER J,K,DE,I; REAL D0,Q1,V1,F1,H,QD,D,Q01,Q21,A1,A3,Y2,DB,H1;
FILE PR(KIND=PRINTER);

$ RESET LIST
V1:=0.4334;F1:=7.08;H:=1.5;D:=72.4;QD:=28.265;Q01:=7.53;                2
Q1:=Q01/D*QD**(-1/3);
X[1]:=0.43;X[2]:=0.43;X[3]:=0.0956;X[4]:=0.513;X[5]:=1.0002;
A1:=Q1*(1-V1*F1**(-2/3))+V1;
A3:=Q1*((F1**2+0.5)*F1**(-4/3)-V1**2*F1**(-2/3))+V1**2/2;
H1:=(H/0.635)*(2*F1**(2/3)/(2*F1**2+1-2*F1**(4/3)*V1));
L:J:=J+1;
Y2:=X[3]*X[4]**(-2/3);
Q21:=X[3]/Q1;
  DZ[1,1]:=X[3]*X[4]**(-2/3)-1;
  DZ[1,2]:=DZ[1,5]:=0;
  DZ[1,3]:=-1+X[1]*X[4]**(-2/3);
  DZ[1,4]:=-2/3*X[3]*X[1]*X[4]**(-5/3);
  DZ[2,1]:=DZ[1,1];
  DZ[2,2]:=1-X[3]*X[5]**(-2/3);
  DZ[2,3]:=-X[2]*X[5]**(-2/3)+X[1]*X[4]**(-2/3);
  DZ[2,4]:=DZ[1,4];
  DZ[2,5]:=2/3*X[2]*X[3]*X[5]**(-5/3);
  DZ[3,1]:=-2*X[1]*X[3]*X[4]**(-2/3)+X[1];
  DZ[3,2]:=DZ[3,5]:=0;
  DZ[3,3]:=(X[4]**2+1/2)*X[4]**(-4/3)-X[1]**2*X[4]**(-2/3);
  DZ[3,4]:=2/3*X[3]*X[4]**(-1/3)-2/3*X[3]*X[4]**(-7/3)+2/3*X[3]*X[1]**2*
  X[4]**(-5/3);
DZ[4,1]:=-X[1];
DZ[4,2]:=X[2];
DZ[4,3]:=H/D/X[3]**2;
DZ[4,4]:=-2/3*X[4]**(-5/3)+2/3*X[4]**(1/3);
DZ[4,5]:=2/3*X[5]**(-5/3)-2/3*X[5]**(1/3);
DZ[5,1]:=DZ[5,4]:=0;
DZ[5,2]:=2*X[2]*X[3]*X[5]**(2/3);
DZ[5,3]:=1-X[5]**2+X[2]**2*X[5]**(2/3);
DZ[5,5]:=2*X[5]*(X[5]**(2/3)-X[3])+(X[5]**2-1)*2/3*X[5]**(-1/3)+2/3*X[5]
 **(-1/3)*X[3]*X[2]**2;
  Z[1]:=A1+X[3]*DZ[1,3]-X[1];
  Z[2]:=X[2]*DZ[2,2]+X[1]*DZ[2,1];
  Z[3]:=DZ[3,3]*X[3]+0.5*X[1]**2-A3;
  Z[4]:=X[4]**(-2/3)+0.5*X[4]**(4/3)-0.5*X[1]**2-X[5]**(-2/3)-H/(D*X[3])
  -0.5*X[5]**(4/3)+0.5*X[2]**2;
  Z[5]:=(X[5]**2-1)*(X[5]**(2/3)-X[3])+X[5]**(2/3)*X[3]*X[2]**2;
DETLINEON(5,DZ,DZ,Z,DX,D0,DE);
  FOR K:=1 STEP 1 UNTIL 5 DO
  BEGIN
IF K=1 THEN D0:=ABS(DX[1]) ELSE IF ABS(DX[K])>D0 THEN D0:=ABS(DX[K]);      2
    X[K]:=X[K]-DX[K]
  END K;
  IF X[4] LEQ 0 OR X[5] LEQ 0 OR D0 < 0.0001 OR D0 > 1000 OR J > 100      2
THEN WRITE(PR,<F5,2,I4,E12.4,F9.5,8F8.4/>,H,J,D0,H1,Q21,Y2,X[1],X[2],
X[3],X[4],X[5],DB) ELSE GO TO L;
END.
```

```
    BURROUGHS B6700 ALGOL COMPILER, VERSION 2.4.175,  THURSDAY, 12/13/73,

                                N E W T O N
                                = = = = = =

  BEGIN ARRAY DZ[0:5,0:5],X,X0,X1,X2,DX,Z[0:5];

  LABEL L,L0,L1;                                                          1
  INTEGER J,K,DE,I; REAL D0,Q1,V1,F1,H,QD,D,Q01,Q21,A1,A3,Y2,DB,H1;
  FILE PR(KIND=PRINTER);

  $ RESET LIST
  V1:=1.0;F1:=8.0;D:=72.4;QD:=26.33;Q01:=7.5565;                          2
  Q1:=Q01/D*QD**(-1/3);
  X[1]:=0.90;X[2]:=0.98;X[3]:=0.0458;X[4]:=0.4;X[5]:=1.0002;
  WRITE (PR[SPACE 1],<"FIRST BRANCH">);
  H:=3.0;
  FOR K:=1 STEP 1 UNTIL 5 DO
  X2[K]:=X1[K]:=X0[K]:=X[K];
  I:=0;
  L1:I:=I+1;
  L0:H:=H-0.01;J:=0;
  A1:=Q1*(1-V1*F1**(-2/3))+V1;
  A3:=Q1*((F1**2+0.5)*F1**(-4/3)-V1**2*F1**(-2/3))+V1**2/2;
  H1:=(H/0.035)*(2*F1**(2/3)/(2*F1**2+1-2*F1**(4/3)*V1));
  L:J:=J+1;
  Y2:=X[3]*X[4]**(-2/3);
  Q21:=X[3]/Q1;
    DZ[1,1]:=X[3]*X[4]**(-2/3)-1;
    DZ[1,2]:=DZ[1,5]:=0;
    DZ[1,3]:=-1+X[1]*X[4]**(-2/3);
    DZ[1,4]:=-2/3*X[3]*X[1]*X[4]**(-5/3);
    DZ[2,1]:=DZ[1,1];
    DZ[2,2]:=1-X[3]*X[5]**(-2/3);
    DZ[2,3]:=-X[2]*X[5]**(-2/3)+X[1]*X[4]**(-2/3);
    DZ[2,4]:=DZ[1,4];
    DZ[2,5]:=2/3*X[2]*X[3]*X[5]**(-5/3);
    DZ[3,1]:=-2*X[1]*X[3]*X[4]**(-2/3)+X[1];
    DZ[3,2]:=DZ[3,5]:=0;
    DZ[3,3]:=(X[4]**2+1/2)*X[4]**(-4/3)-X[1]**2*X[4]**(-2/3);
    DZ[3,4]:=2/3*X[3]*X[4]**(-1/3)-2/3*X[3]*X[4]**(-7/3)+2/3*X[3]*X[1]**2*
    X[4]**(-5/3);
  DZ[4,1]:=-X[1];
  DZ[4,2]:=X[2];
  DZ[4,3]:=H/DX[3]**2;
  DZ[4,4]:=-2/3*X[4]**(-5/3)+2/3*X[4]**(1/3);
  DZ[4,5]:=2/3*X[5]**(-5/3)-2/3*X[5]**(1/3);
  DZ[5,1]:=DZ[5,4]:=0;
  DZ[5,2]:=2*X[2]*X[3]*X[5]**(2/3);
  DZ[5,3]:=1-X[5]**2+X[2]**2*X[5]**(2/3);
  DZ[5,5]:=2*X[5]*(X[5]**(2/3)-X[3])+(X[5]**2-1)*2/3*X[5]**(-1/3)+2/3*X[5]
    **(-1/3)*X[3]*X[2]**2;
    Z[1]:=A1+X[3]*DZ[1,3]-X[1];
    Z[2]:=X[2]*DZ[2,2]+X[1]*DZ[2,1];
    Z[3]:=DZ[3,3]*X[3]+0.5*X[1]**2-A3;
    Z[4]:=X[4]**(-2/3)+0.5*X[4]**(4/3)-0.5*X[1]**2-X[5]**(-2/3)-H/(D*X[3])
    -0.5*X[5]**(4/3)+0.5*X[2]**2;
    Z[5]:=(X[5]**2-1)*(X[5]**(2/3)-X[3])+X[5]**(2/3)*X[3]*X[2]**2;
  DETLINEQN(5,DZ,DZ,Z,DX,DB,DE);
    FOR K:=1 STEP 1 UNTIL 5 DO
    BEGIN
  IF K=1 THEN D0:=ABS(DX[1]) ELSE IF ABS(DX[K])>D0 THEN D0:=ABS(DX[K]);  2
      X[K]:=X[K]-DX[K]
    END K;
    IF X[4] LEQ 0 OR X[5] LEQ 0 OR D0 < 0.0001 OR D0 > 1000 OR J > 100    2
  THEN WRITE(PR,<F5.2,I4,E12.4,F9.5,8F8.4/>,H,J,D0,H1,Q21,Y2,X[1],X[2],
  X[3],X[4],X[5],DB) ELSE GO TO L;
  FOR K:=1 STEP 1 UNTIL 5 DO
  BEGIN X2[K]:=X1[K];X1[K]:=X0[K];X0[K]:=X[K];
  X[K]:=3*X0[K]-3*X1[K]+X2[K] END;                                        2
  IF H>0.0 AND D0<0.0001 THEN GO TO L0;                                   2
  IF I=1 THEN BEGIN H:=3.0;WRITE  (PR[SPACE 1],<"SECOND BRANCH">);
  X[1]:=0.90;X[2]:=0.98;X[3]:=0.035;X[4]:=0.1609;X[5]:=1.0002;            2
  FOR K:=1 STEP 1 UNTIL 5 DO

  X2[K]:=X1[K]:=X0[K]:=X[K];
  GO TO L1 END
  END.
```

```
A.   LINEAR EQUATIONS, MATRIX INVERSION, AND DETERMINANTS

1.   LINPAC - REAL MATRICES

PURPOSE      LINPAC IS A COLLECTION OF PROCEDURES TO SOLVE SYSTEMS OF
   LINEAR EQUATIONS, INVERT MATRICES, AND COMPUTE DETERMINANTS.
   A FULL ACCURACY OPTION ALLOWS SOLUTIONS AND INVERSES TO BE COMPUTED
   TO FULL MACHINE ACCURACY (11+ DECIMAL DIGITS).  THE DIFFERENT
   PROCEDURES GIVEN ALLOW FOR DIFFERENT COMBINATIONS OF OPTIONS.

METHOD       THE BASIC METHOD EMPLOYED IS GAUSSIAN ELIMINATION WITH
   PARTIAL PIVOTING (ROW INTERCHANGES), ALSO KNOWN AS "LU"
   DECOMPOSITION.  THE VERSIONS FOR LINEAR EQUATIONS USE COMBINATIONS
   OF TWO OR MORE BASIC WORKING PROCEDURES, OF WHICH THERE ARE FOUR,
   DECOMPOSE, SOLVE, IMPROVE, AND DETERMINANT.  A DESCRIPTION OF THESE
   FOUR FOLLOWS.
                DECOMPOSE TRANSFORMS A COPY OF THE INPUT MATRIX A (SOME
   PROCEDURES ALLOW A ITSELF TO BE TRANSFORMED, AT THE USER'S OPTION)
   INTO THE PRODUCT OF AN UPPER-TRIANGULAR MATRIX U AND A LOWER
   TRIANGULAR MATRIX L WITH 1 S ALONG THE MAIN DIAGONAL.  U IS
   STORED IN THE UPPER TRIANGULAR HALF OF THE ARRAY LU AND L IS STORED
   IN THE LOWER TRIANGULAR HALF WITH THE 1 S OMITTED.  THE ELIMINATION
   IS CARRIED OUT BY USING A FORM OF SCALING IN ADDITION TO CHOOSING
   MAXIMUM COLUMN PIVOTS.  IT IS DONE AS FOLLOWS: BEFORE THE ELIMIN-
   ATION BEGINS THE RECIPROCAL OF THE MAXIMUM MAGNITUDE ELEMENT IN
   EACH ROW IS RECORDED.  THE ELIMINATION PROCEEDS BY CHOOSING AS THE
   PIVOT ELEMENT THE LARGEST ENTRY, TAKING INTO ACCOUNT THE SCALE FAC-
   TORS, ON OR BELOW THE MAIN DIAGONAL.  RATHER THAN ACTUALLY INTER-
   CHANGE THE ROWS, THE ROW INDICES STORED IN THE ARRAY PS ARE INTER-
   CHANGED.  THE "LU" DECOMPOSITION ACTUALLY SATISFIES THE EQUATION
   LU = PA WHERE P IS A PERMUTATION MATRIX, DUE TO THE ROW INTER-
   CHANGES.
                THE SOLUTION IS COMPUTED IN SOLVE BY SOLVING SUCCESSIVELY
   THE SYSTEMS  LY = B  AND  UX = Y  (THE BACK SOLUTION).
                IMPROVE ITERATES ON THE INITIAL SOLUTION PROVIDED BY
   SOLVE UNTIL FULL MACHINE ACCURACY IS ACHIEVED.  THIS IS DONE AS
   FOLLOWS:  THE RESIDUAL VECTOR  R = AX-B  IS COMPUTED IN DOUBLE
   PRECISION ARITHMETIC AND THE CORRECTION DX1 SATISFYING (APPROXI-
   MATELY)  A DX1 = R  IS COMPUTED BY SOLVE.  THE PROCESS IS REPEATED
   FOR THE NEW RESIDUAL VECTOR  R1 = A(X+DX1)-B  AND CONTINUES UNTIL
   THE CORRECTION BECOMES NEGLIGIBLE.  ITERATIVE IMPROVEMENT REQUIRES
   ONLY A COPY OF A AND A MODEST AMOUNT OF ADDITIONAL TIME BECAUSE
   THE "LU" DECOMPOSITION OF A NEED ONLY BE COMPUTED FOR THE INITIAL
   SOLUTION.
                DETERMINANT COMPUTES THE SIGNIFICANT DIGITS AND EXPONENT
   OF DET(A) SEPARATELY TO AVOID POSSIBLE EXPONENT OVERFLOW OR UNDER-
   FLOW.  DET(A) IS STORED AS A REAL NUMBER, DETBASE, AND AN INTEGER
   POWER OF 10, DETEXP:  DET(A) = DETBASE * 10.0**DETEXP.  IF DET(A)
   LIES WITHIN FLOATING POINT RANGE, THEN DETBASE IS SET TO THE
   VALUE DET(A) AND DETEXP IS SET TO 0.  OTHERWISE DETBASE SATISFIES
   1 LEQ ABS(DETBASE) LSS 8.0@13 AND DETEXP IS THE APPROPRIATE POWER
   OF 10 FOR DETBASE.
                IF A SINGULAR MATRIX IS DETECTED, PROCEDURE SINGULAR
   WILL BE CALLED TO PRINT AN ERROR MESSAGE; THE COMPUTATION WILL
   THEN BE CONTINUED, RESULTING IN A DIVIDE BY ZERO IN SOLVE.  THIS
   MAY BE AVOIDED BY DECLARING A LABEL, SAY ERREXIT, IN THE USER
   PROGRAM, INSERTING THE STATEMENT "GO TO ERREXIT" AT THE END OF
   PROCEDURE SINGULAR, AND LABELING AN APPROPRIATE STATEMENT IN THE
   CALLING PROGRAM WITH THE LABEL ERREXIT.
                PROCEDURE INVERSE OBTAINS THE "LU" DECOMPOSITION FROM A
   BY CALLING DECOMPOSE, AND THEN SOLVES THE N SYSTEMS OF EQUATIONS
   LU X = B[I], WITH B[I] THE I-TH COLUMN OF THE IDENTITY MATRIX,
   I = 1,2,...,N.  RATHER THAN MAKE N CALLS TO SOLVE, INVERSE TAKES
   ADVANTAGE OF THE SPECIAL STRUCTURE OF THE COLUMNS OF THE IDENTITY
   MATRIX TO ACHIEVE FULL EFFICIENCY.  IT IS THE FASTEST OF THE 3
   INVERSION ROUTINES.
                INVMIMPRV USES DECOMPOSE, SOLVE AND IMPROVE TO COMPUTE
   EACH COLUMN OF THE INVERSE TO FULL MACHINE ACCURACY.  NO ADVANTAGE
   IS TAKEN OF THE SPECIAL STRUCTURE OF THE IDENTITY MATRIX.  THIS
   PROCEDURE IS 4-5 TIMES SLOWER THAN INVERSE AND SHOULD ONLY BE USED
   WHEN A FULLY ACCURATE INVERSE IS NECESSARY.

                INVERSEOVERA ALSO COMPUTES THE "LU" DECOMPOSITION OF A,
   BUT INVERTS L AND U IN PLACE, I.E. WITHOUT REQUIRING A SEPARATE
   ARRAY FOR STORAGE OF THE INVERSE.  IT THEREFORE REQUIRES ONLY HALF
   AS MUCH STORAGE AS INVERSE, BUT IS SLOWER.

REFERENCE    "COMPUTER SOLUTION OF LINEAR ALGEBRAIC SYSTEMS", GEORGE
   E. FORSYTHE AND CLEVE B. MOLER, PRENTICE-HALL, 1967, SECTIONS 16-17.


1.2
PROCEDURE    DETLINEQN(N,A,LU,B,X,DETBASE,DETEXP);
VALUE  N;    INTEGER  N,DETEXP;
REAL   DETBASE;
ARRAY  A,LU[0,0], B,X[0];

PURPOSE      SOLVES THE LINEAR SYSTEM AX = B AND CALCULATES THE
   DETERMINANT OF THE COEFFICIENT MATRIX A.

INPUT        N       - DIMENSION OF COEFFICIENT MATRIX A
             A       - COEFFICIENT MATRIX
             B       - RIGHT-HAND-SIDE VECTOR
OUTPUT       LU      - MATRIX CONTAINING THE TRIANGULAR DECOMPOSITION
                       OF A
             X       - SOLUTION VECTOR
             DETBASE - CONTAINS THE SIGNIFICANT DIGITS OF DET(A)
             DETEXP  - CONTAINS THE APPROPRIATE POWER OF 10 FOR DETBASE

REMARKS      DETLINEQN(N,A,A,B,X,DETBASE,DETEXP) OVERWRITES A WITH
   ITS TRIANGULAR DECOMPOSITION AND SAVES N(N+3) WORDS OF STORAGE.
             USES PROCEDURES DECOMPOSE, SOLVE, DETERMINANT,
   AND INDIRECTLY INNERPROD, ELIM, AND SINGULAR.
```

```
(CIVL032)MATHLIB/SYMBOL/DETLINEQN.
DATE 12/12/73          TIME IS 14:30
MAXRECSIZEIN =  14     BLOCKSIZEIN = 420
***-EBCDIC-***         UNITS=WORDS

      1     PROCEDURE    DETLINEQN(N,A,LU,B,X,DETBASE,DETEXP);
      2     VALUE  N;      INTEGER  N,DETEXP;
      3     REAL   DETBASE;
      4     ARRAY  A,LU[0,0], B,X[0];      COMMENT   A,LU[0:N,0:N], B,X[0:N];
      5     COMMENT        DETLINEQN(N,A,A,B,X,DETBASE,DETEXP) OVERWRITES A WITH ITS
      6       TRIANGULAR DECOMPOSITION AND SAVES NIN WORDS OF STORAGE ;
      7     COMMENT        SAME AS LINEQN EXCEPT THAT THE DETERMINANT OF A IS
      8       COMPUTED IN ADDITION:  DET(A) = DETBASE * 10*DETEXP.
      9       IF DET(A) LIES WITHIN FLOATING POINT RANGE THEN DETBASE IS SET TO THE
     10       VALUE DET(A) AND DETEXP IS SET TO 0.  OTHERWISE, DETBASE SATISFIES
     11       1 LEQ DETBASE LSS 8*13 AND DETEXP IS THE APPROPRIATE POWER OF 10.
     12                      USES PROCEDURES DECUMPOSE, SOLVE, DETERMINANT,
     13         AND INDIRECTLY INNERPROD, ELIM, AND SINGULAR ;
     14           BEGIN
     15       INTEGER        DETSIGN;
     16       INTEGER ARRAY  PS[0:N];
     17       PROCEDURE      SINGULAR(WHY);
     18       VALUE  WHY;    INTEGER  WHY;
     19           BEGIN
     20       FILE PRINTER (MYUSE = 2,KIND =  7 ,BUFFERS = 1,MAXRECSIZE = 15);
     21       SWITCH FORMAT  BOMBOUT :=
     22                      ("MATRIX HAS A ZERO ROW"),
     23                      ("MATRIX IS SINGULAR"),
     24                      ("NO CONVERGENCE IN IMPROVE, MATRIX IS NEARLY SINGULAR");
     25                WRITE(PRINTER,BOMBOUT[WHY]);
     26           END  SINGULAR;
     27       PROCEDURE      DECUMPOSE(N,A,LU,PS,DETSIGN);
     28       VALUE  N;      INTEGER  N,DETSIGN;
     29       ARRAY  A,LU[0,0];      COMMENT   A,LU[0:N,0:N];
     30       INTEGER ARRAY PS[0];
     31       COMMENT        DECOMPOSE(N,A,A,PS,DETSIGN) OVERWRITES A WITH ITS
     32         TRIANGULAR DECOMPOSITION AND SAVES NIN WORDS OF STORAGE ;
     33       COMMENT        DECOMPOSE COMPUTES TRIANGULAR MATRICES L AND U AND
     34         PERMUTATION MATRIX P SO THAT LU = PA.  IT STORES L-I AND U IN LU,
     35         ARRAY PS CONTAINS PERMUTED ROW INDICES.  IF MATRIX IS SINGULAR AN
     36         EXIT VIA PROCEDURE SINGULAR TO GLOBAL LABEL RERUN OCCURS.
     37                        USES PROCEDURES ELIM AND SINGULAR ;
     38           BEGIN
     39       INTEGER        I,J,K,PIVOTINDEX;
     40       REAL           NORMROW,PIVOT,SIZE,BIGGEST,MULT,TEMP;
     41       REAL ARRAY     SCALES[0:N];
     42       LABEL          EXIT;
     43       PROCEDURE      ELIM(AI,AK);
     44       ARRAY  AI,AK[0];
     45       COMMENT        EFFICIENT PROCEDURE FOR ELIMINATION STEP.  THE ACTUAL
     46         ARGUMENTS SUPPLIED FOR AI AND AK WILL HAVE ARRAY ROW FORM ;
     47           BEGIN
     48             FOR J := K+1 STEP 1 UNTIL N DO
     49             AI[J] := AI[J] - MULT*AK[J];
     50           END  ELIM;
     51       COMMENT        INITIALIZE PS, LU AND SCALES;
     52             I := 0;  WHILE I := I+1  LEQ N DO
     53             BEGIN
     54               PS[I] := I;      NORMROW := 0;
     55               J := 0;  WHILE J := J+1  LEQ N DO
     56               BEGIN
     57                 TEMP := LU[I,J] := A[I,J];
     58                 NORMROW := MAX(NORMROW,ABS(TEMP));
     59               END;
     60               IF NORMROW NEQ 0 THEN SCALES[I] := 1.0/NORMROW
     61               ELSE  BEGIN  SINGULAR(0);  GO TO EXIT;  END;
     62             END;
     63       COMMENT        PROCEDURE SINGULAR WRITES ERRORMESSAGE AND EXITS ;
     64       COMMENT        GAUSSIAN ELIMINATION WITH PARTIAL PIVOTING NEXT ;
     65             K := 0;  WHILE K := K+1 < N DO
     66           BEGIN
     67               BIGGEST := 0;
     68               FOR I := K STEP 1 UNTIL N DO
     69               BEGIN
     70                 SIZE := ABS(LU[PS[I],K]) * SCALES[PS[I]];
```

```
                    IF BIGGEST LSS SIZE THEN
                      BEGIN BIGGEST := SIZE; PIVOTINDEX := I; END;
                  END;
                  IF BIGGEST = 0 THEN BEGIN SINGULAR(1); GO TO EXIT; END;
                  IF PIVOTINDEX NEQ K THEN
                  BEGIN
                    DETSIGN := -DETSIGN;
                    J := PS[K]; PS[K] := PS[PIVOTINDEX]; PS[PIVOTINDEX]:=J;
                  END;
                  PIVOT := LU[PS[K],K];
                  I := K; WHILE I := I+1 LEQ N DO
                  BEGIN
                    LU[PS[I],K] := MULT := LU[PS[I],K]/PIVOT;
                    IF MULT NEQ 0 THEN
                      ELIM(LU[PS[I],*],LU[PS[K],*]);
                  END;
              END KLOOP;
              IF LU[PS[N],N] = 0 THEN SINGULAR(1);
    EXIT:   ;
        END DECOMPOSE;
    PROCEDURE       SOLVE(N,LU,B,X,PS);
    VALUE   N;      INTEGER N;
    REAL ARRAY      LU[0,0], B,X[0];
    INTEGER ARRAY   PS[0];
     COMMENT        SOLVES AX=B USING LU FROM DECOMPOSE.
                    USES PROCEDURE INNERPROD ;
        BEGIN
    REAL PROCEDURE      INNERPROD(J1,J2,X,Y,C) ;
    VALUE  J1,J2,C;     INTEGER  J1,J2;     REAL  C;
    REAL ARRAY          X,Y[0];
    COMMENT         PROCEDURE WILL ALLOW ARRAY ROW CONSTRUCT OF BURROUGHS
                    ALGOL TO BE UTILIZED FOR EFFICIENCY ;
        BEGIN
            FOR J1 := J1 STEP 1 UNTIL J2 DO
            C := C + X[J1]*Y[J1];
            INNERPROD := C;
        END;
    INTEGER         I;
            I := 0; WHILE I := I+1 LEQ N DO
                X[I] := INNERPROD(1,I-1,LU[PS[I],*],X,B[PS[I]]);
            FOR I := N STEP -1 UNTIL 1 DO
                X[I] := INNERPROD(I+1,N,LU[PS[I],*],X,X[I])/LU[PS[I],I];
        END SOLVE;
    PROCEDURE       DETERMINANT(N,LU,PS,DETSIGN,DETBASE,DETEXP);
    VALUE  N,DETSIGN;  INTEGER  N,DETSIGN,DETEXP;
    REAL  DETBASE;
    ARRAY  LU[0,0];
    INTEGER ARRAY       PS[0];
        BEGIN
    COMMENT         CALCULATES THE DETERMINANT OF A MATRIX WHICH HAS BEEN
       BROUGHT INTO LU FORM BY PROCEDURE DECOMPOSE.
       DETSIGN IS +1 OR -1 TO ACCOUNT FOR ROW INTERCHANGES IN DECOMPOSE.
       THE DETERMINANT IS STORED AS A REAL NUMBER, DETBASE, AND AN INTEGER
       POWER OF 10, DETEXP:  DET(A) = DETBASE * 10**DETEXP.  IF DET(A)
       LIES WITHIN FLOATING POINT RANGE, THEN DETBASE IS SET TO THE VALUE
       DET(A) AND DETEXP IS SET TO 0. OTHERWISE, DETBASE SATISFIES
       1 LEQ DETBASE LSS 8*13  AND DETEXP IS THE APPROPRIATE POWER OF 10 ;
    INTEGER         K,TERMEXP,PRODEXP;
    REAL            TEMP,TERMBASE;
            TERMEXP := DETEXP := 0;
            DETBASE := DETSIGN;
            FOR K := 1 STEP 1 UNTIL N DO
            BEGIN
                TEMP := LU[PS[K],K];
                TERMBASE := TEMP & 0[45:7];
                TERMEXP.[5:6] := TEMP.[44:6];
                TERMEXP.[46:1] := TEMP.[45:1];
                DETBASE := DETBASE*TERMBASE;
                PRODEXP.[5:6] := DETBASE.[44:6];
                PRODEXP.[46:1] := DETBASE.[45:1];
                DETEXP := DETEXP+TERMEXP+PRODEXP;
                DETBASE.[45:7] := 0;
            END;
            IF ABS(DETEXP) LEQ 63 THEN
            BEGIN
                DETBASE := DETBASE & DETEXP[45:46:1] & DETEXP[44:5:6];
                DETEXP := 0;

            END ELSE
            BEGIN
                TEMP := .903089986990 * DETEXP;
    COMMENT         .903089986990 = LOG(8) ;
                DETEXP := ENTIER(TEMP);
                DETBASE := DETBASE * 10.0**(TEMP-DETEXP);
            END;
        END DETERMINANT;
            DETSIGN := 1;
            DECOMPOSE(N,A,LU,PS,DETSIGN);
            SOLVE(N,LU,B,X,PS);
            DETERMINANT(N,LU,PS,DETSIGN,DETBASE,DETEXP);
        END DETLINEQN;
```

APPENDIX G

APPLICATIONS TO THERMAL POWER STATIONS

Power stations require huge volumes of cooling water to condense steam which has passed through the turbines used to drive the generators. The efficiency of the generation cycle is in part dependent on the temperature of the cooling water; the lower the temperature the greater the efficiency.

Cooling water systems may be of the "closed circuit" or "open circuit" type.

The Cooling Pond Problem : Minimum Entrainment

In the closed circuit system water is drawn from a bounded body of water, after passing through the heat exchangers, into the same body of water. The operation of such a system is dependent upon the dissipation of heat to the environment from the pond outlet and intake.

The difference in density of the inflowing and ambient fluids causes the hot water to spread and form a layer at the surface of the reservoir. Density stratification of this type is desirable in cooling ponds since it promotes heat transfer from the heated water to the atmosphere before the cooling water is reused.

Evaporation and radiation are the dominant mechanisms of heat exchange in the pond, and these are optimised when the surface layer is as hot and as thin as possible. This is achieved by minimising mixing of the inflowing and ambient fluids at the outfall.

A density jump will almost always form at a power

station cooling pond outfall since the densimetric Froude Number of the flow at the outfall will almost always be greater than one. Entrainment at the density jump can be reduced by means of a downstream control. One proposal is to anchor a floating barrier downstream of the outfall, and so control entrainment into the jump. The barrier depth necessary to cause the density jump to be non-entraining is calculated. Mixing at the cooling pond outfall can also be inhibited by using a bottom slope to the outfall of less than 15^{o}.

The Open Circuit Cooling Water System

In the open circuit system water is drawn in from a stream of flowing water, and the heated water is discharged into the same stream, usually downstream of the intake. Alternatively, water may be drawn in from one body of water (for example, a lake), and discharged to another (for example, the sea).

In New Zealand most inland waters are classified. The National Water and Soil Conservation Act 1972 for class C and D receiving waters required that "the natural water temperature shall not be changed by more than $3^{o}C$." But in most thermal power stations cooling water is raised in temperature from 8 to $10^{o}C$. One problem for the power station designers is how to dispose of the cooling water without violating the classification restrictions. The simple solution is to promote maximum entrainment of the ambient fluid at the cooling water outfall. Studies made by the writer and others indicate that large entrainments of up to 3 or even 5 times are possible in the maximum entraining hydraulic jump.

A short description of the available cooling water systems for the Huntly Thermal Power Station, and some

related environmental considerations, may be found in the following Appendix.

APPENDIX H

THE HUNTLY THERMAL POWER STATION

It is proposed that a 1000 Mw thermal power station be built at Huntly on the Waikato River, to come into use between 1978 and 1982. Present reports indicate that it is most likely that the once-through cooling system be adopted.

Physical Environment. The annual temperature variation in the Waikato River is from 9.5 to 23.5 ^{o}C. Minimum low flows could be 140 cumecs. The relative humidity of the air along the river is 90-95% in winter. Freshwater lakes in the vicinity of Huntly are Lakes Wahi, Whangape, Kimihia, Waikari, Rotongara. Lake Whangape is about 1½ square miles area. Lake Wahi is less than 10 metres deep, with high summer temperatures (26.7^{o}C). Twenty miles downstream from Huntly is the Meremere Thermal Power Station.

Proposed Once Through Cooling System. It is proposed to take 38 cumecs from the Waikato and discharge it back after being heated 8^{o}C in the condensers. The mean annual Waikato flow is about 390 cumecs. Under mean river conditions, 10% of the river water is withdrawn, giving a 0.8 ^{o}C rise after complete mixing. The design low flow in the Waikato is 190 cumecs, and at this flow, 27% of the Waikato would be required for cooling purposes, raising the river by 2.16 ^{o}C after complete mixing.

The National Water and Soils Conservation Act (1972) for class C and D receiving waters requires that "The natural water temperature shall not be changed by more than $3^{o}C$". It is not stated in these regulations whether the $3^{o}C$ limit applies to spot discharges or the average rise in temperature of the whole body of water after complete mixing, which would allow spot discharges considerably in excess of the $3^{o}C$ limit. It may be better to replace this limit condition by a best practicable means similar to that in the Clean Air Act (1972).

Some measurements have been made at the Meremere thermal power station: water is discharged $15^{o}C$ above ambient. After 100 metres, the plume is $^{3}/_{4}{}^{o}C - 1^{o}C$ above the surrounding fluid, and after 300 yards there is complete mixing.

Two alternative outfall methods for Huntly are (a) to promote local mixing and (b) spread the discharge over the river surface with minimum mixing. It is expected that the designers would endeavour to promote rapid local mixing in an effort to comply with the classification conditions. The stratified transition zone, in this case is expected to extend downstream 1.3 km with a depth of 1.5 m (river depth 3 m).

Alternative Cooling Water Systems: Closed Cycle Systems

(1) Cooling Towers: Four towers would be required, each 115 m high, 92 m base diameter, 46 m top diameter. The cost, $20 m, is prohibitive. Cooling towers may also lead to serious fog and aesthetic problems.

(2) Cooling Pond: Perhaps the best practicable means of dealing with thermal pollution is the cooling pond. The NZED assume that 1 acre would be required per MW, or 1000 acres. Ryan and Harleman (1971) cite 0.75 to 1 - 2 acres per

MW but state that the correct figure depends on local conditions, and that years of meteorological simulation data should be used in the computer simulation. Advantages of cooling ponds include: no thermal pollution of rivers, simplicity, low maintenance, low cost (compared with cooling towers), low power requirements, possible recreational value and possible use as fish farms, high thermal inertia, aesthetic advantages, minimal fogging, and non-dependence on a fluctuating water source. The main disadvantages are cost, large amounts of land required, possible eutrophication problems and lack of experience and confidence in their design.

(3) Spray Canals: Spray canals are new and there is very little data on their performance yet available.

(4) Natural Cooling Ponds: Natural cooling ponds should not be seriously considered because when water is drawn from the hypolimnion and discharged in the ephilimnion, the natural turnover (alteration of stratification) is upset, and the length of time the lake remains stratified each year is increased, reducing oxygen levels in the hypolimnium where trout, food organisms, and other living things consume oxygen. The water in the hypolimnium is rich in available plant nutrients, and by warming it, and discharging it in the lighted zone, the amount of plant growth will be increased. More organic matter will sink to the hypolimnium and use up oxygen when it decays. The threat to the welfare of the lake is very real.

Environmental Considerations. Many eurythermal plants and animals (which can tolerate a wide temperature range) actually breed within a narrower range of temperature

than they can tolerate as adults. Even though animals can survive near heated effluents, it does not preclude the possibility that the species may be prevented from breeding in such a locality and therefore would persist there only if continuously recruited from outside. Conversely, artificial warming might encourage the breeding of non-native species in the area, and nuisance plants and rough fish may flourish.

In temperate regions where sub-polar and sub-tropical species occur together, the higher latitude species breed in winter and low latitude species breed in summer, so heated effluents might be expected to have a differential effect upon these two groups of animals. Low latitude species may become more prolific. Electric power is often produced in greater quantities in winter than summer. Extensive narrowing of the seasonal range of temperature would probably have considerable biological effects since some species exhibit normal growth rates, reproductive rates, sex ratios, and life spans, ONLY under conditions simulating annual fluctuations in the environment.

High temperatures may be associated with low concentrations of dissolved oxygen, particularly in areas receiving oxidizable effluents as well as heat, since the rate of biochemical reactions increases with increasing temperature. Thermal tensions or reduced oxygen often encourage fish to move out of an area temporarily. Of all river animals, fish are the most sensitive to temperature changes, but they are also the most mobile. Fish can perceive temperature differences of less than $1^{o}F$ and can move along temperature gradients.

According to Langford (1970, 1971) and Naylor (1965),

the effect of a once through cooling process of a thermal power station on a river with low concentration of nutrients is minimal. However the Waikato River has high nutrient concentrations and in some of the man-made lakes, lake weed growth is vigorous. Therefore any increase in temperature can only be expected to aggravate the already serious eutrophication problems. There could also be a significant increase in algal growth in the Estuary of the Waikato River. Any improvements in water quality would help to minimise the effects of transient temperature increase.

In the author's opinion the above suggests that it is desirable that a closed cycle cooling system (i.e. the cooling pond) be considered as a practicable alternative to once through cooling.

APPENDIX I

RECOMMENDED MODIFICATIONS

Modifications which should be carried out before any further experiments are attempted include:

(1) Remove the top brass rod just upstream of the downstream platinum wire.

(2) Install beside the 3 Hp pump a $^{3}/_{4}$" self priming pump of 35 gallon per minute capacity, a valve, flow meter and pipe from the downstream end of the flume to the tub. Another grill may be necessary to ensure uniform ambient flow conditions. Alternatively, the space between the two grills could be filled with large irregularly shaped wooden blocks, perspex scraps, or even stones. A second flow meter could be placed in the syphon pipe. The three flow meters could then be used to determine the velocity of the ambient fluid with greater accuracy than with the hydrogen bubble technique. Ambient flow = cold water flow meter reading + syphon flow meter reading - hot water flow meter reading. The 3 Hp pump could still be used for high flows and to mix up the water in the tank to prevent stratification.

(3) Replace the plastic pipe between the large air trap and the hot water inlet by a more rigid but still flexible pipe which will not buckle in hot water.

(4) The cold junction of the adjustable thermocouple should be placed in the ambient fluid, at the bottom of the tank, but removable to permit calibration. The thermocouple could be calibrated with the cold junction at 15°C, and at 20°C. Only a 15°C range in the calibration curves is necessary.

(5) The $^{3}/_{4}$" pipe which is used to maintain a constant head in the tank should be taken from the mains and into the tub. This pipe could be used for priming the 3 Hp pump but must be taken to the tub during an experiment.

(6) The hot water heaters should be increased in power so that a flow of 1 gallon/40 seconds and a temperature rise of 10^{o}C could be maintained indefinitely (1 day?)

(7) A thermometer should be installed in the tank to read the temperature of water near the surface.

APPENDIX J

NOTATION

The following symbols are used in this paper:

D = Total depth

F = Froude No. = densimetric Froude No.

$$F = \left[u^2/(\Delta\rho/\rho)gy \right]^{\frac{1}{2}}$$

F_1 = Froude No. at section (1), upstream Froude No.

F_2 = Froude No. at section (2), downstream Froude No.

F_3 = Froude No. at section (3)

F_* = Froude - Wave Number

f = A function of upstream conditions (Eqn.25)

f^* = Friction factor

g = Gravitational Acceleration

h = Weir height (cm)

k = Δ_1/Δ_2

p = Pressureon the upper surface

q = Discharge = u.y

q_1 = Discharge at section (1)

q_2 = Downstream discharge (section (2))

q_{21} = q_2/q_1

q_F = Flow force (Eqn. 7)

q_m = Mass Flux

q_v = Volume Flux (Eqn. 2)

q_{v_*} = Dimensionless volume flux = $q_v/q_\Delta{}^{1/3}D$

q_u = $v(D-y)$

q_{u_*} = $q_{v_*} - q_*$

q_* = $q/q_\Delta{}^{1/3}D$

q_{*1} = q_* at section (1)

q_{*2} = q_* at section (2)

r = y_2/y_1

T_e = Bernoulli constant in Ambient Fluid

T_{e1} = Bernoulli constant in Density current

u = Velocity in Density current

$\bar{u}$ = Mean velocity in Density current

u_1 = $\bar{u}$ at section (1)

u_2 = $\bar{u}$ at section (2)

v = Velocity in Ambient Fluid

v_1 = v at section (1)

v_2 = v at section (2)

v_* = $v/q_\Delta^{1/3}$

v_{*1} = v_* at section (1)

v_{*2} = v_* at section (2)

w = Wave velocity

w_* = $w/q_\Delta^{1/3}$

x = Distance downstream

y = Depth of Density current

y_1 = y at section (1)

y_2 = y at section (2)

y_* = y/D

z = Wave amplitude

$\rho = \rho_o$ = Density of Ambient Fluid

$\Delta\rho$ = Density difference between current and ambient

Δ_1 = $(\Delta\rho/\rho)g$

Δ_2 = Mass difference at section (2) (Eqn.31)

β_1 = Laminar boundary layer thickness/y

β_2 = Velocity at the edge of a laminar boundary layer/$\bar{u}$

β = $2\beta_2/\beta_1$

β' = Ratio of free stream to jet velocity

τ_w = Boundary shear stress

μ = Dynamic viscosity

APPENDIX K

REFERENCES

Bakke, P. (1957), "An experimental investigation of a wall jet", J. Fluid Mech. 2. pp. 467-472.

Benjamin, T.B. (1962), "Theory of the vortex breakdown phenomenon", J. Fluid Mech. 14. pp. 593-629.

Cole, Lamont C. (1969), "Thermal Pollution", Bioscience, Vol.19, pp.989-992.

Ellison, T.H., and Turner, J.S. (1959), "Turbulent Entrainment in Stratified Flows", J. Fluid Mech. 6. pp.423-448.

Glauert, M.B. (1956), "The Wall Jet", J. Fluid Mech. 1. pp. 625-643.

"Handbook of Chemistry and Physics" (Annual), Chemical Rubber Co., Ohio.

Harleman, D.R.F. (1961), "Stratified Flow" in Handbook of Fluid Dynamics. Ed. Streeter, V.L., McGraw Hill, N.Y.

Henderson, F.M. (1966), "Open Channel Flow", McMillan.

Jenkins, B.S. (1970), "Density Currents and Turbidity Currents in Waste Disposal in the Ocean", University of N.S.W. Water Research Laboratory, Report No. 119.

Kruka, V., and Eskinazi, S. (1964), "The Wall Jet in a Moving Stream", J. Fluid Mech. 20. pp.555-579.

Langford, T.E., "The Biological Assessment of Thermal Effects in Some British Rivers".

Langford, T.E., and Aston, R.J., "The Ecology of Some British Rivers in Relation to Warm Water Discharges from Power Stations".

Langford, T.E. (1971), "River Ecology and the Impact of Man: Thermal Effluents", (A comparative assessment of thermal effects in some British and N. American Rivers) Amherst. Massachusetts.

Langford, T.E. (1970), "Some American Attitudes to Thermal Pollution", Central Electricity Research Laboratories (U.K.)

Lied, N.T. "Stationary Hydraulic Jumps in Katabatic Flow near Davis, Antactica, 1961", Aust. Met. Magazine, No.47, Dec. 1964.

Merriman, Daniel, "The Calefaction of a River".

National Water and Soil Conservation Authority (5 June 1973). Statement.

Naylor, E. (1965). "The Effects of Heated Effluents Upon Marine and Estuarine Organisms", Adv. Mar. Biol. 3:63-103.

N.Z.E.D (1973). "Environmental Impact Statement, Huntly Thermal Power Station".

Ostrowski, A. (1966), "Solution of Equations and Systems of Equations". 2nd Edit., N.Y. Academic Press.

Rouse, H. (1936), "Discharge Characteristics of a Free Overfall" Civil Engineering, Vol.6, No.4, pp.257-260.

Ryan, Patrick, J., and Harleman, D.R.F., (1971), "An Analytical and Experimental Study of Transient Cooling Pond Behaviour". Ralph M. Parsons Laboratory for Water Resources and Hydrodynamics, MIT.

Streeter, B.L. (1971), "Fluid Mechanics", 5th Edition, McGraw-Hill.

Traub, J.F. (1964), "Iterative Methods for the Solution of Equations". N.J., Prentice Hall.

Wilkinson, D.L. (1970), "Studies in Density Stratified Flows", University of N.S.W., Water Research Laboratory, Report No. 118.

Wilkinson, D.L. and Wood, I.R. (1971), "A Rapidly Varied Flow Phenomenon in a Two-Layer Flow", J. Fluid Mech. Vol.47. Part 2, pp.241-256.

Wilkinson, D.L. (1971), "Stratification of Flow from Channel into Deep Lake", Journal of the Hydraulics Division, ASCE, Vol.97, No. HY4, April 1971, pp.602-609.

Wilkinson, D.L. (1972), "Dynamics of Contained Oil Slicks", Journal of the Hydraulics Division, ASCE, Vol.98, No. HY6, June 1972, pp.1013-1029.

Wood, I.R. (1968), "Selective Withdrawal from a Stably Stratified Fluid", J. Fluid Mech. 32, pp. 209-223.

Wood, I.R., (1973), "The Dispersal of Heat in Rivers and Lakes", Proc. Pollution Research Conference, Wairakei, N.Z., pp.347-357.

Yih, C.S. and Guha, C.R. (1965), "Hydraulic Jump in a Fluid System of Two Layers", Tellus, 7, 358-366.

Yih, Chia-Shun (1965), "Dynamics of Nonhomogeneous Fluids", McMillan.